University of Wollongong

Research Online

University of Wollongong Thesis Collection 1954-2016

University of Wollongong Thesis Collections

2016

Development and Evaluation of Novel Biocompatible Microemulsion Formulations for Transdermal Drug Delivery

Fanyu Zhang
University of Wollongong

Follow this and additional works at: https://ro.uow.edu.au/theses

University of Wollongong

Copyright Warning

You may print or download ONE copy of this document for the purpose of your own research or study. The University does not authorise you to copy, communicate or otherwise make available electronically to any other person any copyright material contained on this site.

You are reminded of the following: This work is copyright. Apart from any use permitted under the Copyright Act 1968, no part of this work may be reproduced by any process, nor may any other exclusive right be exercised, without the permission of the author. Copyright owners are entitled to take legal action against persons who infringe their copyright. A reproduction of material that is protected by copyright may be a copyright infringement. A court may impose penalties and award damages in relation to offences and infringements relating to copyright material. Higher penalties may apply, and higher damages may be awarded, for offences and infringements involving the conversion of material into digital or electronic form.

Unless otherwise indicated, the views expressed in this thesis are those of the author and do not necessarily represent the views of the University of Wollongong.

Recommended Citation

Zhang, Fanyu, Development and Evaluation of Novel Biocompatible Microemulsion Formulations for Transdermal Drug Delivery, Master of Science (Research) thesis, School of Biological Sciences, University of Wollongong, 2016. https://ro.uow.edu.au/theses/4962

Research Online is the open access institutional repository for the University of Wollongong. For further information contact the UOW Library: research-pubs@uow.edu.au

School of Biological Science

Development and Evaluation of Novel Biocompatible Microemulsion Formulations for Transdermal Drug Delivery

Fanyu Zhang

"This thesis is presented as part of the requirements for the
award of the Degree of
of the Master of Science (Research)
University of Wollongong"

August 2016

ABSTRACT

Transdermal drug delivery is a noninvasive delivery method which can have numerous advantages for patients. It bypasses first-pass metabolism and can produce a constant and sustained delivery flux when compared to other drug delivery pathways (i.e. oral and injection). To effectively achieve those requirements, microemulsion (ME) formulations have been used as the drug delivery vehicles because they can form spontaneously, are thermodynamically stable and possess high solubilization capacity for drug compounds. This project optimized the composition of topical biocompatible ME formulations and evaluated their transdermal permeation capacity.

In this study, medium chain monoglycerides (MCM) was found can act as the transdermal permeation enhancer in ME formulations. The transdermal permeation rate of sodium fluorescein (NaFlu) produced by both MCM alone and MCM incorporate with surfactant mixture (Tw/Sp) were significantly higher (over 30 and 25-fold, respectively) than that produced by phosphate buffered saline (PBS). Additionally, increasing concentration of MCM leads to an increasing monophasic region (A_T) from 15.2% to 33.2% of pseudo-ternary phase diagrams. When incorporated with MCM, it is observed that ethanol (EtOH) largely expanded the A_T of pseudo-ternary phase diagrams to 52.3% and effectively improved the transdermal delivery rate of ME formulations. The transdermal delivery rate of different surfactants composed with MCM and EtOH based ME formulations was tested *in vitro* through hairless mice skin. Both ME formulation contained surfactant BRIJ O10 and Tween 80 presented great permeation performance (over 33 and 29-fold, respectively) when comparing with PBS in delivery of NaFlu. Besides, either surfactant BRIJ O10, Tween 80 or Kolliphor EL showed great results of gentamicin permeation performance (over 10, 13 and 14-fold, respectively) than in PBS when composed with MCM and EtOH based ME formulations. Therefore, ME formulation contains Tween 80 (ME_T8) was selected to assess the bio-distribution of gentamicin *in vivo*. Results showed that the gentamicin can't go through mouse skin when dissolved in the PBS treatment. It is found that formulation ME_T8 did facilitate the transdermal delivery of gentamicin through mouse skin to produce detectable systemic drug levels. Furthermore, it is observed that the cumulative

amounts of gentamicin in the kidney increasing 2.3-fold when double dose gentamicin was applied in comparison with the single dose ME treatment.

These findings indicate monoglyceride-based MEs can act as transdermal drug delivery vehicles with tunable skin permeation characteristics.

DECLARATION

This thesis is submitted in accordance with the regulations of the University of Wollongong in partial fulfilment of the degree of Master of Science (Research). It does not include any material published by another person without due reference within the text. The laboratory work presented in this thesis was performed by the author, except where acknowledged. This thesis has not been submitted for a degree at any other university.

Fanyu Zhang

August 2016

ACKNOWLEDGEMENTS

I would first like to thank my supervisor, Dr. Jason McArthur, for always being available to give invaluable feedback with regards to my research and writing, for always making the writing much easier when I was struggling with how to start, for always being patient with my progress when I was going through difficulties in life, for always being supportive when I need a help. Without your guidance and persistent help, the thesis would not have been possible.

I would like to thank Prof. Andy Davis, for always being supportive and ready to help.

I would like to thank all the members in our best lab group for always making me feel included and supported. To Oriana, for participating in my lab work. To Simon, for always being ready with a chat. To Martina, for always being kind to me. To Meng Mao, for invaluable advice and help with writing thesis in English.

I would like to thank the Technical Officers, for teaching me to use the lab equipment correctly. To the IHMRI administration, for the best work environment they offer. Thank you.

I would like to thank the International Postgraduate Tuition Award for supporting my study.

Finally, I would like to thank my wife, kid, Mum, Mother-in-law, and all other family members for your encouragement, support, faith in me throughout. Without your unconditional love, I would not be able to have the thesis completed.

TABLE OF CONTENTS

ABSTRACT i
DECLARATION iii
ACKNOWLEDGEMENTS iv
TABLE OF CONTENTS v
LIST OF TABLES xi
LIST OF ABBREVIATIONS xii
1 INTRODUCTION 1
1.1 Introduction of the skin 1
1.1.1 Overview 1
1.1.2 The structure of the skin 1
1.1.3 Skin barrier function 3
1.2 Topical Drug Delivery 5
1.2.1 Advantages and disadvantages 5
1.2.2 Transdermal drug delivery 5
1.2.3 Transdermal drug delivery methods 6
1.3 Medium chain monoglycerides (MCM) as transdermal drug delivery enhancers 8
1.3.1 Structures 8
1.3.2 Transdermal permeation enhancers 8
1.3.3 MCM as transdermal permeation enhancers 9
1.3.4 Antimicrobial properties of MCM 10
1.4 ME formulations as topical drug delivery vehicles 10
1.4.1 Formation and structure of MEs 10
1.4.2 ME formulation for topical drug delivery 11
1.5 The aim of this study 12
2 METHODS AND MATERIALS 13
2.1 Materials 13
2.1.1 Chemicals 13
2.1.2 Equipment 13
2.1.3 Animals 13
2.2 Construction of Pseudo-Ternary Phase Diagram 13
2.3 Measuring transdermal permeation rate through hairless mice skin 14

2.3.1 Collection of skin tissue from mice 14
2.3.2 Mounting full thickness mice skin to Franz diffusion cells 14
2.3.3 Assessing the integrity of full thickness hairless mice skin 15
2.3.4 Measuring the transdermal permeation of sodium fluorescein 15
2.3.5 Measuring the transdermal permeation of gentamicin 17
2.4 Bio-distribution studies in mice 18
2.5 Statistical analysis and software 20
3 DEVELOPING ME FORMULATIONS CONTAINiNG MEDIUM CHAIN GLYCERIDES FOR TRANSDERMAL DELIVERY 21
3.1 Introduction 21
3.1.1 Characterization of a biocompatible ME system containing medium chain glycerides 21
3.1.2 *In vitro* transdermal delivery skin permeation assay 22
3.2 Influence of surfactant type on the transdermal permeation enhancing properties of MCM 25
3.3 The effect of MCM concentration on transdermal permeation 26
3.4 Characterizing the influence of ethanol as a co-surfactant on the ME systems containing MCM 30
3.5 Discussion 34
4 DEVELOPMENT OF TOPICAL ME FORMULATIONS CONTAINING GENTAMICIN 40
4.1 Introduction 40
4.2 Identification of suitable ME systems for gentamicin incorporation 40
4.3 Transdermal permeation kinetics of gentamicin from ME formulations ... 41
4.4 Bio-distribution of gentamicin after topical application of a ME formulation 42
4.5 Discussion 48
5 CONCLUSIONS 51
6 REFERENCES 53
7 APPENDIX 60
7.1 Materials and solutions 60
7.2 Specification Sheets 61
7.3 Transdermal delivery assay of NaFlu (MCM/GTCC based formulations) 64

7.4 Transdermal delivery assay of NaFlu (MCM/EtOH based formulations) . 72
7.5 Transdermal delivery assay of gentamicin (MCM/EtOH based formulations) 74
7.6 Bio-distribution assay of gentamicin (MCM/EtOH based formulations) .. 77

LIST OF FIGURES

Fig 1.1 Cross-section of skin (James et al., 2016). Three layers compose the skin structure: the epidermis, the dermis and subcutaneous tissue. 1

Fig 1.2 The "brick and mortar" pattern of stratum corneum. The corneocyte is protein-based and hydrophobic lipids are extracellularly sequestered in the stratum corneum (Prausnitz et al., 2012). 4

Fig 1.3 The chemical structure of MCM (Moonen and Bas, 2014). OCR is a saturated or an unsaturated hydrocarbon chain with 6 to 12 carbons in length..... 8

Fig 2.1 Location of the electrodes when measuring the resistance across skin mounted in Franz diffusion cells. 15

Fig. 3.1 Pseudo-ternary phase diagram for a mixture of medium chain glycerides (Capmul MCM C8: Crodamol GTCC, 1:3), a mixture of surfactants (Tween 80: Span 80, 3:2) and water. ME formulations were defined as being a single phase that was visually transparent, stable upon ON incubation at room temperature after vigorous vortexing (Garti et al., 2000). The ME phase boundary is indicated with grey shading. Specific formulations assessed for transdermal permeation are indicated with A, marked by the red point. The monophasic ME region is indicated with A_T = 8.8%. 22

Fig 3.2 Cumulative transdermal permeation of NaFlu through mouse skin *in vitro* over 24 h. All formulations contained 1.2 mg/mL NaFlu and are described in Table 3.1 except for the control formulation (PBS) which consisted of NaFlu dissolved in PBS solution. Each point represents the mean ± standard deviation of 3 to 4 biological replicates. (Appendix 7.3, 7.4, 7.5, 7.6, 7.7 and 7.10)..... 24

Fig 3.3 Cumulative transdermal permeation of NaFlu through mouse skin *in vitro* over 24 hours. All formulations contained 1.2 mg/mL NaFlu and are described in Table 1.3. Each point represents a mean ± standard deviation of 3 to 4 biological replicates. (Appendix 7.3, 7.6, 7.8, 7.9, 7.10, 7.11 and 7.12) 26

Fig 3.4 Pseudo-ternary phase diagram for a mixture of (a) medium chain glycerides (Capmul MCM/Crodamol GTCC, 1: 3, w/w), (b) medium chain glycerides Capmul MCM/Crodamol GTCC (1: 1) in combination with surfactant (BRIJ O10) and water. The monophasic ME region is indicated with grey shading with $A_{T(a)}$ = 15.4%; $A_{T(b)}$ = 33.2%. Specific formulations assessed for transdermal permeation ability are marked by red points and labelled with B, C, D, E and F.

A dilution line (indicated by dotted line) was used to demonstrate the maximum water ratio when mixed with certain ratio oil mixture and surfactant mixture. . 27

Fig 3.5 Time course of the *in vitro* transdermal permeation of NaFlu from MCM/GTCC/BRIJ based formulations over 24 hours. Each point represents a mean ± standard deviation of 3 to 4 replicates. ME formulations ME_B, ME_C, ME_D, ME_E and ME_F contained 24.5%, 17.5%, 14%, 10.5% and 7% (w/w) MCM_C8 respectively (Table 3.3). NaFlu was used as model drug with 1.2 mg/mL concentration applied to full thickness mouse skin. (Appendix 7.3, 7.13, 7.14, 7.15, 7.16 and 7.17)..... 28

Fig. 3.6 The relationship between the concentration of MCM in the ME formulation and the corresponding J_s of NaFlu (ng/cm^2/h) through full thickness mouse skin. Each point represents an individual sample replicate. All formulations contained NaFlu at 1.2 mg/mL. 29

Linear regression analysis was processed in Prism 6. The correlation trend is indicated by the blue line and the correlation coefficient is 0.137. (R^2 = 0.019, P-value = 0.555) 30

Fig 3.7 Pseudo-ternary phase diagrams for a mixture of MCM and EtOH (Capmul MCM: EtOH, 1:1, w/w) and surfactants BRIJ O10 (a), Kolliphor EL (b), Tween 20 (c), Tween 80 (d) in combination with water. The A_T is indicated with grey shading with $A_{T(a)}$ = 52.3%; $A_{T(b)}$ = 52.7%; $A_{T(c)}$ = 41.2%; $A_{T(d)}$ = 50.9%. Specific formulations ME_BJ, ME_CO, ME_T2 and ME_T8 assessed for transdermal permeation rate are indicated with G, H, I and J on phase diagrams, marked by red points. 31

Fig 3.8 Cumulative NaFlu transdermal delivery for MCM/EtOH based formulations within 24 hours. BRIJ O10 (ME_BJ), Kolliphor EL (ME_CO), Tween 20 (ME_T2) and Tween 80 (ME_T8) were incorporated with MCM/EtOH (1:1, w/w) respectively, each containing NaFlu 1.2mg/mL. Each point represents means ± standard deviation of 3 to 4 biological replicates. (Appendix 7.3, 7.18, 7.19, 7.20, 7.21 and 7.22)..... 33

Fig 4.1 Cumulative transdermal permeation of gentamicin through mouse skin over 24 h after the application of ME formulation containing gentamicin. Formulations consisted of ME systems containing MCM/EtOH (1: 1, w/w) and either BRIJ O10 (ME_BJ), Kolliphor EL (ME_CO) and Tween 80 (ME_T8)

surfactants which contained 10 mg/mL gentamicin that was spiked with 0.5 μCi of tritium labeled [^{3}H] gentamicin. Each point represents means ± standard deviation of 3 to 4 biological replicates. (Appendix 7.23, 7.24, 7.25 and 7.26) 41

LIST OF TABLES

Table 1.1 Transdermal drug delivery strategies 6

Table 1.2 Permeation rate (Flux) of pentazocine with various glycerol ester of fatty acids (GEFAs) (Furuishi et al., 2007) 9

Table 2.1 Mice grouping use for bio-distribution studies. 19

Table 2.2 Topical formulations used for bio-distribution studies. 19

Table 3.1 Formulation composition and corresponding transdermal permeation parameters of NaFlu (transdermal flux rate (J_s) and cumulative amount permeated (Q24h)) through full thickness mouse skin. All formulations contained 1.2 mg/mL NaFlu. 23

Table 3.2 Formulation composition and corresponding transdermal permeation parameters of NaFlu (J_s and Q_{24h}) through full thickness mouse skin. All formulations contained 1.2 mg/mL NaFlu. 25

Table 3.3 Formulation composition and corresponding transdermal permeation parameters of NaFlu (J_s and Q_{24h}) through full thickness mouse skin. All formulations contained 1.2 mg/mL NaFlu. 28

Table 3.4 Formulation composition and corresponding transdermal permeation parameters of NaFlu (J_s and Q_{24h}) through full thickness mouse skin. All formulations contained 1.2 mg/mL NaFlu. 32

Table 4.1 Permeation parameters of gentamicin (J_s and Q_{24h}) through full thickness mouse skin. All formulations contained 10 mg/mL gentamicin. 42

LIST OF ABBREVIATIONS

A_T ..... monophasic region
BJ ..... BRIJ O10
cm^2 ..... centimetre
CO ..... Kolliphor EL
DPM ..... disintegration per minute
EtOH ..... ethanol
FDA ..... Food and Drug Administration
Flux ..... permeation rate
GEFA ..... glycerol ester of fatty acid
GRAS ..... generally recognized as safe
GTCC ..... medium chain triglycerides
h ..... hour
HLB ..... hydrophile-lipophile balance
IPM ..... isopropyl myristate solution system
J_s ..... transdermal flux rate
kΩ ..... kiloohm
MCM ..... medium chain monoglycerides
ME ..... microemulsion
ME_BJ ..... ME formulations contains BRIJ O10
ME_CO ..... ME formulations contains Kolliphor EL
ME_T2 ..... ME formulations contains Tween 20
ME_T8 ..... ME formulations contains Tween 80
mg ..... milligrams
min ..... minute
mL ..... millilitre
mm ..... millimetre
mM ..... millimolar
NaFlu ..... sodium fluorescein
NaOH ..... sodium hydroxide
ng ..... nanogram

nm ····· nanometre

O/W ····· oil in water

P – value ····· probability value

PBS ····· phosphate buffered saline

Q_{24h} ····· cumulative amount permeated

R^2 ····· total variation

rpm ····· rounds per minute

SSTIs ····· skin and soft tissue infections

T2 ····· Tween 20

T8 ····· Tween 80

Tw/Sp or TS ····· a mixture of surfactants (Tween 80: Span 80, 3:2)

W/O ····· water in oil

w/w ····· weight per weight

µCi ····· microcurie

µg ····· microgram

µL ····· microliter

°C ····· degrees Celsius

1 INTRODUCTION

1.1 Introduction of the skin

1.1.1 Overview

Skin is the largest organ of human body that also provides a series of functions essential for survival. It accounts for up to 16% of body weight with a total surface area of 1.8 m^2. Skin provides physical protection from environmental challenges such as micro-organisms, ultraviolet radiation, toxic agents and mechanical insults but also functions by controlling the inward and outward passage of water, electrolytes and various substances. Since the out layer cells are continuously shed and replaced by inner layer cells moving up to the surface, this constant change contributes to the dynamic state of skin (Bensouilah and Buck, 2007).

1.1.2 The structure of the skin

The skin consists of three main layers (Fig 1.1): the epidermis, the dermis and subcutaneous tissue. The epidermis and dermis are considered as the key components of skin. The subcutaneous tissue is a layer of subcutaneous fat below them.

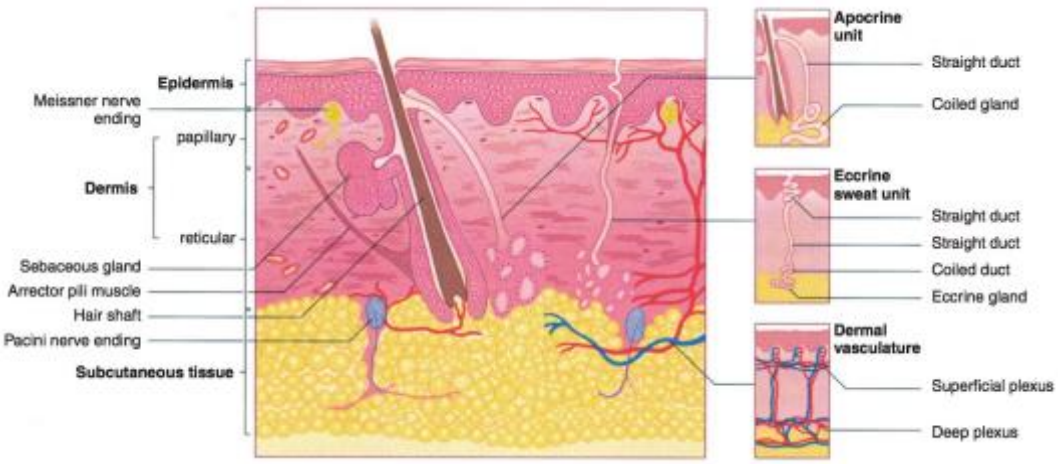

Fig 1.1 Cross-section of skin (James et al., 2016). Three layers compose the skin structure: the epidermis, the dermis and subcutaneous tissue.

1.1.2.1 The epidermis

The epidermis is the external layer composed of layers of keratinocytes but also containing melanocytes, Langerhans cells and Merkel cells. It acts as the physical and chemical barrier between the interior body and exterior environment. There are

four separate layers of the epidermis: Horny cell layer (stratum corneum), granular cell layers (stratum granulosum), squamouse cell layer (stratum spinosum) and basal cell layer (stratum germinativum). These four layers are formed by the various stages of keratinocyte maturation (James et al., 2016, Lever and Elder, 2005).

Basal Layer: The basal cell layer is the deepest layer of the epidermis. It lies close to the dermis and comprises mainly dividing and non-dividing keratinoctytes, which are attached to the basement membrane by hemidesmosomes. Keratinocytes move from this deeper layer to the surface and continually divide and differentiate. Below the basal cell layer are blood vessels in the dermis, which supply nutrients to facilitate this active growth of fresh skin cells. Basal cell will change their content and shape as they move away from this nutrient supply (Murphy, 1997).

Squamous Layer: Above the basal layer there is the squamous layer which comprises irregular shaped cells that are initially formed by reproduction and maturity of basal cells (Murphy, 1997). These cells are connected by intercellular bridges and desmosomes. Langerhans cells that possess dendritic and immunological activity are found mainly in this area (Chu, 2008).

Granular Layer: In the granular cell layer, cells display a flattened appearance, lose their nuclei and their cytoplasm appears granular. Keratin protein also accumulates in these cells (Chu, 2008).

Horny Layer: The outermost layer of the epidermis is the stratum corneum and is the final outcome of keratinocyte maturation. This layer is made up of hexagonal-shaped, non-viable cornified cells named corneocytes (Blank, 1953, Monash, 1958). Corneocytes are arranged in overlapping layers surrounded in stacked lipid bilayers that fill the extracellular space. This spatial arrangement produces a natural physical and waterproof character to the surface. Dead cells are continually sheded, from the skin surface which is balanced by the dividing cells moving up from the basal cell layer. In this layer, melanin is absorbed into the dividing skin cell to protect skin from ultraviolet light (Bensouilah and Buck, 2007).

1.1.2.2 The dermis

Below the epidermis is the dermis which ranges in thickness from 0.6 mm on the eyelids to 3 mm on the soles, back and palms. Two layers comprise the dermis. The

thin papillary layer has many ridges builds human beings individual fingerprints and comprises, thin loosely arranged collagen fibers whilst a thicker reticular layer extends from the base of the papillary layer to the subcutis tissue. Up to 70% of the dermis is made of collagen fibers which provide strength and toughness to skin. The remaining area is made up of elastin fibers, which give skin elasticity and flexibility, and proteoglycan which provides viscosity and hydration. Immune-competent mast cells and macrophages are also present within the dermis layer. Dermal vasculature, lymphatics, nervous cells and fibers, sweat glands, hair roots and small quantities of striated muscle are contained in the fibrous tissue of dermis and these structures contribute to for the various functions of the skin (Bensouilah and Buck, 2007).

1.1.2.3 Subcutaneous fat

The thickness of subcutaneous fat varies in different body regions. This fat layer is located in the deepest region of skin and helps reduce the harmful physical effects from the environment as well as acting as an energy resource (James et al., 2016).

1.1.3 Skin barrier function

The outmost layer of the epidermis is the stratum corneum which largely responsible skin barrier function. The stratum corneum was considered to be biologically inert before the mid-1970’s but in the past 30 years, the complicated biological and chemical properties of stratum corneum have been revealed.

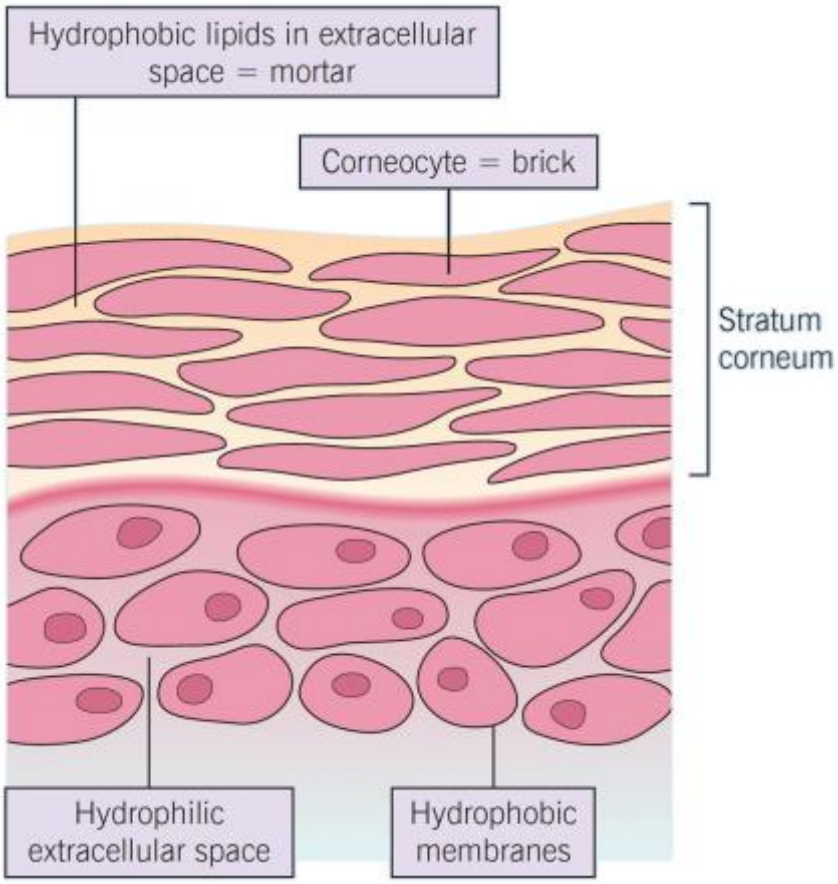

Fig 1.2 The "brick and mortar" pattern of stratum corneum. The corneocyte is protein-based and hydrophobic lipids are extracellularly sequestered in the stratum corneum (Prausnitz et al., 2012).

The structure of stratum corneum is commonly described with a 'brick and mortar' analogy (Fig 1.2). In this model, the corneocytes can be seen as complex proteinaceous bricks which are made of keratin fibers within an organized matrix. Depending on factors such as age, location and exposure to UV, the average thickness of each corneocyte is 1 micrometre. Generally, about 12 to 16 layers of corneocytes are contained in the stratum corneum (Prausnitz et al., 2012). Within the stratum corneum, corneocytes are embedded in a lamellar lipid bilayer enriched in ceramides, cholesterol, and free fatty acids that are released by epidermal organelles known as lamellar bodies (Elias and Menon, 1991). This lipid bilayer is considered as the 'mortar' in the brick and mortar model and has an important role maintaining the barrier property of skin. The hydrophobic layer of ceramide lipids adhering to the cornified cell envelope impede both the outward and inward movement of water producing a stable water balance (Prausnitz et al., 2012).

1.2 Topical Drug Delivery

Topical drug delivery is defined as the application of a drug containing formulation to the skin. It is used to treat cutaneous disorders or the cutaneous manifestations of a general disease with the intent of containing the pharmacological or other effect of the drug to the surface of the skin or within the skin layers.

1.2.1 Advantages and disadvantages

The main advantage of topical delivery is to bypass first pass metabolism. Additionally, it is convenient and easy to apply and avoids the risks and inconveniences of systemic delivery methods. Topical delivery can also be a more efficient vehicle by supplying a consistent and continuous level of drug input that avoids the large drug fluctuations produced by oral and intravenous delivery methods (Paudel et al., 2010, Kumar et al., 2011).

However, topical drug delivery may cause skin irritation, contact dermatitis or allergic reactions due to the drug and/or excipients present in the formulation. Additionally, the enzymatic activity present in epidermis can modify drug compounds reducing their activity. Furthermore, many drug compounds permeate the skin poorly therefore topical drug delivery is mainly used for drug compounds that require limited plasma concentration (Kumar et al., 2011).

1.2.2 Transdermal drug delivery

Topical drug application is used to produce effects at the site of application and doesn't produce high drug concentrations in the blood and other tissues. Transdermal drug delivery refers to the process where drug compounds penetrate through the upper layers of skin and into deeper tissue or even to sites away from the application area. Drugs delivered transdermally can pass into the systemic circulation at a constant concentration, avoiding hepatic first pass metabolism enabling the application of lower dosages and the use of drug compounds with short biological half-life (Gaikwad, 2013).

The primary pathway for the diffusion of drug compounds across skin is trans-epidermal absorption. The biggest barrier to this process is the stratum corneum. The most common mechanism for diffusion through the stratum corneum is via the intercellular lipoid route (Flynn and Stewart, 1988).

Eccrine and sebaceous glands are appendages that can offer a secondary permeation pathway known as the trans-follicular or shunt pathway. Since eccrine and sebaceous glands are present all over the body, these avenues are regarded as shunts which bypass the stratum corneum. However, these pathways have limitations for percutaneous absorption. The orifices of these glands are small and make up a negligible amount of skin surface area. Furthermore, molecules cannot diffuse inwardly against the glands output since they are profusely active and constantly being evacuated. The opening of the follicular pore provides a more useful pathway for percutaneous absorption. The envisioned mechanism of permeation is partitioning into sebum, followed by diffusion through the sebum to the depths of the epidermis. Subsequent systemic entry is via the vasculature located in the dermis (Flynn and Stewart, 1988).

1.2.3 Transdermal drug delivery methods

Several methodologies can be used for transdermal drug delivery. They can be divided into physical or chemical methodologies (Table 1.1). However, transdermal delivery strategies may involve combinations of the various methodologies.

Table 1.1 Transdermal drug delivery strategies

Physical methods	Chemical permeation enhancers
Electroporation	Solvents and organic acids
Iontophoresis	Polyols
Microneedles	Surfactants, fatty acids, fatty acids esters,
Needle-free and ballistic injections	Azone and its derivatives, amides,
Sonophoresis	sulfoxides and terpenes
Photomechanical wave	
Magnetophoresis	

1.2.3.1 Physical Methods:

Utilizing voltage gradients, electroporation and iontophoresis disrupt the SC to promote the permeation of large molecules like peptides through intact skin (Weaver et al., 1999). The local anesthetic compound lidocaine has been successfully delivered transdermally via iontophoresis (Sugar and Neumann, 1984). Some intravenous drugs are also available through iontophoresis (Turner et al., 1997).

However, these techniques require large machines, restricting their clinic availability (Huzil et al., 2011).

Drugs can be transdermally delivered through the use of microneedles and high-pressure needle-free injection. These methods facilitate transdermal drug delivery by bypassing the skin barrier through direct puncturing or abrasion of the SC (Burkoth et al., 1999). Additionally, ultrasonic and electromagnetic energy has been used for transdermal deliver via sonophoresis; and magnetophoresis respectively. Mechanical energy was utilized as photomechanical wave on the skin (Lee et al., 1999). However, these approaches are generally used as complementary methods and display limited transdermal delivery performance (Barry, 2001).

1.2.3.2 Chemical permeation enhancers:

Chemical permeation enhancers that reduce the barrier function of skin can also be used for transdermal drug delivery. There are 3 main groups of chemical permeation enhancers that are classified according to their mechanism of action. The 1st group of enhancers reduce skin barrier function by extracting the lipid layers of the SC, like solvents (e.g., ethanol) and organic acids (e.g., salicylic acid). The 2nd group of enhancers improve transdermal delivery by increasing the solubility of active compounds in the skin and include polyol compounds such as propylene glycol. The 3rd group enhancers like terpenes, surfactants, fatty acids, fatty acid esters, Azone and its derivatives, amides and sulfoxides alter the intercellular lipid. Intercellular lipid phase fluidity is able to improve and its resistance can be limited after applying surfactants (Cócera et al., 1999, Shokri et al., 2001, Honeywell-Nguyen and Bouwstra, 2003).

Chemical penetration enhancers acting within the skin should possess; low toxicity, low irritability and low allergenicity, rapid enhancement with activity and duration being both predictable and reproducible, no pharmacological activity within the body and should work unidirectional (i.e. therapeutic agents should be allowed into the body whilst preventing the loss of endogenous materials from the body) and should be cosmetically acceptable with an appropriate skin feel. Furthermore, skin barrier properties should return both rapidly and fully to normal when the penetration enhancers are removed (Huzil et al., 2011). Although some chemical enhancers possess a subset of the above attributes, currently no single enhancer possess all

these ideal properties. Chemical permeation enhancers were chosen to improve the topical drug applications in this study.

1.3 Medium chain monoglycerides (MCM) as transdermal drug delivery enhancers

1.3.1 Structures

MCM are fatty acid monoesters of glycerol. Due to the orientation of that molecule, two isomeric forms exist (Fig 1.3).

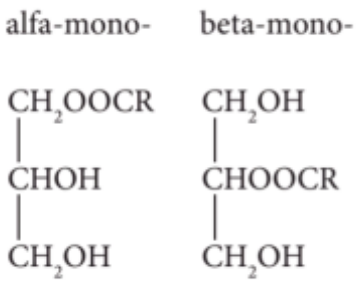

Fig 1.3 The chemical structure of MCM (Moonen and Bas, 2014). OCR is a saturated or an unsaturated hydrocarbon chain with 6 to 12 carbons in length.

1.3.2 Transdermal permeation enhancers

MCM can be formed by both industrial chemical and biological process. By diacylglycerol lipase, MCM are biochemically formed through the release of a fatty acid from diglycerides and can break down by monoglyceride lipase. Either animal or vegetable can be the commercial source, and may be synthetically made as well. Mono- and diglycerides are commonly added to food products in small quantities as emulsifiers and considered as GRAS compounds (Informatics, 1973). Commercial ‘MCM’ were used in the cosmetic production which are mixture of MCM, diglyceirdes and triglycerides before 1969. Then the distilled monoester (94-96%) were manufactured for food and cosmetic formulation purpose (Kabara, 1991). The use of glycerides on medical purpose is already commercially available on US market. For example, transdermal glyceryl trinitrate patch was used to treat stoke topically and approved by FDA (Paudel et al., 2010).

1.3.3 MCM as transdermal permeation enhancers

MCM have enhanced the transdermal permeation rate of numerous drug compounds. Glyceryl monocaprylate (C8) significantly improved the transdermal delivery rate of pentazocine compared with other permeation enhancers (i.e. isopropyl myristate solution alone, carboxylic acids, non-ionic surfactants, l-menthol, alcohols, glycol and urea) from isopropyl myristate solution system (IPM) (Furuishi et al., 2007). In this study, two derivatives of glyceryl monocaprylate (glyceryl diglycerides and glyceryl triglycerides) were proved have no permeation enhancement effect of pentazocine. It also investigated how fatty chain length derived from MCM affect the permeation rate of pentazocine (table 1.2). The flux reached the highest when glyceryl monocaproate (GEFA-C_6) was tested, indicating that the suitable carbon number of glycerol ester of fatty acids is around six. Comparing glyceryl monocaprylate (GRFA-C_8) and glyceryl monocaproate (GRFA-C_6), the former is suitable as a permeation enhancer because of its safety and odorless properties.

Table 1.2 Permeation rate (Flux) of pentazocine with various glycerol ester of fatty acids (GEFAs) (Furuishi et al., 2007)

Enhancer	Flux ($\mu g/cm^2/h$)
IPM alone	14.4 ± 0.8
GEFA-C_2	19.0 ± 3.4
GEFA-C_4	37.5 ± 6.4
GEFA-C_6	158.2 ± 12.5
GEFA-C_8	58.0 ±11.4
GEFA-C_{10}	52.6 ± 3.3
GEFA-C_{12}	27.2 ± 6.8
GEFA-C_{18}	9.7 ± 3.9

In further research, MCM significantly improved the transdermal delivery flux rate of hydrophilic drug (progesterone) and hydrophobic drug (adenoine) though porcine ear skin (Hosmer et al., 2009).

1.3.4 Antimicrobial properties of MCM

Medium chain fatty acids and their corresponding MCM present a broad spectrum of antibacterial properties in numerous studies. Early research found that glycerol monolaurate prohibited the group A, B, F, and G streptococci with 10 to 20 μg/mL concentrations (Schlievert et al., 1992). Glycerol monolaurate has also demonstrated antimicrobial activity against *Staphylococcus aureus* and *Streptococcus pyogenes* (Schlievert and Peterson, 2012). Furthermore, this study also demonstrated that glycerol monolaurate has the ability to inhibit *Haemophilus influenza* and *Staohylococcus aureus* in biofilm cultures, suggesting that glycerol monolaurate has the potential as a broad spectrum topical microbial agent. Monocaprin (10:0) has displayed rapid antimicrobial activity against *Chlamydia trachomatis* (Bergsson et al., 1998) and *Candida albicans* (Bergsson et al., 2001). Furthermore, monocaprin has been shown to reduce biofilm biomass on mucosal surface and medical equipment and devices (Thorgeirsdottir et al., 2006a).

Generally, MCM possess more potent antimicrobial activity than the corresponding fatty acid towards various Gram-positive species. Additionally, other antimicrobial compounds have displayed synergy with MCM. Glycerol monolaurate and lauric acid have displayed synergistic antibacterial/anti-biofilm activity when combined with the aminoglycoside antibiotics, gentamicin and streptomycin (Hess et al., 2014).

1.4 ME formulations as topical drug delivery vehicles

1.4.1 Formation and structure of MEs

MEs are defined as a single, optically isotropic structured solution of surfactant, oil and water is called a microemulsion (Danielsson and Lindman, 1981). MEs can be formed with a wide range of oil-surfactant-water compositions and can be either water-in-oil (W/O) or oil-in-water (O/W) with a characteristic droplet size of 150 nm or less (Kreilgaard, 2002). As it is difficult to predict ME formation based on the complex physical-chemical interactions between components, pseudo-ternary phase diagrams are commonly used to determine the specified oil-surfactant-water concentration ranges required for the formation of MEs (Chen et al., 2004, Saint Ruth et al., 1995, Aboofazeli and Lawrence, 1993, Kale and Allen, 1989, Rushforth et al., 1986).

A variety of structures and phases can be formed with an oil, surfactant and water mixture. Visual inspection can easily recognise many of these structures and phases from their physical appearance. Emulsions are non-transparent and the water and oil phases will eventually separate; lamellar structures and cubic phases have increased viscosity; crystalline phases can be discerned by polarised microscopy. (Kreilgaard, 2002) The interface in the MEs is continuously and spontaneously fluctuating. MEs are dynamic systems and are significantly affected by the composed components. Both the physio-chemical properties of the components and the ratio between the components can affect the structure of ME systems (Lam and Schechter, 1987). Monophasic ME are of consideration as potential drug delivery vehicle in this study since they are stable, can be easily prepared and have a high capacity for a wide range drug solubilisation, including lipophilic and hydrophilic compounds in the one formulation (Lawrence and Rees, 2000). Depending on the properties of the components, the structure of a ME, can range from being spherical droplets to coarse agglomerates (Santos et al., 2008).

1.4.2 ME formulation for topical drug delivery

MEs can satisfy all requirements for liquid drug delivery vehicles including thermodynamic stability (long shelf-life), easy production (zero interfacial tension and almost spontaneous formation), low viscosity with Newtonian behavior, and high solubilization capacity. MEs were chosen as ideal liquid vehicles for drug delivery since the small droplets have better ability to adhere to membranes and to transport bioactive molecules in a more controlled fashion. (Shakeel et al., 2008) MEs can be administered into the body orally, topically on the skin, or nasally, as an aerosol for direct entry into the lung (Kogan, 2006).

MEs have been studied in the last decades since their great potential in many applications. Significant efforts have obtained due to MEs' complicated phase behavior and fascinating microstructures in ME forming systems (Hellweg, 2002, Langevin, 1992, Schulman et al., 1959, Strey, 1994, Strey, 1996). In spite of these benefits, only few drug formulations are commercially available in the market. The dog shampoo "Allermyl®" produced by Virbac® in USA is a ME based application for dogs and cats. It is designed to clean and release the irritation condition in pets' skin (Virbac, 2011). Another ME based formulation "Solvium" containing Ibuprofen

were commercially used to topical treatment, which was produced by Chefaro (Akzo) (Verma and Hassan, 2013). However, the function of human skin provides a primary barrier to transdermal delivery (Kreilgaard, 2002).

1.5 The aim of this study

MCM (C6-12) are known transdermal penetration enhancers that have been used for the transdermal delivery of a range of compounds (Lopes et al., 2005, Lopes et al., 2009, Hosmer et al., 2009, Lopes et al., 2007). Furthermore, MCM display broad spectrum antimicrobial activity against a variety of human pathogens (Isaacs et al., 1995, Thorgeirsdottir et al., 2006b, Bunkova et al., 2011, Hyldgaard et al., 2012). This combination of activities displayed by MCM may be useful in the development of novel antimicrobial formulations for topical use. MEs are stable mixtures of oils, surfactants and water and are ideal for the development of topical formulations containing MCM and water-soluble drug compounds. Therefore, the broad aim of this project was to investigate the use of MCM as a transdermal permeation enhancer for water soluble compounds in ME formulations. The specific aims were:

1. To identify suitable surfactant/co-surfactant combinations that enable stable incorporation of MCM into ME formulations.
2. To examine the effect of surfactant/co-surfactant combinations on the transdermal permeation enhancing properties of MCM.
3. To develop and assess a topical ME formulation for the transdermal delivery of the topical antibiotic, gentamicin.

2 METHODS AND MATERIALS

2.1 Materials

2.1.1 Chemicals

Span 80-LQ-(SG) and Crodamol GTCC-LG-(SG) were supplied as a gift by CRODA, Singapore Pty Ltd. Tween 80-LQ-(SG) and BRIJ-O10-SS-(R13) were purchased from CRODA Australia. Tween 20, Tween 40 and Tween 60 were purchased from Sigma-Aldrich (USA). Kolliphor EL was a gift from BASF Australia. Gentamicin sulfate salt and 1, 2 - Decanediol (C8) were from SIGMA – ALDRICH. Capmul MCM (C8) (EP) and Captex 300 EP/NF were supplied as a gift from ABITEC Corporation. Gentamicin [3H(G)] sulfate was purchased from American Radiolabeled Chemicals, Inc. Fluorescein sodium salt was purchased from Fluka Analytical Sigma. Monocaprylin (C8) was obtained from NU-CHEK Prep (USA). Hydrogen peroxide (30%) and ethanol 100% undenatured (Ethyl Alcohol 100%) were supplied by Liem Supply and Chem-Supply. Solvable and Ultima Gold were purchased from PerkinElmer (USA). All other solvents and reagents were commercial products of analytical grade and were used without further purification. Milli-Q water (MilliPore, VIC) was used throughout.

2.1.2 Equipment

The Franz diffusion cells (9mm diameter, 5mL volume) and 6 place stirrers were manufactured by PermeaGear (USA) and the circulating water bath was manufactured by HAAKE (USA). Handheld LCR Meter U1733C was manufactured by Agilent (Australia). POLARstar Omega plate reader and Liquid Scintillation Analyzer were ordered from BMG LABTECH (Australia) and PerkinElmer (USA), respectively.

2.1.3 Animals

Mice: C57BL/6J mice aged 8-12 weeks. C57BL-6J mice were sourced from Australian BioResources, Moss Vale.

2.2 Construction of Pseudo-Ternary Phase Diagram

Pseudo-ternary phase diagrams were prepared according to the procedure described by (Li et al., 2005). Mixtures of oil and surfactant were prepared in 5 mL flat bottom

tube in the following ratios: 1: 9, 2: 8, 3: 7, 4: 6, 5: 5, 6: 4, 7: 3, 8: 2 and 9: 1. After equilibration for 10 min at room temperature, aliquots of the oil/surfactant mixtures were mixed with varying amounts of Milli-Q water (10% to 90% w/w). After shaking for 5 min, the solutions were allowed to equilibrate overnight. The solutions were characterised by visual observation and classified as either: (1) MEs which appeared as clear or translucent, single phase solutions or (2) unstable emulsions which appeared as cloudy solutions that phased-separated overtime or after centrifugation at 14000 x *g* for 5 min.

A Microsoft Excel spreadsheet named "Tri-plot v1.4.2" was used to prepare the triangular phase diagrams for particle shape and tri-variate date. Adobe Photoshop CS6 was used to describe variable phases and specific ME samples. The monophasic region (A_T) was the percentage of ME area in the total phase diagram area. In this article, the pixel amounts of ME area and total phase diagram area were counted by Adobe Photoshop CS6, which can be used to calculate the A_T.

2.3 Measuring transdermal permeation rate through hairless mice skin

2.3.1 Collection of skin tissue from mice

For transdermal permeation experiments conducted *in vitro*, murine skin tissue was collected from animals made available through a tissue sharing arrangement with different researchers at the University of Wollongong with approval from the University's Animal Ethics Committee (AE14/23). Mice that had been sacrificed via CO_2 exposure (within 30 min prior), had their backs shaved using electric hair clippers. The shaved skin area was then surgically excised, removed of all subcutaneous fat and tissue before being laid flat in a labelled snap lock bag and stored at -20 °C.

2.3.2 Mounting full thickness mice skin to Franz diffusion cells

The skin tissue was defrosted at 4 °C for 20 minutes, then allowed to heat to room temperature for 10 minutes. The skin was cut into small sections that completely covered the reception chamber (approximately 1.5 cm^2). The skin was placed onto the receptor chamber (epidermal side was up). The donor chamber was then placed on top of the skin and clamped in position (Fig 2.1). The reception chamber was filled with 5 mL of degassed phosphate buffered saline (PBS) pH 7.4 ensuring no air

bubbles were trapped under the skin. A stirrer bar was added to receptor chamber and the assembled diffusion cell was placed into the 6-place magnetic stirrer. The Franz cells were connected to a recirculating water bath to maintain the temperature at 35 °C.

2.3.3 Assessing the integrity of full thickness hairless mice skin

The integrity of mouse skin was assessed by measuring the electrical resistance across the skin when mounted in the Franz cell. 400 µl PBS was added in the donor chamber and allowed to be equilibrated for 5 minutes. Resistance was measured using a handheld LCR meter (Agilent U1733C) fitted with platinum wire electrodes, set at 100 Hz in parallel (PAR) mode. The electrodes were inserted into Franz cell as shown in Fig 2.1 taking care not to touch the skin. For intact skin, resistance was in the range of 6 to 15 kΩ/cm^2 (Novotny et al., 2009). Skin sections with resistance below this range were discarded.

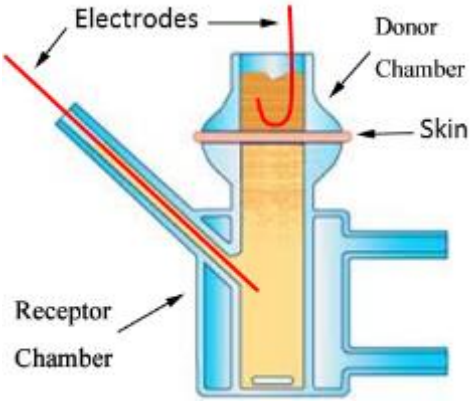

Fig 2.1 Location of the electrodes when measuring the resistance across skin mounted in Franz diffusion cells.

2.3.4 Measuring the transdermal permeation of sodium fluorescein

For formulations containing sodium fluorescein (NaFlu), a 200 µL aliquot was applied to the donor chamber at NaFlu concentration of 1.2 mg/mL. Aluminium foil was used to loosely cover the top of the receptor chamber and donor chamber to prevent excessive evaporation. A 100 µL or 200 µL aliquot of receptor fluid was collected at specified time points during the course of the experiment (24 h) and was immediately mixed with an equal volume of 10 mM NaOH. To maintain constant sink conditions, the receptor chamber fluid was maintained at 5 mL by adding an

equal volume of degassed PBS to replace the aliquot that was withdrawn. For the duration of the experiment, the Franz cell apparatus and collected samples were protected from light. The fluorescence intensity of each sample was measured using a POLARstar Omega plate reader (BMG LABTECH). Plate reader setting are given below. The optimal gain setting was set automatically on samples from the last time point. The amount of NaFlu present in each sample was determined from a standard curve of NaFlu (0 μg/ml to 20 μg/mL) which was included on each plate. The standard curve was linear in the range of 0 to 1.3 μg/mL. 100 μl samples were added in the same plate.

The transdermal flux rate (J_s) was the ratio of the change in cumulative drug amount per mouse skin area against the different of collect time point (ng/cm^2/h):

$$\text{Flux rate} = \frac{\Delta m}{S \cdot \Delta t}$$

$\Delta m =$ The different of cumulative drug amount (ng)

$\Delta t =$ The change in diffusion time (h)

$S =$ The area of mouse skin (0.64 cm^2)

The cumulative amount permeated (Q_{24h}) through full thickness mouse skin was the total amount of drug accumulated in the reception chamber after 24 hours divided by the mouse skin area (ng/cm^2).

$$The\ cumulative\ amount\ permeated = \frac{m}{S}$$

m = The drug amount collected after 24 hours (ng)

S = The area of mouse skin (0.64 cm^2)

Details of the protocol:

Emission: 520	Excitation: 485-12
Orbital Averaging: ON	Diameter: 4 mm
Top optic	Position delay: 0.1
Measurement start time: 0.0	Number of flashes per well: 10
Replicates Number: 2	Unit: nmL

Start concentration: 2,000,000	Factor: 0.5
Start Volume: 200	Factor: 1
Shaking Model: Orbital	Shaking Frequency: 500 rpm

2.3.5 Measuring the transdermal permeation of gentamicin

For formulations containing tritium labelled gentamicin, 20 µl aliquot was applied to the donor chamber at gentamicin concentration. Each contains 10 mg/mL gentamicin that was spiked with 0.5 µCi of tritium labelled gentamicin. Aluminium foil was used to loosely cover the top of the receptor chamber and donor chamber to prevent excessive evaporation. A 200 µl aliquot of receptor fluid was collected at specified time points during the course of the experiment (24 h). To maintain constant sink conditions, the receptor chamber fluid was maintained at 5 mL by adding an equal volume of degassed PBS to replace the aliquot that was withdrawn.

After all samples in the receptor chamber were collected, 400 µl PBS was used to wash the skin while in the donate chamber of Franz cell, repeat this and store the wash in tubes. Donor chambers and clamps were taken off after the wash. Skin tissue was removed and placed in glass scintillation vials containing 3mL Solvable. The vials were incubated in the incubator at 50 °C for 4 hours or more, until the tissue is completely dissolved. Remain buffer from receptor chamber was removed into a radioactivity waste bottle. 10 µl original radiolabelled formulation was diluted with 90 µl PBS and filled in glass scintillation vials. 100 µl of sample from the wash buffer, the skin solution and the receptor chamber were mixed with 5 mL Ultima Gold scintillation cocktail (PerkinElmer), respectively, adding in each scintillation vial. All vials were numbered on lids and mixed thoroughly by inversion. Remain buffer from receptor chamber was removed into a radioactivity waste bottle.

All the bottles were placed in the Liquid Scintillation Analyzer (PerkinElmer Tri-Cab 2810TR) and run protocol (Flag 2: JMC dpm) to measure the level of radioactivity. The protocol (Flag 2: JMC dpm) has the following parameters:

Assay Type: Direct DPM	Radionuclide Name: Direct DPM 3H-UG
Normalization Std DPM: 259700	Quench Set: 3H-UG Quench
Indicator: tSIE/AEC	External Std Terminator: 0.5 2s%

Static Controller was selected.

After measurement finish, the value of raw DPM was obtained (recorded in the DPM1 row). The value of raw DPM times the dilution factor to get the corrected DPM. The absolute amounts of accumulated gentamicin through the skin area present in the samples (ng/cm^2) was able to be calculated by the following equation:

$$Absolute\ amount\ of\ accumulated\ drug\ through\ skin = \frac{m(st)}{S} \cdot \frac{DPM(s)}{DPM(st)}$$

$DPM(s) =$ The raw DPM of sample times dilution factor (50)

$DPM(st) =$ The raw DPM of 100% dose sample times dilution factor (4)

$m(st) =$ The amount of drug applied in the 100% dose sample (200 µg)

$S =$ The area of mouse skin (0.64 cm^2)

2.4 Bio-distribution studies in mice

To permit the topical application of formulations directly to skin, the rear flank region of mice was shaved using electric animal clippers. This was performed two days prior to the commencement of the experiment.

Mice were divided into 3 treatment groups of 20 individuals as shown in table 2.1. Mice were topically treated with either PBS containing 10 mg/mL gentamicin, one dose of the ME containing 10 mg/mL or 2 identical doses of the ME containing 10 mg/mL (See Table 2.2). All formulations were spiked with 1 µCi of tritium labelled gentamicin (American Radiochemicals, St. Louis USA). To topically apply the radiolabeled formulations, each mouse was anaesthetised using isoflurane and 20 µl of the specified formulation was pipetted onto the shaved area skin. To avoid mice ingesting the formulation applied to their flanks, animals were fitted with an Elizabethan collar (Kent Scientific, Torrington, USA) while anaesthetised. After treatment, mice were caged individually for the duration of the experiment (maximum 48 hours) to prevent inter-animal grooming. These cages were also free of nesting material and PVC enrichment tubes for this period.

At specified time points post treatment (Table 2.1), 4 mice from each group were sacrificed using CO_2, dissected and blood/tissues collected for analysis. Blood/tissues were stored frozen at -20°C until processed. Tissues collected post mortem included skin (site of application and a distant site) and muscle (underneath the site of skin

collected), blood and major clearance organs such as spleen, liver, lungs, kidney. To determine if lymphatic circulation is influencing bio-distribution post topical drug delivery (King et al., 2003), the major lymph nodes (lumbar, axillary and brachial) were also collected. To demonstrate mice weren't ingesting the topically applied formulations, small intestine tissue was also collected and assessed.

Table 2.1 Mice grouping use for bio-distribution studies.

Group \ Time Points (h)	3	6	12	24	48	Total
PBS Group	n=4	n=4	n=4	n=4	n=4	20
ME Group	n=4	n=4	n=4	n=4	n=4	20
MEx2 Group	n=4	n=4	n=4	n=4	n=4	20
Overall Total						60

Table 2.2 Topical formulations used for bio-distribution studies.

Formulation	Ingredients	Concentration	Dose Applied
PBS Group	Phosphate buffered saline	100%	6.67 mg/kg
	Gentamicin	10 mg/mL	
ME Group	Capmul MCM C8	10% w/w	6.67 mg/kg
	Ethanol	10% w/w	
	Tween 80	20% w/w	
	Water	60% w/w	
	Gentamicin	10 mg/mL	
MEx2 Group	Capmul MCM C8	10% w/w	13.34 mg/kg
	Ethanol	10% w/w	
	Tween 80	20% w/w	
	Water	60% w/w	
	Gentamicin	10 mg/mL	

For each organ and blood collected from the mice, 1 mL Solvable (Pekin Elmer) was added. The mixture was incubated at 50°C overnight. After which taking 100 µl from the mixture and add 5 mL Ultima Gold scintillation cocktail (PerkinElmer) in the scintillation vial, 0.2 mL of 30% H_2O_2 was added. All vials were measured by Liquid Scintillation Analyzer (PerkinElmer Tri-Cab 2810TR) and run protocol (Flag 2: JMC

dpm) to measure the level of radioactivity. The tissue uptakes were calculated as the percentage of the accumulated gentamicin per gram of tissue (mg/g or mg/mL).

2.5 Statistical analysis and software

Original data was initially recorded and calculated in Microsoft Excel. Statistical analyses and comparison figures were generated by Prism 6. One-way ANOVA (and nonparametric) was used to analyze *in vitro* permeation test. Two-way ANOVA was used to analyze *in vivo* bio-distribution test.

3 DEVELOPING ME FORMULATIONS CONTAINING MEDIUM CHAIN GLYCERIDES FOR TRANSDERMAL DELIVERY

3.1 Introduction

Medium chain (C6~C12) chain fatty acids, mono-, di-, and tri-glycerides have been used in emulsion formulations as absorption enhancers for a variety of drug compounds (Constantinides et al., 1994). Furthermore, MCM have also been shown to act as transdermal permeation enhancers (Cornwell et al., 1998, Furuishi et al., 2007). Previous research using the biocompatible components; medium chain triglycerides (Crodamol GTCC), medium chain monoglycerides (Capmul MCM C8), surfactants polysorbate 80 (Tween 80) and sorbitan mono-oleate (Span 80) and water indicated that ME can be formed with specific ratios of these substances (Watnasirichaikul et al., 2000). Recently, a ME formulation from this system was used to facilitate the transdermal delivery of proteins (Russell-Jones and Himes, 2011, Himes et al., 2011).

3.1.1 Characterization of a biocompatible ME system containing medium chain glycerides

To investigate the transdermal permeation enhancing properties of these ME formulations, a representative pseudo-ternary phase diagram of the same system containing Capmul MCM C8: Crodamol GTCC (1:3, w/w), as the oil phase, Tween80: Span80) (3:2, w/w, as the surfactant phase and water was constructed and is shown in Fig 3.1. The ME formulation identified in a previous study (Watnasirichaikul et al., 2000) and used in the following experiments (76% MCM: GTCC (1:3) and 14% Tween80: Span80 (3:2), 10% water) is indicated at position A (Fig 3.1).

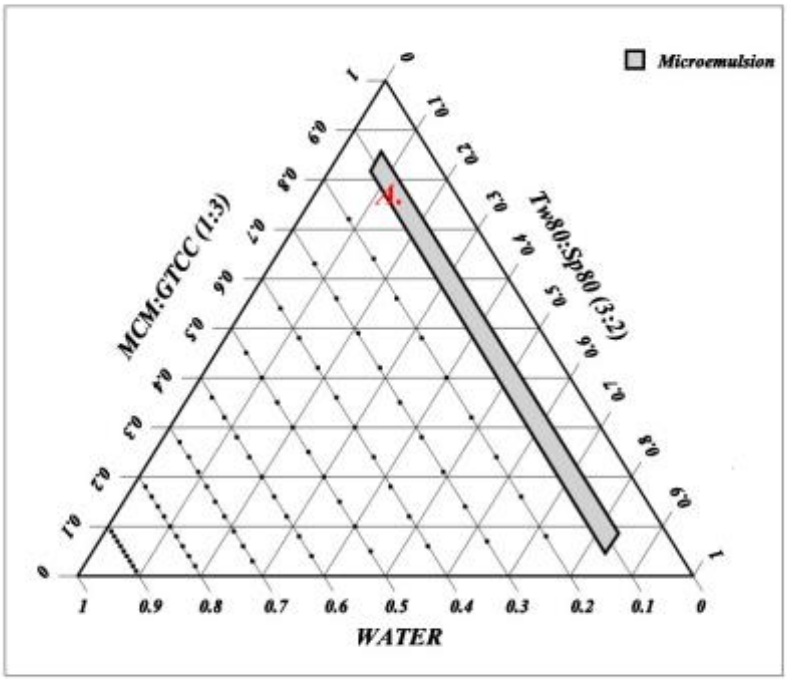

Fig. 3.1 Pseudo-ternary phase diagram for a mixture of medium chain glycerides (Capmul MCM C8: Crodamol GTCC, 1:3), a mixture of surfactants (Tween 80: Span 80, 3:2) and water. ME formulations were defined as being a single phase that was visually transparent, stable upon ON incubation at room temperature after vigorous vortexing (Garti et al., 2000). The ME phase boundary is indicated with grey shading. Specific formulations assessed for transdermal permeation are indicated with A, marked by the red point. The monophasic ME region is indicated with A_T = 8.8%.

3.1.2 *In vitro* transdermal delivery skin permeation assay

In a previous study, the formulation ME_A (Fig 3.1 and Table 3.1) effectively delivered peptides and proteins through the stratum corneum into living epidermal tissue (Himes et al., 2011). To characterize the potential of this formulation for the transdermal delivery of small molecules, sodium fluorescein (NaFlu) was used as a model small compound. Additionally, the influence of individual formulation components on transdermal flux was also assessed (Table 3.1). All formulations contained 1.2 mg/mL of NaFlu and transdermal permeation of this compound

through full thickness mouse skin from the various formulations was determined using Franz diffusion cells.

Table 3.1 Formulation composition and corresponding transdermal permeation parameters of NaFlu (transdermal flux rate (J_s) and cumulative amount permeated (Q24h)) through full thickness mouse skin. All formulations contained 1.2 mg/mL NaFlu.

Formulation	MCM (% w/w)	GTCC (% w/w)	Surfactant (% w/w)	Water (% w/w)	J_s (ng/cm^2/h)	Q_{24h} (ng/cm^2)
ME_A	19	57	14	10	270±47	3,990±255
MCM*	19	-	-	81	754±185	12,368±1,852
Tw/Sp*	-	-	14	86	11±2	166±27
MCM_TS	19	-	14	67	599±126	10,274±2,130
GTCC_TS	-	57	14	29	15±11	148±46
PBS	-	-	-	-	25±10	475±172

* indicates the formulation was a visible emulsion; Abbreviations: Tw/Sp – a mixture of surfactants (Tween 80: Span 80, 3:2)

The transdermal permeation profile of NaFlu from each of the formulations applied to full thickness mouse skin is shown in Fig 3.2. From these graphs, the maximum J_s of NaFlu produced by each formulation and the total amount of NaFlu accumulated in the receptor chamber (Q_{24h}) was determined and is presented in Table 3.1. Application of NaFlu dissolved in PBS produced a J_s of 25 ng/cm^2/h indicating that NaFlu does not readily pass through mouse skin. The J_s produced by formulation ME_A (270 ng/cm^2/h) was significantly higher (over 10-fold) when compared to the J_s produced by PBS ($p < 0.05$). This indicates ME_A can act as a transdermal permeation enhancer for small compounds.

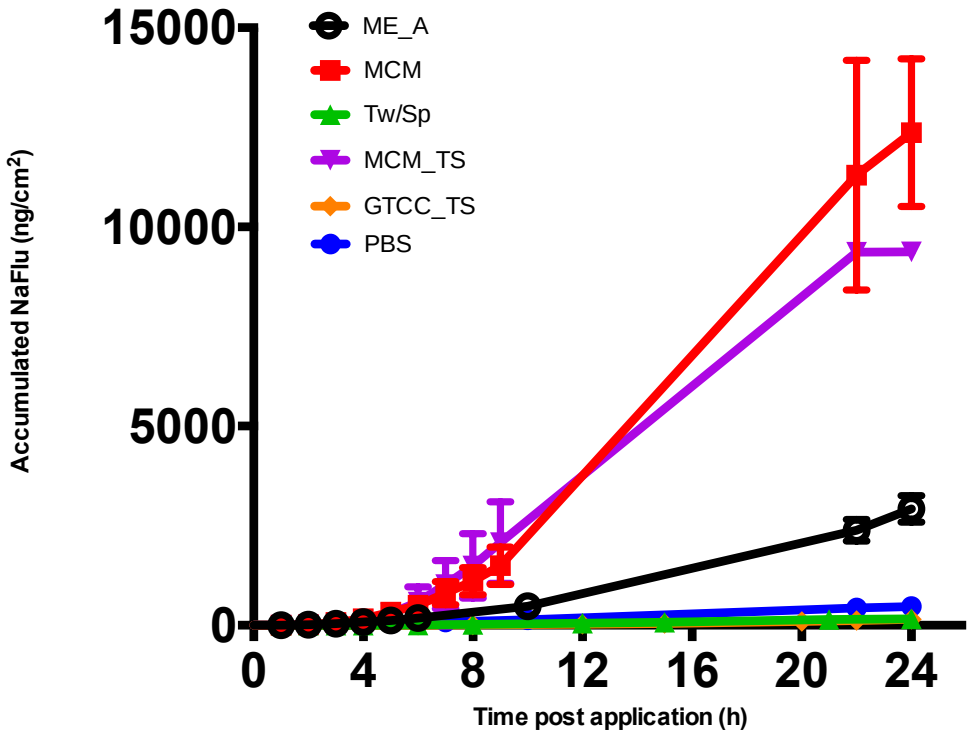

Fig 3.2 Cumulative transdermal permeation of NaFlu through mouse skin *in vitro* over 24 h. All formulations contained 1.2 mg/mL NaFlu and are described in Table 3.1 except for the control formulation (PBS) which consisted of NaFlu dissolved in PBS solution. Each point represents the mean ± standard deviation of 3 to 4 biological replicates. (Appendix 7.3, 7.4, 7.5, 7.6, 7.7 and 7.10)

To determine how the individual components in formulation ME_A influenced the transdermal permeation of NaFlu, formulations containing these individual components were also examined. The application of NaFlu dissolved in either diluted surfactant (Tween 80: Span 80 (3:2, w/w)) or GTCC and surfactant mixture (GTCC_TS) to mouse skin resulted in low J_s of 11 ng/cm^2/h and 15 ng/cm^2/h, respectively. Taken together, this indicates these components do not affect the transdermal permeation of NaFlu through mouse skin. By contrast, the J_s produced by formulation MCM_TS (599 ng/cm^2/h) and MCM alone (754 ng/cm^2/h) was significantly higher (over 25 and 30-fold, respectively) when compare to the J_s produced by PBS ($p<0.05$). This indicates MCM can act as transdermal permeation enhancer for small compounds. Furthermore, as there was no significant difference between flux rates for MCM_TS and MCM alone ($p>0.05$), this indicates the

surfactant blend (Tween 80: Span 80 (3:2, w/w)) does not influence the transdermal permeation enhancing properties of MCM.

3.2 Influence of surfactant type on the transdermal permeation enhancing properties of MCM

Surfactants are required to form stable ME formulations that are suitable for topical applications. Therefore, to determine how different surfactants influence the transdermal permeation enhancing properties of MCM, several surfactants were mixed with/without MCM (Table 3.3) and these formulations were assessed for transdermal permeation using NaFlu (Fig 3.3).

Table 3.2 Formulation composition and corresponding transdermal permeation parameters of NaFlu (J_s and Q_{24h}) through full thickness mouse skin. All formulations contained 1.2 mg/mL NaFlu.

Formulation	MCM (% w/w)	GTCC (% w/w)	Surfactant (% w/w)	Water (% w/w)	J_s (ng/cm^2/h)	Q_{24h} (ng/cm^2)
MCM_CO	19	0	14	67	180±122	1,427±523
MCM_BJ	19	0	14	67	991±52	17,850±1336
CO	0	0	14	86	94±46	1,507±879
BJ	0	0	14	86	140±90	1,162±875
PBS					25±10	475±172

Abbreviations: CO - Kolliphor EL, BJ - BRIJ O10

The transdermal permeation profile of NaFlu from each of the formulations applied to full thickness mouse skin is shown in Fig 3.3. From these graphs, the J_s produced and Q_{24h} were determined and are shown in Table 3.3. The J_s produced by application of CO (94 ng/cm^2/h) and BJ (140 ng/cm^2/h) were higher than the J_s produced by PBS (25 ng/cm^2/h) ($p<0.05$). However, these surfactants had contrasting effects on the transdermal permeation enhancing properties of MCM. The J_s produced by formulation MCM_BJ (991 ng/cm^2/h) was significantly higher when compared to the J_s produced by formulation MCM alone (754 ng/cm^2/h), suggesting a possible synergistic interaction between these compounds. In contrast, the J_s produced by MCM_CO (180 ng/cm^2/h) was significantly lower ($p<0.05$) when compared to the J_s produced by MCM alone, indicating a possible antagonistic interaction between the MCM and Kolliphor EL. As the J_s produced by MCM_BJ

was significantly ($p<0.05$) higher than the J_s produced by MCM_TS and the J_s of MCM_TS was significantly ($p<0.05$) higher than the J_s produced by MCM_CO, this suggests the enhancing effect of the different surfactants on the rate of NaFlu transdermal permeation mediated by MCM was found to be: BRIJ O10 > Tween80/Span80 (1:3, w/w) > Kolliphor EL.

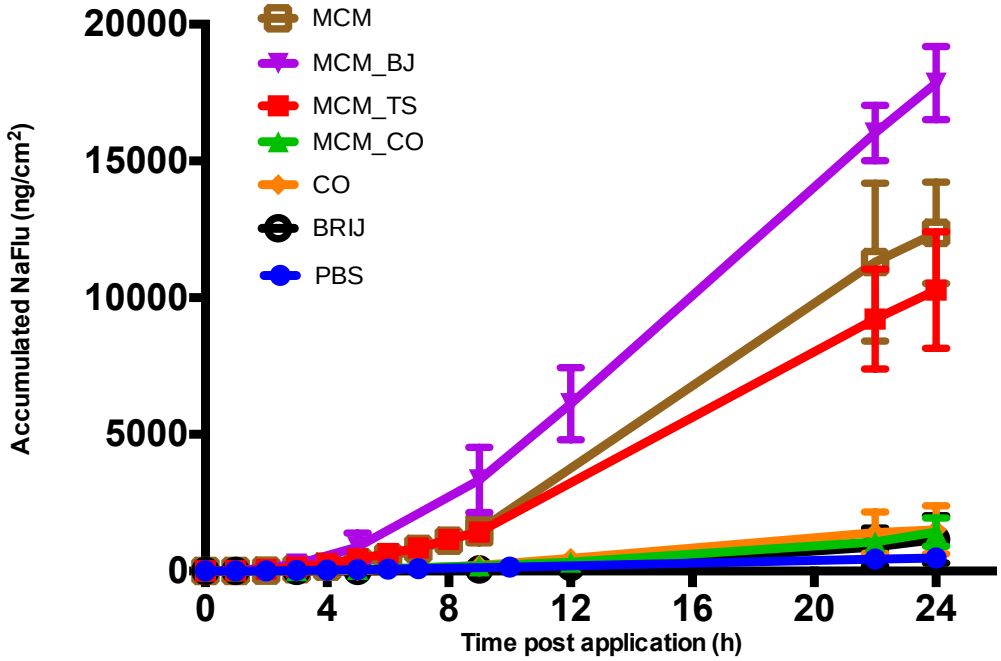

Fig 3.3 Cumulative transdermal permeation of NaFlu through mouse skin *in vitro* over 24 hours. All formulations contained 1.2 mg/mL NaFlu and are described in Table 1.3. Each point represents a mean ± standard deviation of 3 to 4 biological replicates. (Appendix 7.3, 7.6, 7.8, 7.9, 7.10, 7.11 and 7.12)

The J_s chosen from the application of MCM was between time point 9 h and 22 h and from the application of MCM_BJ was between time point 12 h to 22h, which are both long time gap. This is because during the *in vitro* experiments of NaFlu, the sample collection time points were not unified, therefore J_s may different with the actual flux rate and need to be tested in a smaller time interval in the future experiment. In the next set of experiments of gentamicin, those collection time points were consistently chosen.

3.3 The effect of MCM concentration on transdermal permeation

Based on the data presented in Table 3.2, it is evident that the combination of MCM and the BRIJ O10 surfactant produced the highest transdermal permeation activity.

To determine how BRIJ O10 can be incorporated into the ME system containing the MCM: GTCC oil phase, pseudo-ternary phase diagrams were constructed using the water titration method at ambient temperature (25 °C) and are shown in Fig 3.4.

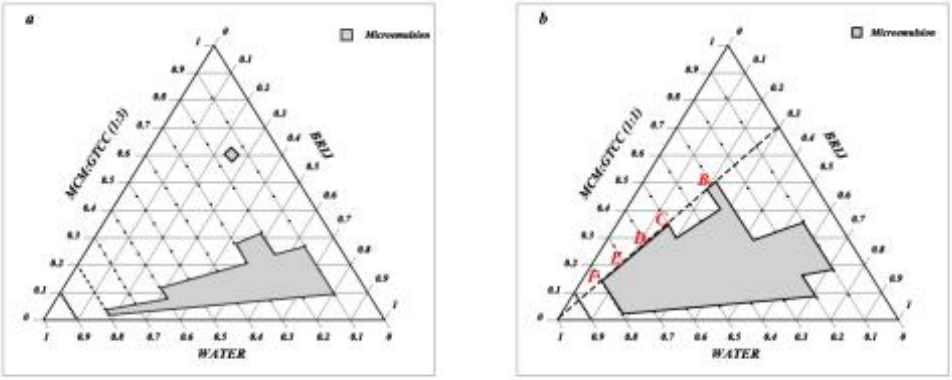

Fig 3.4 Pseudo-ternary phase diagram for a mixture of (a) medium chain glycerides (Capmul MCM/Crodamol GTCC, 1: 3, w/w), (b) medium chain glycerides Capmul MCM/Crodamol GTCC (1: 1) in combination with surfactant (BRIJ O10) and water. The monophasic ME region is indicated with grey shading with $A_{T(a)}$ = 15.4%; $A_{T(b)}$ = 33.2%. Specific formulations assessed for transdermal permeation ability are marked by red points and labelled with B, C, D, E and F. A dilution line (indicated by dotted line) was used to demonstrate the maximum water ratio when mixed with certain ratio oil mixture and surfactant mixture.

It is evident that the A_T in Fig. 3.4(a) is less than that in Fig. 3.4(b). This suggests that increasing the ratio of MCM in oil phase from 25% to 50% in the MCM/GTCC/BRIJ system produces a larger A_T.

From the pseudo-ternary phase diagram in Figure 3.4 (b), a dilution line within the single-phase region at the lowest possible concentration of surfactant was identified. A selection of formulations from along this dilution line (labelled ME_C, ME_, MG_D, MG_E and MG_F; see Fig 3.4 and Table 3.3) were used to investigate how MCM concentration influences the transdermal permeation properties of MCM/GTCC based formulations.

Table 3.3 Formulation composition and corresponding transdermal permeation parameters of NaFlu (J_s and Q_{24h}) through full thickness mouse skin. All formulations contained 1.2 mg/mL NaFlu.

Formulation	MCM (% w/w)	GTCC (% w/w)	Surfactant[a] (% w/w)	Water (% w/w)	J_s (ng/cm^2/h)	Q_{24h} (ng/cm^2)
ME_B	24.5	24.5	21	30	570±284	8,489±1029
ME_C	17.5	17.5	15	50	716±179	7,369±1436
ME_D	14	14	12	60	324±217	5,300±3161
ME_E	10.5	10.5	9	70	254±225	3,119±2289
ME_F	7	7	6	80	1,021±396	10,583±4324
PBS	-	-	-	-	25±10	475±172

[a] The surfactant used in all formulations was BRIJ O10.

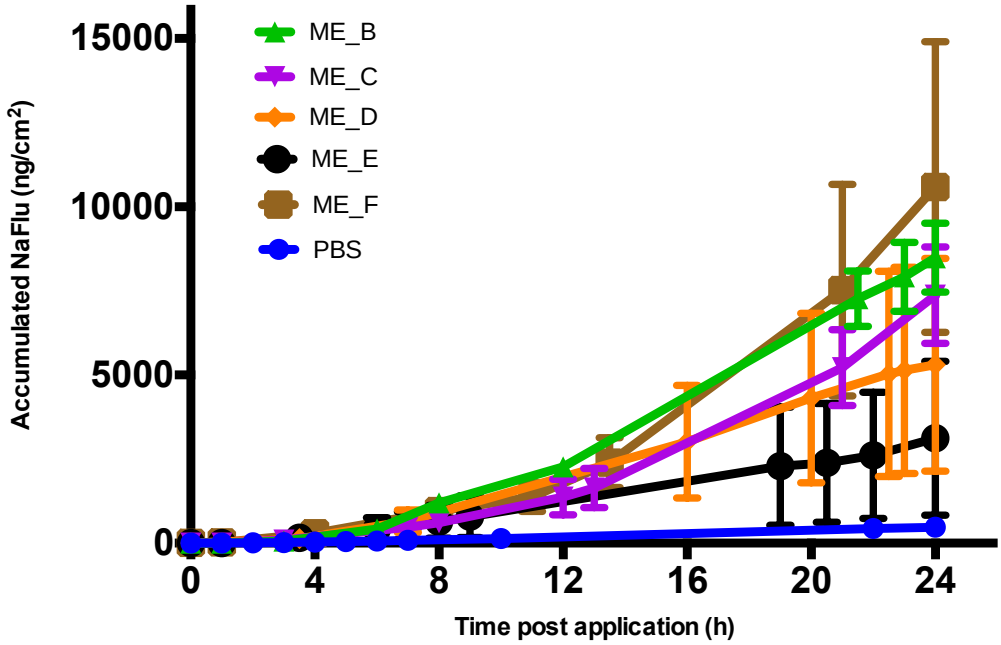

Fig 3.5 Time course of the *in vitro* transdermal permeation of NaFlu from MCM/GTCC/BRIJ based formulations over 24 hours. Each point represents a mean ± standard deviation of 3 to 4 replicates. ME formulations ME_B, ME_C, ME_D, ME_E and ME_F contained 24.5%, 17.5%, 14%, 10.5% and 7% (w/w) MCM_C8 respectively (Table 3.3). NaFlu was used as model drug with 1.2 mg/mL concentration applied to full thickness mouse skin. (Appendix 7.3, 7.13, 7.14, 7.15, 7.16 and 7.17)

The transdermal permeation profile of NaFlu from each of the formulations applied to full thickness mouse skin is shown in Fig 3.5. From these graphs, the maximum J_s of NaFlu produced by each formulation and the accumulated amount of NaFlu in the receptor chamber (Q_{24h}) was determined (Table 3.3). Application of NaFlu dissolved in PBS was used as a negative control group.

All formulations were able to significantly enhance the transdermal permeation of NaFlu through mouse skin ($p<0.05$) although the flux rates produced by the different formulations were variable. Formulation ME_F (7% w/w MCM) produced the highest J_s (1,021 ng/cm^2/h) which was over 40-fold greater than the J_s produced by NaFlu in PBS. Formulation ME_E produced the lowest J_s (254 ng/cm^2/h). The J_s produced by ME_E was the lowest and was significantly lower comparing to the J_s produced by ME_F ($p<0.05$). While these data demonstrate the ability of all formulations to enhance the transdermal permeation of NaFlu, there was no correlation between the MCM concentration and the transdermal flux produced by the formulation (Fig 3.6).

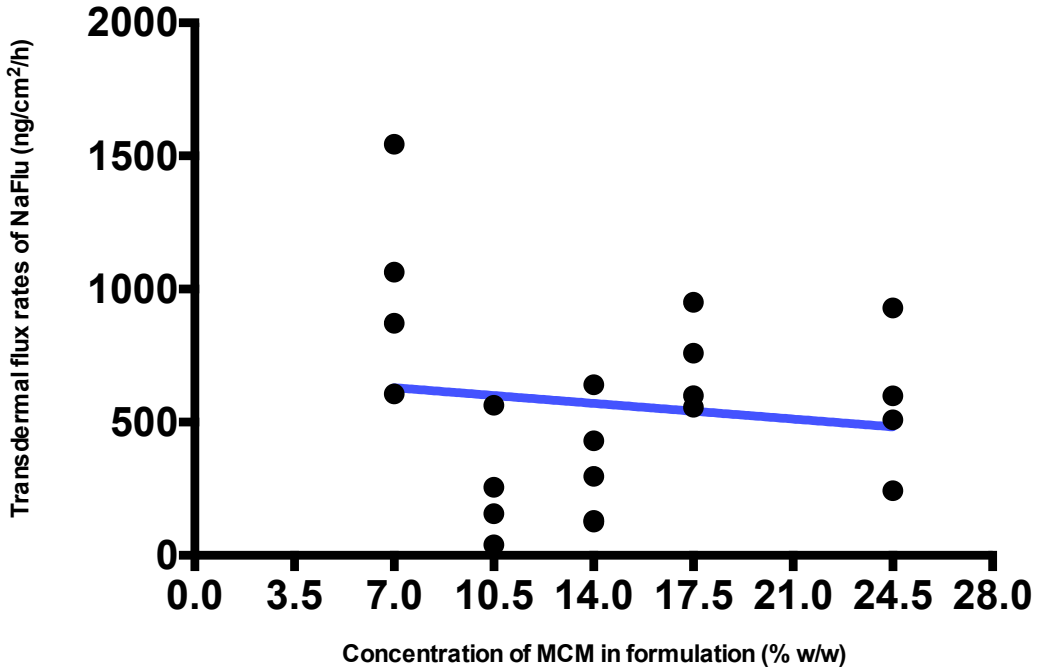

Fig. 3.6 The relationship between the concentration of MCM in the ME formulation and the corresponding J_s of NaFlu (ng/cm^2/h) through full thickness mouse skin. Each point represents an individual sample replicate. All formulations contained NaFlu at 1.2 mg/mL.

Linear regression analysis was processed in Prism 6. The correlation trend is indicated by the blue line and the correlation coefficient is 0.137. (R^2 = 0.019, P-value = 0.555)

3.4 Characterizing the influence of ethanol as a co-surfactant on the ME systems containing MCM

In previous studies, the co-surfactants such as a short- or medium-chain alcohols are used to reduce the interfacial tension of ME formulations. While alcohols may potentially cause skin irritation and dehydration, ethanol is considered safe for topical formulations where the contact time on skin is short (Morgan et al., 1998). Therefore, to characterize the influence of ethanol on MEs systems containing MCM, pseudo-ternary phase diagrams were constructed using different amounts of Capmul MCM C8: ethanol (1:1, w/w) as the oil phase, surfactants (either BRIJ O10, Kolliphor EL, Tween 20 and Tween 80) and water (Fig 3.8). Comparing the A_T value of single phase areas between these systems that utilised different surfactants indicated there were only slight differences with Kolliphor EL (52.7%) > BRIJ O10 (52.3%) > Tween 80 (50.9%) > Tween 20 (41.2%).

Comparing the A_T values of Fig 3.7 (a) to Fig 3.4 (b), it is evident that the monophasic areas in MCM/EtOH based phase diagrams are larger than that of MCM/GTCC based phase diagram, indicating the ethanol increased the A_T when incorporated with Capmul MCM and BRIJ O10.

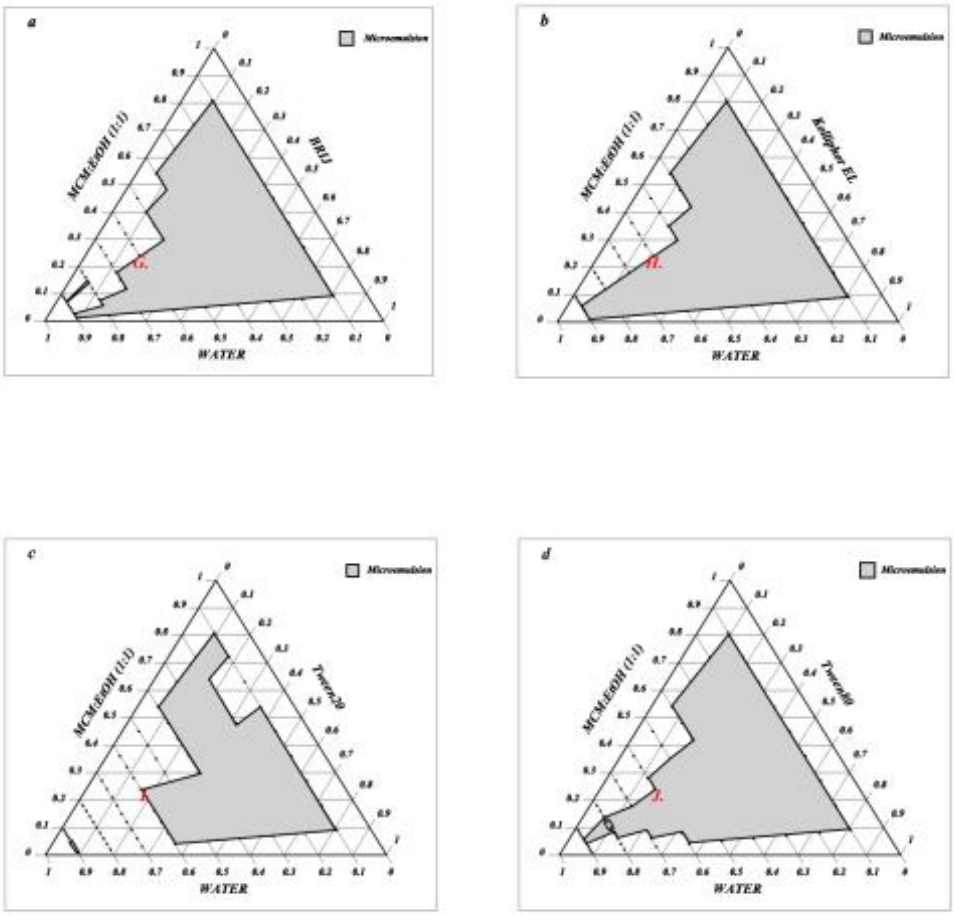

Fig 3.7 Pseudo-ternary phase diagrams for a mixture of MCM and EtOH (Capmul MCM: EtOH, 1:1, w/w) and surfactants BRIJ O10 (a), Kolliphor EL (b), Tween 20 (c), Tween 80 (d) in combination with water. The $\mathbf{A_T}$ is indicated with grey shading with $A_{T(a)}$ = 52.3%; $A_{T(b)}$ = 52.7%; $A_{T(c)}$ = 41.2%; $A_{T(d)}$ = 50.9%. Specific formulations ME_BJ, ME_CO, ME_T2 and ME_T8 assessed for transdermal permeation rate are indicated with G, H, I and J on phase diagrams, marked by red points.

Formulation ME_BJ (G), ME_CO (H), ME_T2 (I) and ME_T8 (J) (Table 3.4) were selected by identifying the lowest surfactant concentration present in the ME region that was common to all four surfactant systems examined. The transdermal permeation profile of NaFlu from each of the formulations applied to full thickness mouse skin is shown in Fig 3.8. The maximum J_s of NaFlu produced by each

formulation and the total amount of NaFlu accumulated in the receptor chamber was determined and is presented in Table 3.4. The J_s produced by formulation ME_BJ was significantly higher (over 33-fold) when compared to the J_s produced by PBS ($p<0.05$). The J_s produced by formulation ME_T8 was significantly higher (over 29-fold) when compared to the J_s produced by PBS ($p<0.05$). The J_s produced by formulation ME_CO was significantly higher (over 10-fold) when compared to the J_s produced by PBS ($p<0.05$). The J_s produced by formulation ME_T2 was significantly higher (over 4-fold) when compared to the J_s produced by PBS ($p<0.05$). All above indicate that ME_BJ ME_T8, ME_CO and ME_T2 can act as a transdermal permeation enhancer for small compounds.

Table 3.4 Formulation composition and corresponding transdermal permeation parameters of NaFlu (J_s and Q_{24h}) through full thickness mouse skin. All formulations contained 1.2 mg/mL NaFlu.

Formulation[a]	MCM (% w/w)	EtOH (% w/w)	Surfactant (% w/w)	Water (% w/w)	J_s (ng/cm^2/h)	Q_{24h} (ng/cm^2)
ME_BJ	10	10	20	60	846±159	13,523±2,135
ME_CO	10	10	20	60	269±187	4,109±1,974
ME_T2	10	10	20	60	123±28	1,817±303
ME_T8	10	10	20	60	732±169	13,225±1,154
MCM/EtOH	10	10	0	80	2,267±926	33,111±11451
PBS	-	-	-	-	25±10	475±172

[a] Surfactants used in the following formulations: BRIJ O10 (ME_BJ); Kolliphor EL (ME_CO); Tween 20 (ME_T2); Tween80 (ME_T8). No surfactant was used in MCM/EtOH. Abbreviations used; MCM - Monoglycerides, EtOH - ethanol.

There is no significant difference between the J_s produced by ME_BJ (846 ng/cm^2/h) and ME_T8 (732 ng/cm^2/h) ($p > 0.05$). Meanwhile, there is no significant difference between the J_s produced by ME_CO (269 ng/cm^2/h) and ME_T2 (123 ng/cm^2/h) ($p > 0.05$). However, the J_s produced by both application of ME_BJ and ME_T8 were significantly higher when compared to the J_s produced by both application of ME_CO and ME_T2, respectively ($p<0.05$). The application of NaFlu dissolved in MCM/EtOH produced the highest J_s of 2267 ng/cm^2/h comparing to all other

formulations (P<0.05) indicating the MCM/EtOH mixture promotes the transdermal permeation for small compounds.

Comparing the transdermal permeation properties of MCM/EtOH and MCM alone (Table 3.1), the J_s produced by formulation MCM/EtOH (2267 ng/cm^2/h) was significantly higher (3-fold) than the J_s produced by MCM (754 ng/cm^2/h) ($p < 0.05$). Since the concentration of MCM/EtOH (20%) is quite close to the concentration of MCM (19%), this suggests there may be a possible synergistic interaction between MCM and ethanol which increases the transdermal permeation performance of formulations that contain both substances. Besides, the J_s produced by ME_BJ was the highest (846 ng/cm^2/h) comparing to other MCM/EtOH based ME formulations. This result is quite similar to the performance of BRIJ O10 containing formulation in MCM/GTCC based formulations (Table 3.2).

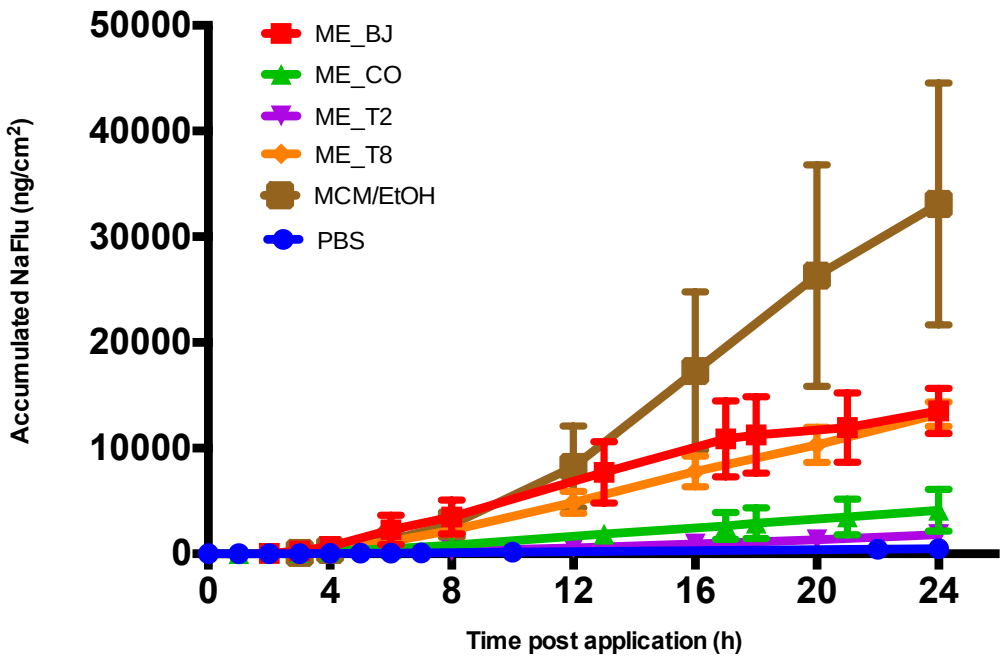

Fig 3.8 Cumulative NaFlu transdermal delivery for MCM/EtOH based formulations within 24 hours. BRIJ O10 (ME_BJ), Kolliphor EL (ME_CO), Tween 20 (ME_T2) and Tween 80 (ME_T8) were incorporated with MCM/EtOH (1:1, w/w) respectively, each containing NaFlu 1.2mg/mL. Each point represents means ± standard deviation of 3 to 4 biological replicates. (Appendix 7.3, 7.18, 7.19, 7.20, 7.21 and 7.22)

Taken together, these data suggest that the combination of MCM/EtOH significantly enhanced the formulation transdermal delivery property for small compounds.

Moreover, surfactant BRIJ O10 and Tween80 performed better permeation enhancer property than other surfactants along the MCM/EtOH based systems.

3.5 Discussion

To initially characterise the ME formulation used by Himes et al. (2011) and Russell-Jones and Himes (2011) for the transdermal delivery of protein, a pseudo-ternary phase diagram was constructed using the same components (i.e. a 3:1 mixture of medium chain triglycerides (Crodamol GTCC) and MCM (Capmul MCM C8), a 3:2 mixture of polysorbate 80 (Tween 80) and sorbitan mono-oleate (Span80) surfactants and water). Comparing this phase diagram (Fig 3.1) with a similar one constructed previously by Watnasirichaikul et al. (2000), MEs were formed under similar conditions (where oil/surfactant ratio is between 10:90 and 90:10 with water ≤ 10% w/w). The maximum percentage of water solubilized in the system was found to be 10% w/w, which is lower than 14% w/w in the study by Watnasirichaikul et al. (2000). However, if smaller increments of water were used for the titration, a more accurate phase diagram would be produced allowing for a better comparison between the two-phase diagrams.

For transdermal permeation studies, NaFlu was used as a model, small hydrophilic compound as it can be readily quantified using fluorescence spectroscopy. This model compound is commonly used in transdermal permeation studies (Santos et al., 2008, Valenta and Schultz, 2004). In this study, formulation ME_A (Himes et al. (2011) promoted the transdermal delivery of NaFlu through full thickness mouse skin at a flux rate of 270 ng/cm^2/h, which was over 10-fold higher when compared to NaFlu in PBS (25 ng/cm^2/h). This indicates that formulation ME_A has the potential to be used as a transdermal permeation enhancing formulation for small compounds.

To further characterise this formulation, individual components of the ME_A formulation were examined alone or in combination to evaluate how they influenced the transdermal permeation flux rate of NaFlu. While GTCC and the surfactant blend had no effect on the transdermal permeation of NaFlu when used alone, MCM significantly increased (over 30-fold) the J_s of NaFlu (754 ng/cm^2/h) when compared to the J_s produced by NaFlu in PBS indicating MCM acts as the permeation enhancer in formulation ME_A. In this study, a core role of the *in vitro* transdermal

experiment is to determine the ME formulation with relative high J_s value. However, when GTCC and the surfactant blend were mixed with MCM in the ME_A formulation, the J_s was significantly lower ($p < 0.05$) when compared to the J_s produced by MCM alone. Taken together, these experiments indicate that presence of GTCC in the formulation decreased the transdermal permeation enhancing properties of MCM.

It should be noted that the J_s chosen from the application of MCM was between time point 9 h and 22 h and from the application of MCM_BJ was between time point 12 h to 22h, which are both long time gap (Fig 3.3). This is because during the *in vitro* experiments of NaFlu, the sample collection time points were not unified, therefore J_s may different with the actual flux rate and need to be tested in a smaller time interval in the future experiment. In the next set of experiments of gentamicin, those collection time points were consistently chosen.

In this study, the influence of different surfactants on the transdermal permeation enhancing properties of MCM were investigated. The inclusion of surfactants in the topical formulations can enhance transdermal permeation via partially extracting extracellular lamellar lipids from the stratum corneum (Albanesi et al., 2005). Additionally, surfactants may also increase the fluidity of the intercellular lipid phase permitting increased diffusion of small molecules (Huzil et al., 2011). Furthermore, as many chemical permeation enhancers act by increasing the partition of active compounds in the stratum corneum, a titration of drug concentrations should be the subject of future studies to determine how this influences the transdermal flux rates for various compounds (Barry, 1983).

The transdermal permeation profiles of surfactant test alone (Tween 80: Span 80 (3:2, w/w), BRIJ O10 and Kolliphor EL) were all significantly lower ($p < 0.05$) in comparison with that produced by ME_A application. In comparison with the transdermal permeation profile of PBS application (25 ng/cm^2/h), the application of BJ (140 ng/cm^2/h) and CO (94 ng/cm^2/h) were slightly higher ($p < 0.05$) while the application of Tw/Sp (11 ng/cm^2/h) was slightly lower ($p < 0.05$). These results show that either BRIJ O10, Kolliphor EL or Tw/Sp could only slightly influence the transdermal permeation rate when applying individually. However, when the surfactants were individually mixed with MCM and assessed for transdermal

permeation, the NaFlu J_s produced by the MCM_BJ formulation (991 ng/cm^2/h) was significantly higher ($p < 0.05$) when compared to that produced by MCM alone (754 ng/cm^2/h), while the J_s of NaFlu produced by the MCM_CO formulation (180 ng/cm^2/h) was significantly lower ($p < 0.05$). The J_s of NaFlu produced by MCM_TS (599 ng/cm^2/h) similar to that produced by MCM alone. Taken together, these data indicate different surfactants can have varying effects on the transdermal permeation enhancing activity of MCM and suggest BRIJ O10 may act synergistically with MCM, Kolliphor EL may act antagonistically and the Tween 80: Span 80 (3:2, w/w) blend has no effect. The different behaviours of BRIJ O10, Tween 80: Span 80 (3:2, w/w) and Kolliphor EL may be the result of distinct interactions with the stratum corneum. Savić et al. (2009) assessed the colloidal structures and *in vitro* permeation performance of topical vehicles contain two model drugs (diclofenac sodium and caffeine) incorporated with three different lipophilic excipients (GTCC, decyl oleate and isopropyl myristate). The results suggested that the colloidal structures of topical delivery vehicles may affect the diffusion through the vehicles and influence their permeation performance. Formulations used to produce pseudo-ternary phase diagrams can be further characterized by measuring their electrical conductivity and rheological properties (Podlogar et al., 2005, Kreilgaard et al., 2000). Conductivity can be used to identify inversion points where the formulations transition from oil in water to water in oil emulsion. Furthermore, viscosity and conductivity are known to sharply increase when emulsion droplets cluster at the percolation threshold (i.e. in a bicontinuous ME) (Promod Kumar; Mittal, 1999, Gradzielski and Hoffman, 1999, Podlogar et al., 2004).

To further evaluate, it is necessary to characterize those vehicles with polarization micrographs, conductivity measure and rheological test. Now that stable, transdermal permeation enhancing formulations have been identified in this study, specific formulations should be examined in more detail in future studies to characterize the physical properties (such as the size and morphology of particles) of the formulations. Furthermore, the solubility of various hydrophilic and hydrophobic compounds should be assessed and a titration of different drug concentrations in formulations should be assessed to determine how these properties influence transdermal permeation kinetics.

As can be seen in the pseudo-ternary phase diagram of the original MCM/GTCC/Tween 80: Span 80 (3:2, w/w) system used by Himes et al. (2011), the range of suitable component concentrations that can be utilized for the production of single phase, stable, biocompatible ME formulations is reflected by the A_T zone (see Fig 3.1). Systems with greater A_T zones, as determined in pseudo-ternary phase diagrams have a larger range of stable ME formulations that can be selected for their biocompatibility and drug solubilizing properties. Different surfactants and co-surfactants can influence the interfacial forces in emulsions, a selection of surfactants/co-surfactants were assessed for their effect on ME formation. The non-ionic surfactant BRIJ O10 has been used successfully in ME systems previously (Kogan, 2006), therefore a new pseudo-ternary phase diagram consisting of MCM/GTCC (1:3, w/w), BRIJ O10 and water was constructed in Fig 3.4 (a). The use of this surfactant produced a larger A_T (26.5%) when compared to the ME_A which contained the Tween 80: Span 80 (3:2, w/w) surfactant blend (A_T=12.5%). In research conducted by Prajapati et al. (2012), it was determined that ME regions can be expanded by increasing the concentration of MCM in the oil phase of mixture systems. Therefore, a mixture system of MCM: GTCC (1:1, w/w), BRIJ O10 and water was characterized through the construction of a new phase diagram (Fig 3.4(b)) and compared to the MCM/GTCC (1:3, w/w), BRIJ O10 and water system (Fig 3.4 (a)). Increasing the concentration of MCM in these systems did produce an increased monophasic area. The alternative of MCM content may influence ME system converting gel region (bicontinuous structures) into W/O or O/W systems (Kreilgaard, 2002). Later research concluded that MCM composed with GTCC at 1:1 ratio effectively reduced the gel region, thus ME region was expanded and the particle size was decreased (Prajapati et al., 2012). This suggested that the MCM act as the co-surfactant with surfactant BRIJ O10 as it has an intermediate hydrophile-lipophile balance (HLB) value. To further validate, the particle size of MCM/GTCC/BRIJ system should be measured.

A complete dilution line within the ME region was identified in the phase diagram of the MCM: GTCC (1:1, w/w) /BRIJ system (Fig 3.4 (b)) and specific formulations along this line were used to evaluate the effect of MCM concentration on transdermal permeation rate. When these ME formulations were assessed for transdermal permeation using NaFlu, no correlation (R^2 = 0.019) between MCM concentration

and J_s was observed (Fig 3.6). The immiscible water and oil phase composed with the interfacial surfactant film can form distinct internal structure in the ME regions (Kreilgaard, 2002). This internal structure is significantly affected by the compounds formed, and the ratio between those compounds. In the dilution system of present study, the content change of MCM and other composition may alter the ME structures between oil-in-water structures, water-in-oil structures or bicontinuous structures. A variety studies has confirmed that the transdermal drug delivery of micro-emulsion is dependent not only on the its composition, but also on the internal structures (Kreilgaard et al., 2000, Podlogar et al., 2005). Therefore, the change of ME internal structure caused by the composition content alternative would be a reason that produces irregular J_s between each formulation. To further evaluate, using the conductivity measurement and rheological methods would be help to characterize the ME phase inversion phenomena (Podlogar et al., 2004).

In ME systems, short chain alcohols such as EtOH can act as a co-surfactant and further decrease the interfacial tension to produce larger areas of A_T (Santos et al., 2008). Therefore, EtOH was mixed with MCM in the ratio of 1: 1 (w/w) in the oil phase and pseudo-ternary phase diagrams were generated using water and a selection of different surfactants. A large A_T (52.3%) was obtained in Fig 3.7 (a) comparing to the A_T (33.2%) of Fig 3.4 (b), indicating that EtOH incorporated with MCM/BRIJ eliminated the gel region then particle size has been reduced and ME region was expanded (Prajapati et al., 2012). It is suggested that EtOH is acting as co-surfactant with surfactant BRIJ O10 as it has an intermediate HLB value. The particle size in this system may be worthwhile to measure in further studies.

EtOH facilitates transdermal drug delivery as a solvent type enhancer (Barry, 1991). In the study of Morimoto et al. (1993), EtOH (40%) composed with 1-menthol exhibited synergistic transdermal permeation enhancement of morphine hydrochloride (2,467 $\mu g/cm^2$) when compared with EtOH applied alone (73 $\mu g/cm^2$). Significant permeation enhancement effect of ketotifen fumarate was also observed when EtOH incorporated with isopropyl myristate system (Nakamura et al., 1996). In this study, MCM/EtOH mixture significantly increased the J_s of NaFlu in relative to MCM alone. Thus, we demonstrated that EtOH enhanced the transdermal permeation properties of MCM, for the first time. For the future studies, assessing different

concentrations of MCM and EtOH combinations would facilitate the development of more effective delivery formulations.

To evaluate the effect of variable surfactants, different surfactants were combined with MCM-EtOH and corresponding transdermal permeation parameters were presented (Table 3.4). Permeation data presented the NaFlu J_s produced by the MCM-EtOH combinations was significantly higher when compared to the rest MCM/EtOH based formulations ($p < 0.05$). The NaFlu J_s produced by ME_T8 (732 ng/cm^2/h) similar ($p > 0.05$) to that produced by ME_BJ (846 ng/cm^2/h), which were significantly higher ($p < 0.05$) than the NaFlu J_s produced by both ME_CO (269 ng/cm^2/h) and ME_T2 (123 ng/cm^2/h). Additional, the NaFlu J_s produced by ME_CO was significantly higher ($p < 0.05$) than that produced by MCM_T2. Taken together, these data present different surfactant can have distinct influences on the transdermal permeation enhancing activity of MCM-EtOH combinations and suggest surfactant BRIJ O10, Kolliphor EL, Tween 20 and Tween 80 may act antagonistically with MCM-EtOH combinations. The different performance of ME_BJ, ME_CO, ME_T8 and ME_T2 may be the result of distinct interactions with the stratum corneum. It has been mentioned that colloidal structures of topical delivery formulations may influence the diffusion through the formulations and affect their permeation profile (Savić et al., 2009). Thus, it is necessary to further evaluate those formulations with polarization micrographs, conductivity measure and rheological test. Furthermore, to observe similar trend exist or not, other drug compounds would be tested.

As the ME_BJ and ME_T8 formulations were found to be the most potent transdermal permeation enhancers, these formulations were further investigated for the transdermal delivery of the topical antibiotic, gentamicin.

4 DEVELOPMENT OF TOPICAL ME FORMULATIONS CONTAINING GENTAMICIN

4.1 Introduction

Skin and soft tissue infections (SSTIs) are the most common bacterial infections in humans and represent a large burden on global healthcare systems. SSTIs can be superficial, uncomplicated infections (including impetigo, erysipelas and cellulitis) or may be more severe, complicated infections involving deeper tissues which can require significant surgical intervention (including infected ulcers, major abscesses and necrotizing fasciitis). Additionally, recent evidence suggests that bacteria associated with many SSTIs (such as cutaneous abscesses and chronic wound ulcers) are present as highly persistent biofilm communities that are notoriously difficult to treat effectively due to the impermeable nature of these bacterial communities (James et al., 2008).

Topical treatment of SSTIs represents the most direct approach for the delivery of antimicrobials to local sites of infection. Traditionally, topical antimicrobials are formulated as ointments/creams for direct application or are incorporated into wound dressings allowing controlled release at the wound surface. As traditional topical formulations display limited skin penetration of active antimicrobial compounds, topical treatment of SSTIs often produces incomplete bacterial eradication leading to increased rates of bacterial resistance (Lipsky and Hoey, 2009). Therefore, the development of more efficient and effective delivery mechanisms of topical antibiotic therapy for SSTIs is needed.

In a recent study by Hess et al. (2014), gentamicin was shown to act synergistically with glycerol monolaurate to eliminate detectable viable biofilm bacteria. Similarly, glycerol monocaprylate has also demonstrated synergistic anti-biofilm activity in combination with gentamicin against *S. aureus* biofilms (Proctor, 2015b). Therefore, this part of the study focused on the development of topical ME formulations containing MCM C8 and gentamicin.

4.2 Identification of suitable ME systems for gentamicin incorporation

To optimise ME formulations containing gentamicin, solubility testing was conducted to ensure gentamicin was soluble at suitable concentrations in various ME systems. Gentamicin solubility was assessed in the MCM: GTCC (1: 1)/BRIJ

O10/water ME system shown in Fig 3.4. Gentamicin was not soluble at 10mg/mL in any of the specific formulations (ME_B to ME_F) along the minimum surfactant dilution line identified in Fig 3.4. Gentamicin was soluble in the MCM: EtOH (1: 1)/Surfactant/water ME systems (Fig 3.7) at 10 mg/mL.

4.3 Transdermal permeation kinetics of gentamicin from ME formulations

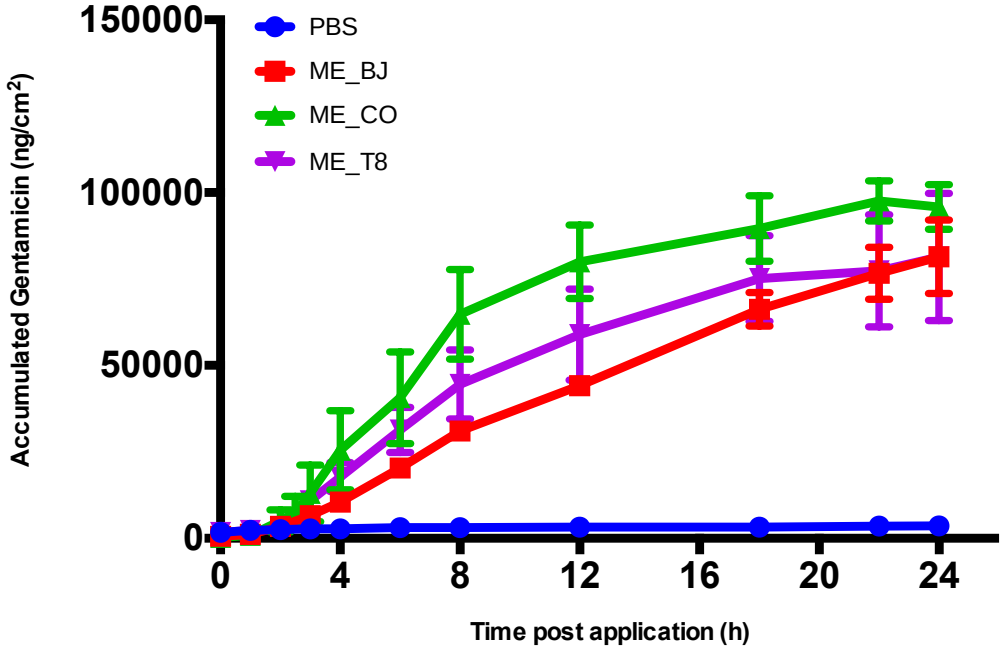

Fig 4.1 Cumulative transdermal permeation of gentamicin through mouse skin over 24 h after the application of ME formulation containing gentamicin. Formulations consisted of ME systems containing MCM/EtOH (1: 1, w/w) and either BRIJ O10 (ME_BJ), Kolliphor EL (ME_CO) and Tween 80 (ME_T8) surfactants which contained 10 mg/mL gentamicin that was spiked with 0.5 µCi of tritium labeled [^{3}H] gentamicin. Each point represents means ± standard deviation of 3 to 4 biological replicates. (Appendix 7.23, 7.24, 7.25 and 7.26)

ME formulations identified to be compatible with gentamicin (ME_BJ, ME_CO and ME_T8) were characterized for transdermal permeation. The composition of the formulations is shown in Table 4.1. All formulations contained 10 mg/mL of gentamicin and were spiked with 0.5 µCi of tritium labeled [^{3}H] gentamicin to enable monitoring of transdermal permeation through mouse skin mounted in Franz diffusion cells. The transdermal permeation profile of gentamicin produced by these formulations is shown in Fig 4.1. From these graphs, the J_s and accumulated amount

of gentamicin in the receptor chamber after 24-hour application (Q_{24h}) were determined and presented in Table 4.1.

Application of gentamicin dissolved in PBS produced a low J_s of 525 ng/cm^2/h indicating that gentamicin does not readily pass through full thickness mouse skin (Fig 4.1). By comparison to PBS, all ME formulations significantly enhanced the transdermal permeation of gentamicin through mouse skin ($p<0.05$). The J_s produced by formulations ME_CO (7,633 ng/cm^2/h) and ME_T8 (6,948 ng/cm^2/h) were similar ($p>0.05$) while the J_s produced by formulations ME_T8 (6,948 ng/cm^2/h) and ME_BJ (5,350 ng/cm^2/h) were similar ($p>0.5$). The J_s produced by application of ME_CO was significantly higher (over 1.4-fold) than the J_s produced by application of ME_BJ ($p<0.05$).

Table 4.1 Permeation parameters of gentamicin (J_s and Q_{24h}) through full thickness mouse skin. All formulations contained 10 mg/mL gentamicin.

Formulation[a]	MCM (% w/w)	EtOH (% w/w)	Surfactant (% w/w)	Water (% w/w)	J_s (ng/cm^2/h)	Q_{24h} (ng/cm^2)
ME_BJ	10	10	20	60	5,350±251	81,464±10,701
ME_CO	10	10	20	60	7,633±957	95,833±6,506
ME_T8	10	10	20	60	6,948±1,960	81,378±18,375
PBS	-	-	-	-	525±250	3,575±585

4.4 Bio-distribution of gentamicin after topical application of a ME formulation

Although formulation ME_CO presented higher J_s and Q_{24h} values, the MCM/EtOH/Kolliphor EL system was found to display limited stability when used to solubilise gentamicin. Therefore, the more stable, ME_T8 gentamicin formulation which effectively enhanced the transdermal permeation of this compound through full thickness mouse skin (see Fig 4.1), was further assessed in *in vivo* studies to determine the bio-distribution of gentamicin after topical application of the formulation to mice. In this study, gentamicin was dissolved in the ME formulation ME_T8 (Table 3.4), at 10 mg/mL gentamicin which was spiked with 0.5 µCi of tritium labeled [^{3}H] gentamicin and topically applied on the shaved dorsal skin of mice. For the single dose (ME), the formulation was applied as a 10 µl aliquot on the right side of the dorsal region while the double dose (MEx2) was applied as two

separated 10 µl aliquots, one on each dorsal side. The negative control formulation consisted of 10 mg/mL gentamicin dissolved in PBS which was spiked with 0.5 µCi of tritium labelled [^{3}H] gentamicin that was topically applied on the right side of the shaved dorsal skin of mice. The gentamicin amount in the mice tissue skin, muscle (underneath the site of skin collected), blood, small intestine, major lymph nodes (lumbar, axillary and brachial) and major clearance organs such as kidney, liver, spleen, lungs, and the wash buffer were measured.

The results of wash buffer, skin, blood and kidney are showing below, the rest results are presented in the appendix (Appendix 7.27, 7.28, 7.29, 7.30, 7.31 and 7.32).

In Fig 4.2 (a), at all time points except 3 h, the amount of gentamicin stay in the wash buffer was significantly higher after PBS treatment when compared to both ME treatment and MEx2 treatment (indicated with **, $p < 0.05$) while at 3 h that was significantly higher after PBS treatment comparing to the ME treatment (indicated with *, $p < 0.05$). At time 6h and 24 h, the amount of gentamicin accumulated in the MEx2 treatment was significantly higher than that accumulated in the ME treatment (indicated with ***, $p < 0.05$).

In Fig 4.2 (a), the amount of gentamicin remains in the wash buffer after PBS treatment wasn't significantly changed during 48 h ($p>0.05$) and it is significantly higher comparing to that of ME treatment at all time point ($p<0.05$). Those results suggested that the gentamicin of PBS treatment didn't transdermal delivered into skin. It is evidence that the decrease trend can be observed in the wash buffer of MEx2 treatment, indicating the gentamicin was transdermal delivered into the skin. Similar trend should be observed in the ME treatment as well. Since the amount of gentamicin in the wash buffer after ME treatment was low and the its SEMs are relevant big, it didn't show significant decrease trend in the static analysis.

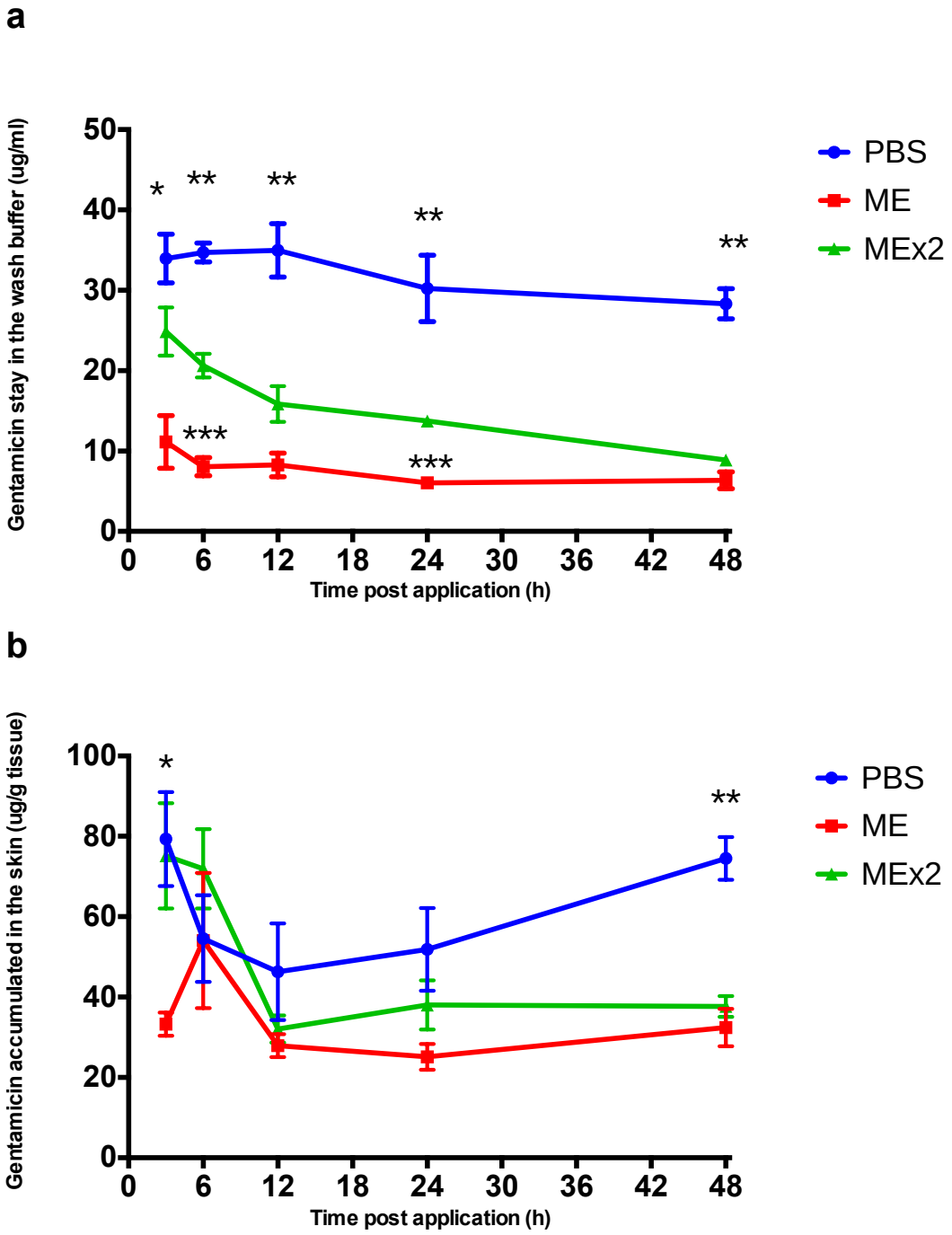

Fig 4.2 The amount of gentamicin present in the skin buffer (a) and the amount of gentamicin accumulated in the skin tissue at the site of topical application (b) over 48 hours post application. All formulations contained 10 mg/mL gentamicin that was spiked with 0.5 µCi of tritium labelled gentamicin and are described in Table 3.4. Each point represents a mean ± standard error of the mean (SEM) of 3 to 4 biological replicates.

In Fig 4.2 (b), at 3 h the amount of gentamicin in the skin was significantly lower after ME treatment when compared to the PBS treatment (indicated with *, $p < 0.05$). At 48 h, the amounts of gentamicin in the skin were significantly lower after the application of both ME and MEx2 when compared to the application of PBS treatment (indicated with **, $p < 0.05$).

In Fig 4.2 (b), the amount of gentamicin accumulated in the skin after PBS treatment wasn't significantly changed during 48 h ($p>0.05$). However, it is as high as the MEx2 treatment at the first 24 hours ($p>0.05$). If the gentamicin of PBS treatment didn't penetrate through the skin, one possible reason here would be the gentamicin precipitation was hard to washed off, it adhered on the skin until the skin was dissolved in the Solvable and measured. In comparison, the gentamicin amount accumulated in the skin of MEx2 treatment presented a decrease trend between 3 h and 12 h ($p<0.05$), suggesting the gentamicin of MEx2 treatment was transdermal delivered through the skin. Similar trend supposed to be observed in the ME treatment as well as the MEx2 treatment. However, since its SEMs were big and amounts of gentamicin accumulated were low, it didn't show such a trend in the static analysis.

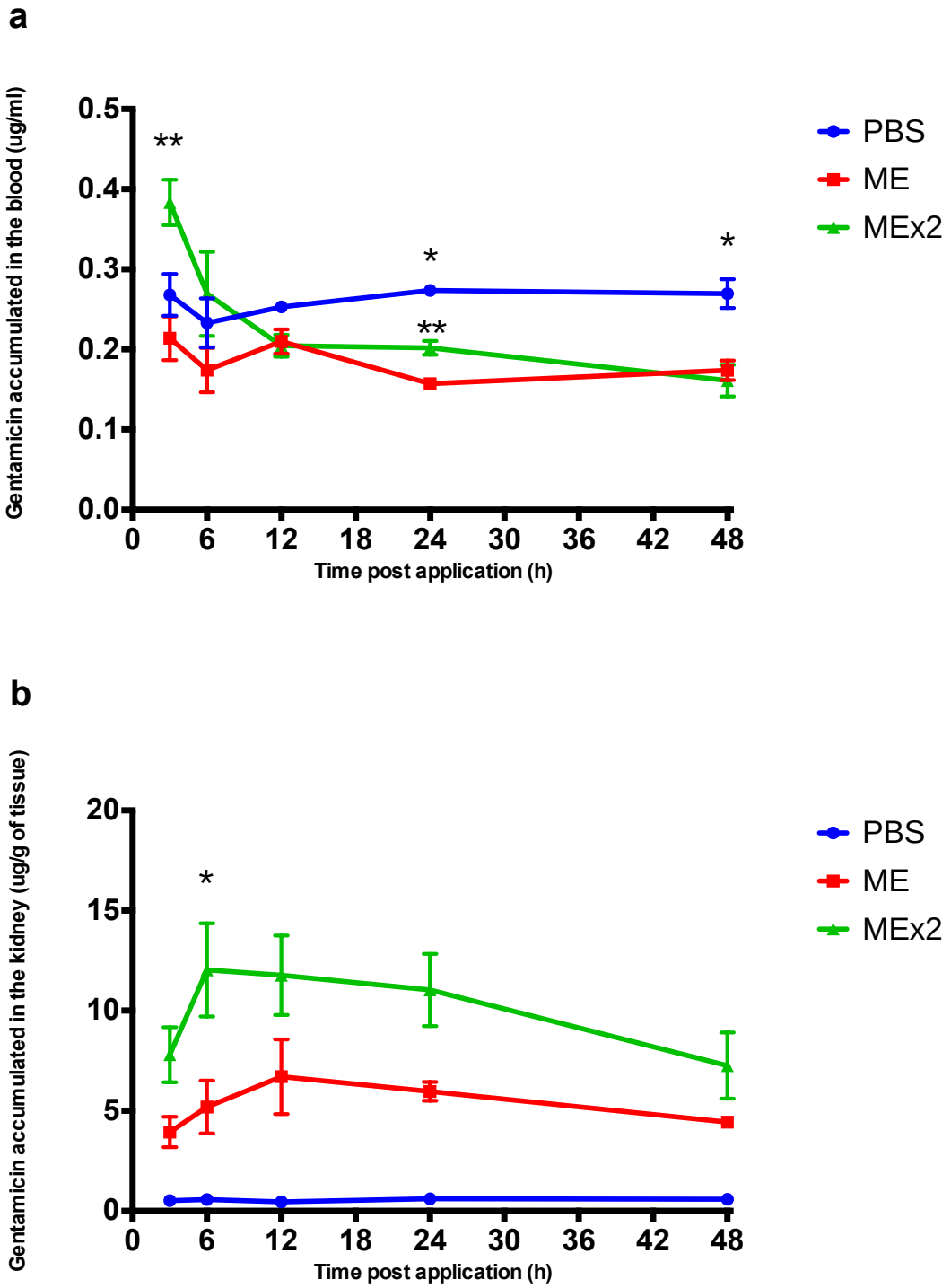

Fig 4.3 The amount of gentamicin accumulated in the blood (a) and the kidney (b) over 48 hours post application. All formulations contained 10 mg/mL gentamicin that was spiked with 0.5 µCi of tritium labelled gentamicin and are described in Table 3.4. Each point represents a mean ± standard error of the mean (SEM) of 3 to 4 biological replicates.

In Fig 4.2 (a), at 24 h and 48 h, the amount of gentamicin accumulated in the blood was significantly lower after ME treatment and MEx2 treatment (indicated with *, $p < 0.05$) when compared with that after PBS treatment. At 3 h and 24 h, the amount of gentamicin accumulated in blood was significantly higher after MEx2 treatment comparing to the ME treatment (indicated with **, $p < 0.05$).

In Fig 4.3 (a), the amount of gentamicin accumulated in the blood was significantly higher when compared with that of ME treatment at 3 h, proving that the gentamicin was transdermal delivered into the blood after MEx2 treatment. There is a dramatic decrease trend ($p<0.05$) for gentamicin amount accumulated in the blood of MEx2 treatment between 3 h and 12 h, indicating the gentamicin was take part in to the systemic circle after MEx2 treatment. There is no significant difference ($p>0.05$) of gentamicin amount accumulated in blood after both PBS and ME treatment over 24 h.

In Fig 4.2 (b), the gentamicin accumulated in the kidney after MEx2 treatment was significantly higher than that in both ME and PBS treatment at all time points ($p < 0.05$). At 6 h, the gentamicin amount accumulated in the kidney of MEx2 treatment was significantly higher than that in the MEx2 treatment (indicated with *, $p < 0.05$).

In Fig 4.3 (b) the gentamicin amount accumulated in the kidney after both ME and MEx2 treatment were significantly higher than that after PBS treatment. Taken together, above results suggested the amount of gentamicin was transdermal delivered into the blood and accumulated in the kidney via the systemic circle after ME and MEx2 treatment. The reason that no significant different was observed of gentamicin amount in the blood after ME treatment over 24 h may because it’s low amount of gentamicin and relative high SEM of ME treatment. However, since there is significantly lower rate of gentamicin accumulated in the kidney after PBS treatment comparing with that after ME and MEx2 treatment, suggesting that the gentamicin didn’t transdermal delivered through the skin and take part into the systemic circle. It is also noticed that the gentamicin amount accumulated in the kidney demonstrated an increase trend between 3 h and 6 h after ME treatment when compared with the decrease trend observed in the blood between 3 h and 6 h, suggesting that the gentamicin was accumulating in the kidney via the blood during this period.

4.5 Discussion

Topical gentamicin preparations are commercially available and are used to treat minor skin infections (such as impetigo, folliculitis) or infections associated with other skin conditions (such as eczema, psoriasis, minor burns/cut/wound) (Zanca, 1969). Topical gentamicin formulations are currently available as an ointment (Binenbaum et al., 2010), spray pack solution (Osawa et al., 2016) or a cream (AlShwaimi et al., 2016). However, previous study observed that the transdermal delivery of gentamicin from water-miscible bases was greater and faster than from ointment bases (Stone et al., 1968). Moreover, several former experiments proved that gel and ointment based topical formulations performed lower value than W/O emulsions or O/W emulsions in terms of transdermal drug delivery (Gomes et al., 2004, Fini et al., 2008). These researches suggest that ME could be an interesting alternative to improve topical delivery of gentamicin. With recent studies demonstrating synergistic, anti-biofilm activity between MCM and gentamicin, ME formulations containing MCM and gentamicin were developed and characterised (Proctor, 2015a, Hess et al., 2014).

Gentamicin was readily soluble in the MCM/EtOH based formulations and three gentamicin containing formulations (ME_BJ, ME_CO and ME_T8) were assessed for transdermal delivery (Table 4.1). The gentamicin J_s produced by ME_BJ (5,350 ng/cm^2/h), ME_CO (7,633 ng/cm^2/h) and ME_T8 (6,948 ng/cm^2/h) were significantly higher when compared with that produced by PBS (525 ng/cm^2/h). The gentamicin J_s produced by ME_BJ reaching statistical difference in comparison with that produced by ME_CO. These data indicate that different surfactants can have different influence on the transdermal permeation enhancing activity of MCM-EtOH based formulations and suggest ME_BJ, ME_CO and ME_T8 has the potential to effectively transdermal deliver gentamicin. It is suggested that the colloidal structures of topical permeation formulations may affect the difference through the formulation and alter their permeation ability. Furthermore, it is observed that the performance of gentamicin J_s was superior to the performance of NaFlu J_s of formulation ME_CO. Savić et al. (2009) concluded that permeation performance of two different model drugs may principally affected by the vehicle/solute interaction. This suggests the transdermal permeation of small compounds can be influenced by specific interactions with surfactants present in ME formulations (Karande et al.,

2007, Karande et al., 2004). To investigate, the nature of drug compounds such as partition coefficient within the formulation and its effect to permeation profile would be promising to verify in future studies.

Tween 80 is widely used in a variety of drug formulation vehicles and as formulation ME_T8 produced high transdermal flux for gentamicin *ex vivo*, this formulation was assessed for *in vivo* transdermal delivery using mice (Hosmer et al., 2009, Watnasirichaikul et al., 2002, Constantinides et al., 1994).

In the bio-distribution experiment performed, mice were topically treated with either PBS containing 10 mg/mL gentamicin, one dose of the ME containing 10 mg/mL or two identical doses of the ME containing 10 mg/mL. At each time point, the topical application site was washed to assess how much of the gentamicin in formulation remained on the surface of the skin. The amount of gentamicin present in the skin wash buffer from mice treated with PBS was high and remained relatively constant over the 48 hours post treatment. The amount of gentamicin present in the skin wash buffer from mice treated with the ME formulations was consistently lower when compared to the PBS treated group and was also seen to decline overtime. Taken together, this suggests that when mice were topically treated with PBS, high quantities of gentamicin remained on the skin surface and when treated with ME, gentamicin permeated through the skin more readily.

The profile of gentamicin accumulation in the skin after ME treatment suggests gentamicin rapidly permeated into deeper skin tissue. After this rapid accumulation post ME treatment, the concentration of gentamicin was then seen to slowly decline over time suggesting gentamicin could be spreading systemically. This is further supported by the gentamicin accumulation profile in kidney whereby after the ME treatment, gentamicin concentration increases in the first 12 h post application and then declines over the next 36 hours.

The high amount of gentamicin seen in PBS treated skin may be the result of gentamicin penetration into skin or inefficient removal of gentamicin from skin surface by the wash method used. This could be investigated further by using stronger wash buffers (e.g. those containing higher concentrations of detergent or ethanol). The penetration of gentamicin into skin layers could be assessed more

accurately via strip taping striping which has been used to determine the depth and lateral spread of compounds through skin tissue. (Hahn et al., 2010, Gee et al., 2012).

In the present study, mice treated with ME formulations were shown to accumulate gentamicin in the kidney. Those treated with PBS formulations did not. This indicates ME formulations were facilitating transdermal permeation of gentamicin producing systemic delivery. This effect was found to be dose dependent as indicated by those mice in the MEx2 treatment group accumulating 2.3-fold more gentamicin in the kidney when compared to the single ME treatment at 6 h post application. In addition, the kidney concentration of gentamicin of MEx2 treatment reach the highest at 6 h while that of ME treatment reach the highest at 12 h. This suggests that the MEx2 treatment produces faster transdermal permeation when compared to the ME treatment. While the majority of drug compounds are excreted from the body via the kidney, gentamicin is known to cause nephrotoxicity as it binds to phospholipids within the membrane of the proximal tubule cell specific in the kidney (Smith et al., 1980). While this may be a potential problem for the topical gentamicin formulation produced in this project, the data presented in this thesis does indicate that ME formulations containing the transdermal permeation enhancer, monocaprylate, can facilitate systemic drug delivery after topical application. However, producing high systemic drug concentrations post topical application may have unwanted side effects if the compounds have known systemic toxicity properties Therefore, in future studies, it will be necessary to optimize the ME formulation to get good penetration through the skin but reduced systemic dose. The J_s generated in this study would be optimized to produce better localized drug concentrations versus systemic concentrations (i.e. different drug concentration elaboration and dosing regimens, systemic concentration). Moreover, based on the equivalent surface area dosage conversion factors between animal and human (Rockville, 2005), the gentamicin dose applied in this study (6.67 and 13.34 mg/kg) would be optimized to use in the next set of *in vivo* experiments. Last but not least, the pharmacokinetics should be evaluated *in vivo* in the future study. For example, the process of antibiotics release from the ME based formulations and the removal of gentamicin from the body should be designed and evaluated.

5 CONCLUSIONS

ME formulations have great potential for use as transdermal drug delivery vehicles due to their thermodynamic stability and spontaneous formation (Shakeel et al., 2008). The composition and internal structure of ME can affect the internal mobility of the drugs in the vehicle, which influences the transdermal drug delivery performance of ME (Kreilgaard, 2002). MCM are approved for human use and have been incorporated into commercial formulations for decades (Paudel et al., 2010). MCM are known transdermal permeation enhancers and can be easily incorporated into ME formulations (Furuishi et al., 2007, Russell-Jones and Himes, 2011). Furthermore, MCM have broad spectrum antimicrobial properties including anti-biofilm activity (Schlievert et al., 1992, Bergsson et al., 2001, Hess et al., 2014, Proctor, 2015a). Taken together, these properties of MCM make them highly attractive for use in more effective, topical antimicrobial formulations.

The aim of this project was to utilize MCM in biocompatible ME formulations for transdermal drug delivery. The influence of medium chain mono and triglyceride concentration, non-ionic surfactants and co-surfactants on ME systems was characterized through the construction of pseudo-ternary phase diagrams and the transdermal permeation properties of selected formulations was assessed *in vitro* and *in vivo*.

Present project demonstrated that formulation ME_A effectively enhanced the transdermal delivery rate of NaFlu through full thickness mouse skin. Further assessment revealed MCM act as the permeation enhancer in formulation ME_A while the presence of GTCC in the formulation ME_A decreased the transdermal permeation enhancing properties of MCM. When investigating the permeation profiles of variable surfactants incorporated with MCM, Surfactant BRIJ O10 demonstrated synergistic effect on transdermal permeation delivery of NaFlu. It is proved that increasing MCM can expand the A_T at a ratio to GTCC of 1: 1. Moreover, phase diagrams which established with MCM/EtOH and surfactants produced larger monophasic area in comparison with that of MCM/GTCC based formulations, suggesting EtOH is potent to form stable ME formulations. After evaluating the effect of different surfactants on the transdermal delivery profiles, permeation results presented that the NaFlu J_s produced by formulation ME_T8 = ME_BJ > ME_CO > ME_T2.

Previous researches have shown that gentamicin acts synergistically with MCM to eradicate on *S. aureus* biofilm (Proctor, 2015b, Hess et al., 2014). Therefore, the incorporation of gentamicin into ME formulations was assessed. Results showed that formulation ME_T8, ME_CO and ME_BJ all effectively enhanced the transdermal delivery rate of gentamicin through full thickness mouse skin. ME_T8 was chosen to test the bio-distribution *in vivo*. The bio-distribution results showed that gentamicin accumulated in the kidney reaching statistical significance after application of formulation ME_T8 (both single dose and double dose groups) in comparison with the control group. This indicates that ME_T8 facilitated the transdermal delivery of gentamicin through mouse skin to produce detectable systemic drug levels.

In conclusion, ME formulations composed by MCM and EtOH are favourable for the transdermal drug delivery. In future studies, it is recommended that characterizing ME formulations with conductivity measure, rheology test and polarization microscopy would be promising. What's more, it is promising to examine variable antibiotic drugs incorporated with ME formulations.

Overall, this set of topical ME formulations with enhanced permeation capacity for the antibiotics (gentamicin) were constructed and evaluated in mice body. Greater range of ME formulations were found to use as transdermal delivery vehicles in this article, indicating that optimized ME formulations have more potential to fulfil variable requirement. The permeation enhancement ability of ME formulations presented in this study, informing ME formulations have a great capacity to incorporate with antibiotic drugs to replace current commercial antibiotic cream/ointment/gel.

6 REFERENCES

ABOOFAZELI, R. & LAWRENCE, M. J. 1993. Investigations into the formation and characterization of phospholipid microemulsions. I. Pseudo-ternary phase diagrams of systems containing water-lecithin-alcohol-isopropyl myristate. *International Journal of Pharmaceutics,* 93**,** 161-175.

ALBANESI, C., SCARPONI, C., GIUSTIZIERI, M. L. & GIROLOMONI, G. 2005. Keratinocytes in inflammatory skin diseases. *Curr Drug Targets Inflamm Allergy,* 4**,** 329-34.

ALSHWAIMI, E., MAJEED, A. & ALI, A. A. 2016. Pulpal Responses to Direct Capping with Betamethasone/Gentamicin Cream and Mineral Trioxide Aggregate: Histologic and Micro-Computed Tomography Assessments. *Journal Of Endodontics,* 42**,** 30-35.

BARRY, B. W. 1983. *Dermatological formulations : percutaneous absorption*, New York : M. Dekker, c1983.

BARRY, B. W. 1991. Lipid-Protein-Partitioning theory of skin penetration enhancement. *Journal of Controlled Release,* 15**,** 237-248.

BARRY, B. W. 2001. Novel mechanisms and devices to enable successful transdermal drug delivery. *European Journal Of Pharmaceutical Sciences: Official Journal Of The European Federation For Pharmaceutical Sciences,* 14**,** 101-114.

BENSOUILAH, J. & BUCK, P. 2007. *Aromadermatology; aromatherapy in the treatment and care of common skin conditions*, Book News, Inc.

BERGSSON, G., ARNFINNSSON, J., KARLSSON, S. M., STEINGRÍMSSON, O. & THORMAR, H. 1998. In vitro inactivation of Chlamydia trachomatis by fatty acids and monoglycerides. *Antimicrobial Agents And Chemotherapy,* 42**,** 2290-2294.

BERGSSON, G., ARNFINNSSON, J., STEINGRÍMSSON, O. & THORMAR, H. 2001. In vitro killing of Candida albicans by fatty acids and monoglycerides. *Antimicrobial Agents And Chemotherapy,* 45**,** 3209-3212.

BINENBAUM, G., BRUNO, C. J., FORBES, B. J., SNYDER, M., MOLLEN, T. J., SCHMIDT, B. & PETERSIDE, I. 2010. Periocular ulcerative dermatitis associated with gentamicin ointment prophylaxis in newborns. *The Journal Of Pediatrics,* 156**,** 320-321.

BLANK, I. H. 1953. Further Observations on Factors Which Influence the Water Content of the Stratum Corneum1. *Journal of Investigative Dermatology,* 21**,** 259.

BUNKOVA, L., BUNKA, F., POLLAKOVA, E., PODESVOVA, T. & DRAB, V. 2011. The effect of lactose, NaCl and an aero/anaerobic environment on the tyrosine decarboxylase activity of Lactococcus lactis subsp. cremoris and Lactococcus lactis subsp. lactis. *Int J Food Microbiol,* 147**,** 112-9.

BURKOTH, T. L., BELLHOUSE, B. J., HEWSON, G., LONGRIDGE, D. J., MUDDLE, A. G. & SARPHIE, D. F. 1999. Transdermal and transmucosal powdered drug delivery. *Critical Reviews In Therapeutic Drug Carrier Systems,* 16**,** 331-384.

CHEN, H., CHANG, X., WENG, T., ZHAO, X., GAO, Z., YANG, Y., XU, H. & YANG, X. 2004. A study of microemulsion systems for transdermal delivery of triptolide. *J Control Release,* 98**,** 427-36.

CHU, D. H. 2008. *Overview of biology, development, and structure of skin.,* New York, McGraw-Hill.

CÓCERA, M., LOPEZ, O., CODERCH, L., PARRA, J. L. & DE LA MAZA, A. 1999. Influence of the level of ceramides on the permeability of stratum corneum lipid liposomes caused by a C12-betaine/sodium dodecyl sulfate mixture. *International Journal of Pharmaceutics,* 183**,** 165-173.

CONSTANTINIDES, P. P., SCALART, J. P., LANCASTER, C., MARCELLO, J., MARKS, G., ELLENS, H. & SMITH, P. L. 1994. Formulation and intestinal absorption enhancement evaluation of water-in-oil microemulsions incorporating medium-chain glycerides. *Pharm Res,* 11**,** 1385-90.

CORNWELL, P. A., TUBEK, J., VAN GOMPEL, H. A. H. P., LITTLE, C. J. & WIECHERS, J. W. 1998. Glyceryl monocaprylate/caprate as a moderate skin penetration enhancer. *International Journal of Pharmaceutics,* 171**,** 243-255.

DANIELSSON, I. & LINDMAN, B. 1981. Brief note: The definition of microemulsion. *Colloids and Surfaces,* 3**,** 391-392.

ELIAS, P. M. & MENON, G. K. 1991. Structural and lipid biochemical correlates of the epidermal permeability barrier. *Adv Lipid Res,* 24**,** 1-26.

FINI, A., BERGAMANTE, V., CESCHEL, G. C., RONCHI, C. & DE MORAES, C. A. 2008. Control of transdermal permeation of hydrocortisone acetate from hydrophilic and lipophilic formulations. *AAPS PharmSciTech,* 9**,** 762-8.

FLYNN, G. L. & STEWART, B. 1988. Percutaneous drug penetration: Choosing candidates for transdermal development. *Drug Development Research,* 13**,** 169-185.

FURUISHI, T., ODA, S., SAITO, H., FUKAMI, T., SUZUKI, T. & TOMONO, K. 2007. Effect of permeation enhancers on the in vitro percutaneous absorption of pentazocine. *Biol Pharm Bull,* 30**,** 1350-3.

GAIKWAD, A. K. 2013. Transdermal drug delivery system: Formulation aspects and evaluation. *Comprehensive Journal of Pharmaceutical Sciences,* 1(1).

GARTI, N., CLEMENT, V., FANUN, M. & LESER, M. E. 2000. Some characteristics of sugar ester nonionic microemulsions in view of possible food applications. *Journal Of Agricultural And Food Chemistry,* 48**,** 3945-3956.

GEE, C. M., NICOLAZZO, J. A., WATKINSON, A. C. & FINNIN, B. C. 2012. Assessment of the lateral diffusion and penetration of topically applied drugs in humans using a novel concentric tape stripping design. *Pharmaceutical Research,* 29**,** 2035-2046.

GOMES, S. F. D. O., NUNAN, E. D. A. & FERREIRA, L. A. M. 2004. Influence of the formulation type (o/w, w/o/w emulsions and ointment) on the topical delivery of paromomycin.

GRADZIELSKI, M. & HOFFMAN, H. 1999. Rheological Properties of Microemulsions. *In:* MITTAL, K. L. & KUMAR, P. (eds.) *Handbook of microemulsion science and technology.* New York : Marcel Dekker, 1999.

HAHN, T., HANSEN, S., NEUMANN, D., KOSTKA, K. H., LEHR, C. M., MUYS, L. & SCHAEFER, U. F. 2010. Infrared densitometry: a fast and non-destructive method for exact stratum corneum depth calculation for in vitro tape-stripping. *Skin Pharmacology And Physiology,* 23**,** 183-192.

HELLWEG, T. 2002. Phase structures of microemulsions. *Current Opinion in Colloid & Interface Science,* 7.

HESS, D. J., HENRY-STANLEY, M. J. & WELLS, C. L. 2014. Antibacterial synergy of glycerol monolaurate and aminoglycosides in Staphylococcus aureus biofilms. *Antimicrob Agents Chemother,* 58**,** 6970-3.

HIMES, R., LEE, S., MCMENIGALL, K. & RUSSELL-JONES, G. 2011. The influence of molecular adjuvants in the cutaneous response to antigen after topical vaccination. *Vaccine,* 29**,** 5393-8.

HONEYWELL-NGUYEN, P. L. & BOUWSTRA, J. A. 2003. The in vitro transport of pergolide from surfactant-based elastic vesicles through human skin: a suggested mechanism of action. *Journal of Controlled Release,* 86**,** 145-156.

HOSMER, J., REED, R., BENTLEY, M. V. L. B., NORNOO, A. & LOPES, L. B. 2009. Microemulsions Containing Medium-Chain Glycerides as Transdermal Delivery Systems for Hydrophilic and Hydrophobic Drugs. *AAPS PharmSciTech***,** 589.

HUZIL, J. T., SIVALOGANATHAN, S., KOHANDEL, M. & FOLDVARI, M. 2011. Drug Delivery Through the Skin: Molecular Simulations of Barrier Lipids to Design more Effective Noninvasive Dermal and Transdermal Delivery Systems for Small Molecules Biologics and Cosmetics. *WIREs Nanomedicine and Nanobiotechnology*.

HYLDGAARD, M., SUTHERLAND, D. S., SUNDH, M., MYGIND, T. & MEYER, R. L. 2012. Antimicrobial mechanism of monocaprylate. *Appl Environ Microbiol,* 78**,** 2957-65.

INFORMATICS, I. 1973. Monograph on glycerine and glycerides.

ISAACS, C. E., LITOV, R. E. & THORMAR, H. 1995. Antimicrobial activity of lipids added to human milk, infant formula, and bovine milk. *J Nutr Biochem,* 6**,** 362-366.

JAMES, G. A., SWOGGER, E., WOLCOTT, R., PULCINI, E., SECOR, P., SESTRICH, J., COSTERTON, J. W. & STEWART, P. S. 2008. Biofilms in chronic wounds. *Wound Repair Regen,* 16**,** 37-44.

JAMES, W. D., ELSTON, D. M. & BERGER, T. G. (eds.) 2016. *Andrews' Diseases of the skin : clinical dermatology*: Philadelphia, PA : Elsevier, [2016]

Twelfth edition / William D. James, MD, Paul R Gross, Professor of Dermatology, Department of Dermatology, University of Pennsylvania School of Medicine, Philadelphia, Pennsylvania; Dirk M. Elston, MD, Professor and Chairman, Department of Dermatology and Dermatologic Surgery, Medical University of South Carolina, Charleston, South Carolina, Former Director, Ackerman Academy of Dermatopathology, New York, New York; Timothy G. Berger, MD, Professor of Clinical Dermatology, Executive Vice Chair and Residency, Program Director, Chair in Dermatology Medical Student Education, University of California, San Francisco, San Francisco, California.

KABARA, J. J. 1991. *Chemisrty and Biology of Monoglycerides in Cosmetic Formulations,* CSC Press.

KALE, N. J. & ALLEN, J. L. V. 1989. Research paper: Studies on microemulsions using Brij 96 as surfactant and glycerin, ethylene glycol and propylene glycol as cosurfactants. *International Journal of Pharmaceutics,* 57**,** 87-93.

KARANDE, P., JAIN, A., ARORA, A., HO, M. J. & MITRAGOTRI, S. 2007. Synergistic effects of chemical enhancers on skin permeability: A case study of sodium lauroylsarcosinate and sorbitan monolaurate. *European Journal of Pharmaceutical Sciences,* 31**,** 1-7.

KARANDE, P., JAIN, A. & MITRAGOTRI, S. 2004. Discovery of transdermal penetration enhancers by high-throughput screening. *Nature Biotechnology*, 192.

KING, M. J., MICHEL, D. & FOLDVARI, M. 2003. Evidence for lymphatic transport of insulin by topically applied biphasic vesicles. *J Pharm Pharmacol,* 55, 1339-44.

KOGAN, A. G., NISSIM 2006. Microemulsions as transdermal drug delivery vehicles. *Advances in Colloid and Interface Science,* 123, 369-385.

KREILGAARD, M. 2002. Influence of microemulsions on cutaneous drug delivery. *Adv Drug Deliv Rev,* 54 Suppl 1, S77-98.

KREILGAARD, M., PEDERSEN, E. J. & JAROSZEWSKI, J. W. 2000. NMR characterisation and transdermal drug delivery potential of microemulsion systems. *Journal of Controlled Release,* 69, 421-433.

KUMAR, K. K., SASIKANTH, K., SABAREESH, M. & DORABABU, N. 2011. FORMULATION AND EVALUATION OF DIACEREIN CREAM. *Asian Journal of Pharmaceutical & Clinical Research,* 4, 93.

LAM, A. C. & SCHECHTER, R. S. 1987. The theory of diffusion in microemulsion. *Journal of Colloid and Interface Science,* 120, 56-63.

LANGEVIN, D. 1992. Micelles and Microemulsions. *Annual Review of Physical Chemistry,* 43, 341-369.

LAWRENCE, M. J. & REES, G. D. 2000. Microemulsion-based media as novel drug delivery systems. *Advanced Drug Delivery Reviews,* 45, 89-121.

LEE, S., KOLLIAS, N., MCAULIFFE, D. J., FLOTTE, T. J. & DOUKAS, A. G. 1999. Topical drug delivery in humans with a single photomechanical wave. *Pharmaceutical Research,* 16, 1717-1721.

LEVER, W. F. & ELDER, D. E. 2005. *Lever's histopathology of the skin.,* Philadelphia : Lippincott Williams & Wilkins, 2008. 10th ed.

LI, P., GHOSH, A., WAGNER, R. F., KRILL, S., JOSHI, Y. M. & SERAJUDDIN, A. T. M. 2005. Effect of combined use of nonionic surfactant on formation of oil-in-water microemulsions. *International Journal of Pharmaceutics,* 288, 27-34.

LIPSKY, B. A. & HOEY, C. 2009. Topical antimicrobial therapy for treating chronic wounds. *Clin Infect Dis,* 49, 1541-9.

LOPES, L. B., COLLETT, J. H. & BENTLEY, M. V. L. B. 2005. Research paper: Topical delivery of cyclosporin A: an in vitro study using monoolein as a penetration enhancer. *European Journal of Pharmaceutics and Biopharmaceutics,* 60, 25-30.

LOPES, L. B., MURPHY, N. & NORNOO, A. 2009. Enhancement of transdermal delivery of progesterone using medium-chain mono and diglycerides as skin penetration enhancers. *Pharmaceutical Development & Technology,* 14, 524-529.

LOPES, L. B., SPERETTA, F. F. & BENTLEY, M. V. 2007. Enhancement of skin penetration of vitamin K using monoolein-based liquid crystalline systems. *Eur J Pharm Sci,* 32, 209-15.

MONASH, S. B., H. 1958. Location and reformation of the epithelial barrier to water vapor. *AMA Arch Derm,* 78, 710-4.

MOONEN, H. & BAS, H. 2014. Mono- and Diglycerides. *Emulsifiers in Food Technology.* John Wiley & Sons, Ltd.

MORGAN, T. M., REED, B. L. & FINNIN, B. C. 1998. Enhanced skin permeation of sex hormones with novel topical spray vehicles. *J Pharm Sci,* 87, 1213-8.

MORIMOTO, Y., SUGIBAYASHI, K., KOBAYASHI, D., SHOJI, H., YAMAZAKI, J.-I. & KIMURA, M. 1993. A new enhancer-coenhancer system to increase skin permeation of morphine hydrochloride in vitro. *International Journal of Pharmaceutics,* 91**,** 9-14.

MURPHY, G. F. 1997. *Histology of the skin.,* Philadelphia, Lippincott Williams & Wilkins.

NAKAMURA, H., SUGIBAYASHI, K. & MORIMOTO, Y. Effect of Lipophilic Multicomponent System on Skin Permeation of Ketotifen Fumarate. *In:* BRAIN, K. R., JAMES, V. J. & WALTERS, K. A., eds., 1996. STS Publishing Ltd, 150-153.

NOVOTNY, J., KOVARIKOVA, P., NOVOTNY, M., JANUSOVA, B., HRABALEK, A. & VAVROVA, K. 2009. Dimethylamino acid esters as biodegradable and reversible transdermal permeation enhancers: effects of linking chain length, chirality and polyfluorination. *Pharm Res,* 26**,** 811-21.

OSAWA, H., YOSHII, S., ABRAHAM, S. J. K., OKAMOTO, Y., HOSAKA, S., FUKUDA, S., TSUCHIYA, K., NAKAJIMA, M., HONDA, Y. & TAKIZAWA, K. 2016. Topical spraying of cefazolin and gentamicin reduces deep sternal wound infections after heart surgery: a multicenter, large volume, retrospective study. *General Thoracic And Cardiovascular Surgery,* 64**,** 197-202.

PAUDEL, K. S., MILEWSKI, M., SWADLEY, C. L., BROGDEN, N. K., GHOSH, P. & STINCHCOMB, A. L. 2010. Challenges and opportunities in dermal/transdermal delivery. *Therapeutic delivery,* 1**,** 109-131.

PODLOGAR, F., BESTER ROGAC, M. & GASPERLIN, M. 2005. The effect of internal structure of selected water-Tween 40-Imwitor 308-IPM microemulsions on ketoprofene release. *Int J Pharm,* 302**,** 68-77.

PODLOGAR, F., GASPERLIN, M., TOMSIC, M., JAMNIK, A. & ROGAC, M. B. 2004. Structural characterisation of water-Tween 40/Imwitor 308-isopropyl myristate microemulsions using different experimental methods. *Int J Pharm,* 276**,** 115-28.

PRAJAPATI, H. N., DALRYMPLE, D. M. & SERAJUDDIN, A. T. 2012. A comparative evaluation of mono-, di- and triglyceride of medium chain fatty acids by lipid/surfactant/water phase diagram, solubility determination and dispersion testing for application in pharmaceutical dosage form development. *Pharm Res,* 29**,** 285-305.

PRAUSNITZ, R. M., ELIAS, M. P., FRANZ, J. T., SCHMUTH, M., TSAI, J.-C., MENON, K. G., W., H. M. & K., F. R. 2012. Skin Barrier and Transdermal Drug Delivery. *MEDICAL THERAPY.*

PROCTOR, E.-J. 2015a. *Exploring anti-bacterial interactions between monocaprylin and broad-spectrum antimicrobials on Staphylococcus aureus biofilms.* Bachelor of Medical Biotechnology (Advanced) with Honours, University of Wollongong.

PROCTOR, R. A. 2015b. Recent developments for Staphylococcus aureus vaccines: clinical and basic science challenges. *Eur Cell Mater,* 30**,** 315-26.

PROMOD KUMAR; MITTAL, K. L. 1999. *Handbook of microemulsion science and technology,* 270 Madison Ave., New York, NY 10016, USA; Marcel Dekker Inc. Gillette Res. Inst., Gaithersburg, MD, USA.

ROCKVILLE, M. 2005. Guidance for industry: estimating the maximum safe starting dose in initial clinical trials for therapeutics in adult healthy

volunteers. U.S. Dept. of Health and Human Services, Food and Drug Administration, Center for Drug Evaluation and Research, [2005].

RUSHFORTH, D. S., SANCHEZ-RUBIO, M., SANTOS-VIDALS, L. M., WORMUTH, K. R., KALER, E. W., CUEVAS, R. & PUIG, J. E. 1986. Structural study of one-phase microemulsions. *J. Phys. Chem.; (United States)*, 6668.

RUSSELL-JONES, G. & HIMES, R. 2011. Water-in-oil microemulsions for effective transdermal delivery of proteins. *Expert Opin Drug Deliv,* 8**,** 537-46.

SAINT RUTH, H., ATTWOOD, D., KTISTIS, G. & TAYLOR, C. J. 1995. Phase studies and particle size analysis of oil-in-water phospholipid microemulsions. *INTERNATIONAL JOURNAL OF PHARMACEUTICS,* 116**,** 253.

SANTOS, P., WATKINSON, A. C., HADGRAFT, J. & LANE, M. E. 2008. Application of microemulsions in dermal and transdermal drug delivery. *Skin Pharmacol Physiol,* 21**,** 246-59.

SAVIĆ, S., WEBER, C., SAVIĆ, M. M. & MÜLLER-GOYMANN, C. 2009. Natural surfactant-based topical vehicles for two model drugs: Influence of different lipophilic excipients on in vitro/in vivo skin performance. *International Journal of Pharmaceutics,* 381**,** 220-230.

SCHLIEVERT, P. M., DERINGER, J. R., KIM, M. H., PROJAN, S. J. & NOVICK, R. P. 1992. Effect of glycerol monolaurate on bacterial growth and toxin production. *Antimicrobial Agents And Chemotherapy,* 36**,** 626-631.

SCHLIEVERT, P. M. & PETERSON, M. L. 2012. Glycerol Monolaurate Antibacterial Activity in Broth and Biofilm Cultures. *PLoS ONE,* 7**,** 1-12.

SCHULMAN, J. H., STOECKENIUS, W. & PRINCE, L. M. 1959. Mechanism of Formation and Structure of Micro Emulsions by Electron Microscopy. *The Journal of Physical Chemistry,* 63**,** 1677-1680.

SHAKEEL, F., BABOOTA, S., AHUJA, A., ALI, J. & SHAFIQ, S. 2008. Skin permeation mechanism and bioavailability enhancement of celecoxib from transdermally applied nanoemulsion. *Journal of Nanobiotechnology,* 6**,** 1-11.

SHOKRI, J., NOKHODCHI, A., DASHBOLAGHI, A., HASSAN-ZADEH, D., GHAFOURIAN, T. & BARZEGAR JALALI, M. 2001. The effect of surfactants on the skin penetration of diazepam. *International Journal of Pharmaceutics,* 228**,** 99-107.

SMITH, C. R., LIPSKY, J. J., LASKIN, O. L., HELLMANN, D. B., MELLITS, E. D., LONGSTRETH, J. & LIETMAN, P. S. 1980. Double-blind comparison of the nephrotoxicity and auditory toxicity of gentamicin and tobramycin. *The New England Journal Of Medicine,* 302**,** 1106-1109.

STONE, H. H., KOLB, L. P. J. & SMITH, R. B. 1968. The systemic absorption of an antibiotic from the burn wound surface. *Am Surg,* 34**,** 639-43.

STREY, R. 1994. Microemulsion microstructure and interfacial curvature. *Colloid & Polymer Science,* 272**,** 1005.

STREY, R. 1996. Phase behavior and interfacial curvature in water-oil-surfactant systems. *Current Opinion in Colloid & Interface Science,* 1**,** 402-410.

SUGAR, I. P. & NEUMANN, E. 1984. Stochastic model for electric field-induced membrane pores. Electroporation. *Biophysical Chemistry,* 19**,** 211-225.

THORGEIRSDOTTIR, T. O., KRISTMUNDSDOTTIR, T., THORMAR, H., AXELSDOTTIR, I. & HOLBROOK, W. P. 2006a. Antimicrobial activity of

monocaprin: a monoglyceride with potential use as a denture disinfectant. *Acta Odontol Scand,* 64**,** 21-6.

THORGEIRSDOTTIR, T. O., THORMAR, H. & KRISTMUNDSDOTTIR, T. 2006b. Viscoelastic properties of a virucidal cream containing the monoglyceride monocaprin: effects of formulation variables: a technical note. *AAPS PharmSciTech,* 7**,** E44.

TURNER, N. G., KALIA, Y. N. & GUY, R. H. 1997. The effect of current on skin barrier function in vivo: recovery kinetics post-iontophoresis. *Pharm Res,* 14**,** 1252-7.

VALENTA, C. & SCHULTZ, K. 2004. Influence of carrageenan on the rheology and skin permeation of microemulsion formulations. *Journal of Controlled Release,* 95**,** 257-265.

VERMA, G. & HASSAN, P. A. 2013. Self assembled materials: design strategies and drug delivery perspectives. *Physical Chemistry Chemical Physics: PCCP,* 15**,** 17016-17028.

VIRBAC. 2011. *ALLERMYL® Shampoo* [Online]. Available: http://www.virbacvet.com/pdf/product_pdfs/ALLERMYL_Shampoo_msds.pdf [Accessed 2016].

WATNASIRICHAIKUL, S., DAVIES, N. M., RADES, T. & TUCKER, I. G. 2000. Preparation of biodegradable insulin nanocapsules from biocompatible microemulsions. *Pharm Res,* 17**,** 684-9.

WATNASIRICHAIKUL, S., RADES, T., TUCKER, I. G. & DAVIES, N. M. 2002. In-vitro release and oral bioactivity of insulin in diabetic rats using nanocapsules dispersed in biocompatible microemulsion. *J Pharm Pharmacol,* 54**,** 473-80.

WEAVER, J. C., VAUGHAN, T. E. & CHIZMADZHEV, Y. 1999. Theory of electrical creation of aqueous pathways across skin transport barriers. *Advanced Drug Delivery Reviews,* 35**,** 21-39.

ZANCA, A. 1969. [Gentamicin for topical use in dermatology]. *Giornale Italiano Di Chemioterapia,* 16**,** 354-359.

7 APPENDIX

7.1 Materials and solutions

Phasphate buffered salin (PBS) (1 x)

NaCl	8 g/L
KCl	0.2 g/L
Na_2HPO_4	1.44 g/L
KH_2PO_4	0.24 g/L

7.2 Specification Sheets

Appendix 7.1 Certificate of analysis of Crodamol GTCC-LQ-(SG), listing the percentage breakdown of the oil components, indicating 57.8 caprylic and 42.2% capric triglycerides

CRODA

Certificate prepared at

Croda Singapore Pte Ltd
30 Seraya Avenue
Singapore 627884

Certificate of Analysis

A quality management system registered to the international standard ISO 9001 was used to manufacture and test this material.

Customer details

Croda Australia (Samples and Parcels)
Suite 102
447 Victoria Street
PO BOX 6079
Wetherill Park NSW 2164
Australia

Customer Ref.
Inspection Lot 080000083435
C of A Printed. 12.03.2012
Croda Order No. 1206806
Croda Del. No. 81300410
Quantity. 2.000KG

Batch Details

Product Name: CRODAMOL GTCC-LQ-(SG)
Product Code: GE83907/SAMP
Batch No: 24424

Date of test: 23.02.2012
Date of manufacture: 14.02.2012
Retest date: 13.02.2014

Specification: REV. 06 01.03.2012

Quality Control Results

Analytical Test Method No.	Characteristic	Specification Limit Lower	Upper	Value	Unit	Status
	Addendum 00	PASS OR FAIL		Pass	-	P
AS039010	APPEARANCE @ 25°C (CLARITY)	CLEAR		Pass	-	P
AS039010	APPEARANCE @ 25°C (STATE)	LIQUID		Pass	-	P
ES001010	ACID VALUE	0.00	0.10	0.03	mg KOH/g	P
AS006010	COLOUR (HAZEN)	0	50	15		P
ES011010	IODINE VALUE	0.0	0.5	0.2	gI2/100g	P
ES014030	PEROXIDE VALUE (PH EUR)	0.0	1.0	0.0	meqO2/kg	P
FS017010	REFRACTIVE INDEX @ 20°C	1.4400	1.4510	1.4496		P
ES018010	SAPONIFICATION VALUE	325.0	345.0	336.7	mg KOH/g	P
ES019010	SOAP CONTENT	0.00	0.01	0.00	%	P
FS020010	SPECIFIC GRAVITY@ 20 °C	0.920	0.960	0.945		P
FS021010	VISCOSITY (U-TUBE)@ 20°C	27.0	33.0	29.6	mPas	P
FS022010	WATER CONTENT	0.00	0.15	0.06	%	P
AS040010	ODOUR	ESSENTIALLY ODOURLESS		Pass	-	P
FS026010	UNSAPONIFIABLES	0.5% MAX		Pass	-	P
LS008010	FATTY ACID DISTRI-			Pass	-	P

CRODA

Certificate prepared at

Croda Singapore Pte Ltd
30 Seraya Avenue
Singapore 627884

Certificate of Analysis

A quality management system registered to the international standard ISO 9001 was used to manufacture and test this material.

Customer details

Croda Australia (Samples and Parcels)
Suite 102
447 Victoria Street
PO BOX 6079
Wetherill Park NSW 2164
Australia

Customer Ref.	
Inspection Lot	080000083435
C of A Printed.	12.03.2012
Croda Order No.	1206806
Croda Del. No.	81300410
Quantity.	2.000KG

	BUTION (PhEUR)					
LS008010	C6:0	0.0	1.0	0.0	%	P
LS008010	C8:0	50.0	63.0	57.8	%	P
LS008010	C10:0	36.0	45.0	42.2	%	P
LS008010	C12:0	0.0	2.0	0.0	%	P
AS040010	ODOUR	CHARACTERISTIC		Pass	-	P

If you received only a sample of this product, please request updated specification before placing the first purchase order.

Batch Status: Pass
Our quality tests on this batch are reported above. The tests carried out are those necessary to demonstrate compliance with our product specification and are not intended to guarantee the product as suitable for any application beyond those contained in the specification. We recommend you perform your own quality and or identification checks on receipt

The name printed at the end of this document is an electronic signature.

Confirmed by

Bee Kim Tan QA Coordinator

Appendix 7.2 Certificate of analysis of Capmul MCM, listing the percentage breakdown of the oil components, indicating 58.4% MCM, glyceryl monocaprylate (C8) and glyceryl caprate (C10).

ABITEC
AN ABF INGREDIENTS COMPANY

1530 S. Jackson Street
Janesville, WI 53546
608-752-9007

Contact information
Customer Service:
ph: 800- 555-1255
email: sales@abiteccorp.com

Certificate of Analysis

Capmul MCM C-8, EP
Lot Number: 111119-6
Date of Manufacture: November 19, 2011
Re-Test Date: 20 Months from Date of Manufacture

European Pharmacopeia Monograph: Glycerol Monocaprylate (Type I)

Test	Test Result	Specification
Identification		
A) Fatty Acid Composition	Pass	Pass
B) Meets Assay	Pass	Pass
Acid Value	1.5	3.0 max.
Composition of Fatty Acids:		
6:0 Caproic Acid %	0.1	1.0 max.
8:0 Caprylic Acid %	97.3	90.0 min.
10:0 Capric Acid %	2.6	10.0 max.
12:0 Lauric Acid %	0.1	1.0 max.
14:0 Myristic Acid %	0.0	0.5 max.
Free Glycerol %	1.1	3.0 max.
Assay/Content:		
Monoacylglycerols %	58.4	45.0 - 75.0
Diacylglycerols %	34.3	20.0 - 50.0
Triacylglycerols %	5.8	10.0 max.
Water, by KF (%)	0.1	1.0 max.
Total Ash (w/w)	0.0	0.5 max.

Prepared by:
QC Technician
ABITEC Corporation
Date: March 19, 2012

Reviewed By:

7.3 Transdermal delivery assay of NaFlu (MCM/GTCC based formulations)

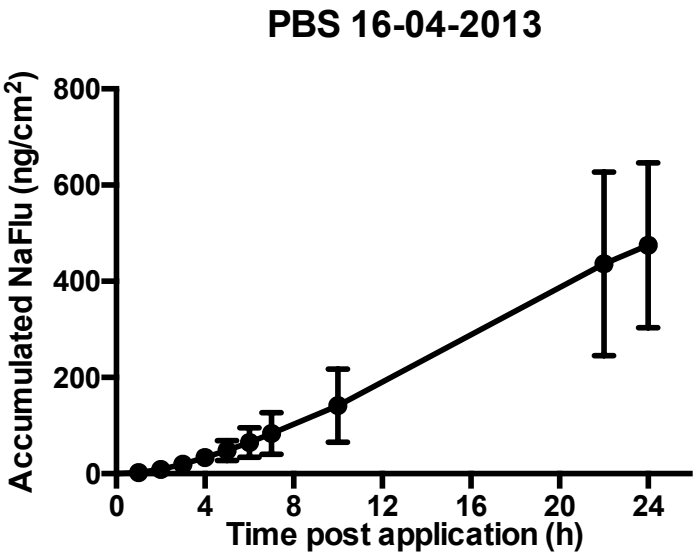

Appendix 7.3 Cumulative transdermal delivery of NaFlu through mouse skin *in vitro* over 24 hours. This formulation contained 1.2 mg/mL NaFlu and was described in Table 3.1. Each point represents means ± standard deviation of 3 to 4 biological replicates.

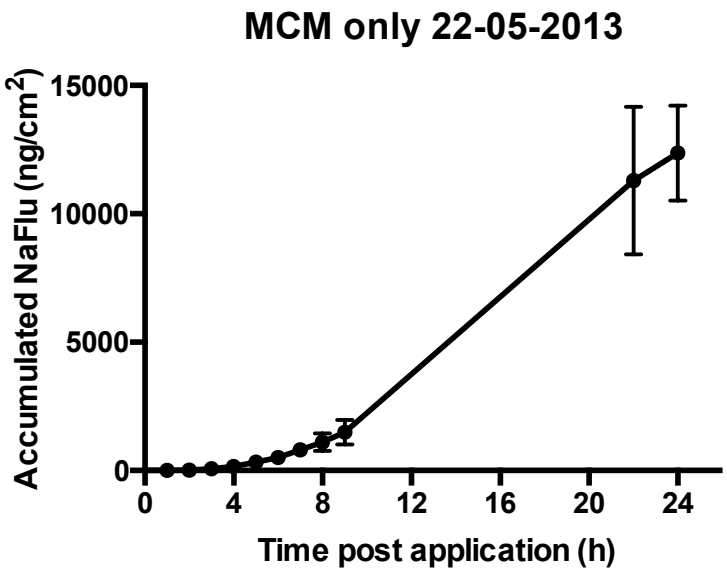

Appendix 7.4 Cumulative transdermal delivery of NaFlu through mouse skin *in vitro* over 24 hours. This formulation contained 1.2 mg/mL NaFlu and was described in Table 3.1. Each point represents means ± standard deviation of 3 to 4 biological replicates.

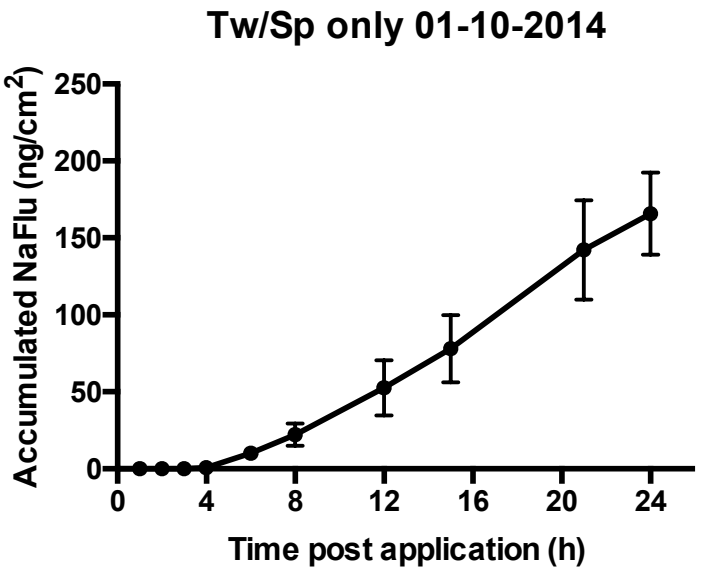

Appendix 7.5 Cumulative transdermal delivery of NaFlu through mouse skin *in vitro* over 24 hours. This formulation contained 1.2 mg/mL NaFlu and was described in Table 3.1. Each point represents means ± standard deviation of 3 to 4 biological replicates.

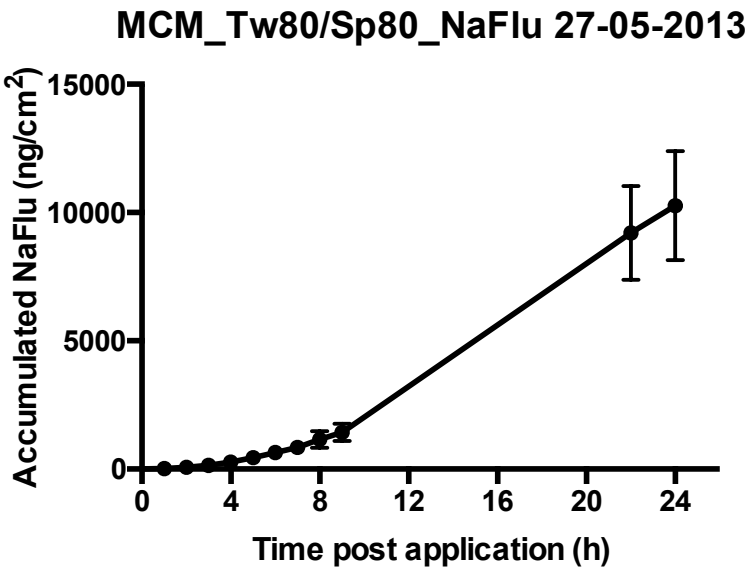

Appendix 7.6 Cumulative transdermal delivery of NaFlu through mouse skin *in vitro* over 24 hours. This formulation contained 1.2 mg/mL NaFlu and was described in Table 3.1. Each point represents means ± standard deviation of 3 to 4 biological replicates.

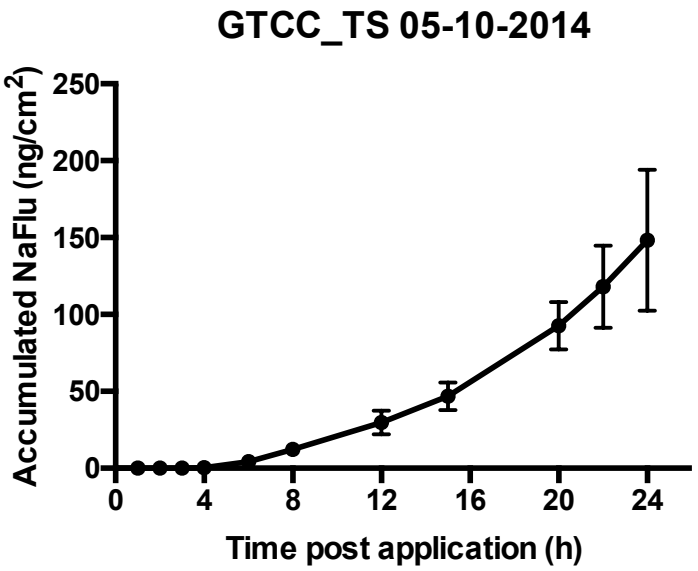

Appendix 7.7 Cumulative transdermal delivery of NaFlu through mouse skin *in vitro* over 24 hours. This formulation contained 1.2 mg/mL NaFlu and was described in Table 3.1. Each point represents means ± standard deviation of 3 to 4 biological replicates.

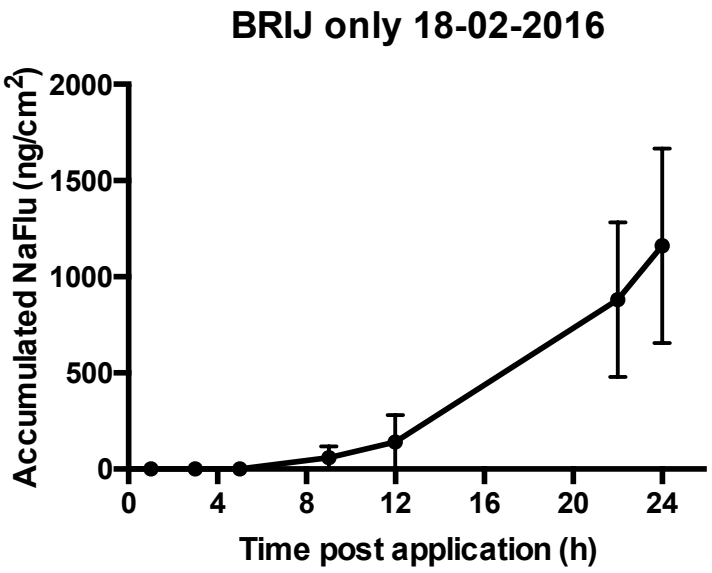

Appendix 7.8 Cumulative transdermal delivery of NaFlu through mouse skin *in vitro* over 24 hours. This formulation contained 1.2 mg/mL NaFlu and was described in Table 3.2. Each point represents means ± standard deviation of 3 to 4 biological replicates.

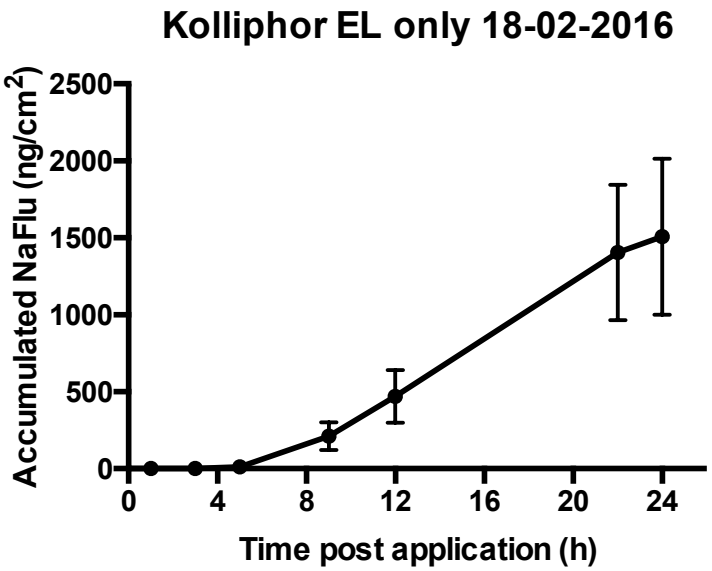

Appendix 7.9 Cumulative transdermal delivery of NaFlu through mouse skin *in vitro* over 24 hours. This formulation contained 1.2 mg/mL NaFlu and was described in Table 3.2. Each point represents means ± standard deviation of 3 to 4 biological replicates.

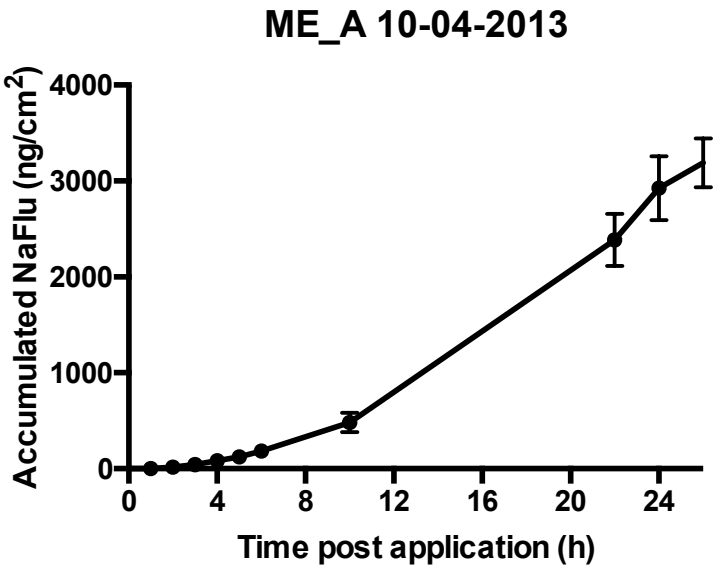

Appendix 7.10 Cumulative transdermal delivery of NaFlu through mouse skin *in vitro* over 24 hours. This formulation contained 1.2 mg/mL NaFlu and was described in Table 3.1. Each point represents means ± standard deviation of 3 to 4 biological replicates.

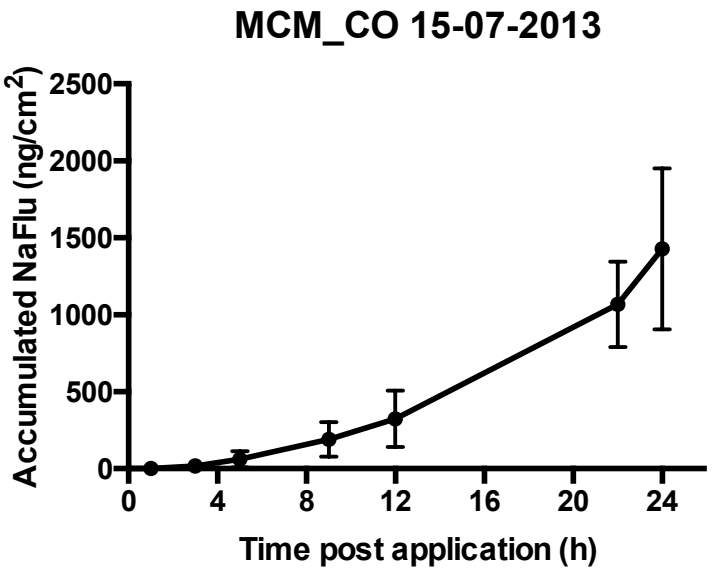

Appendix 7.11 Cumulative transdermal delivery of NaFlu through mouse skin *in vitro* over 24 hours. This formulation contained 1.2 mg/mL NaFlu and was described in Table 3.2. Each point represents means ± standard deviation of 3 to 4 biological replicates.

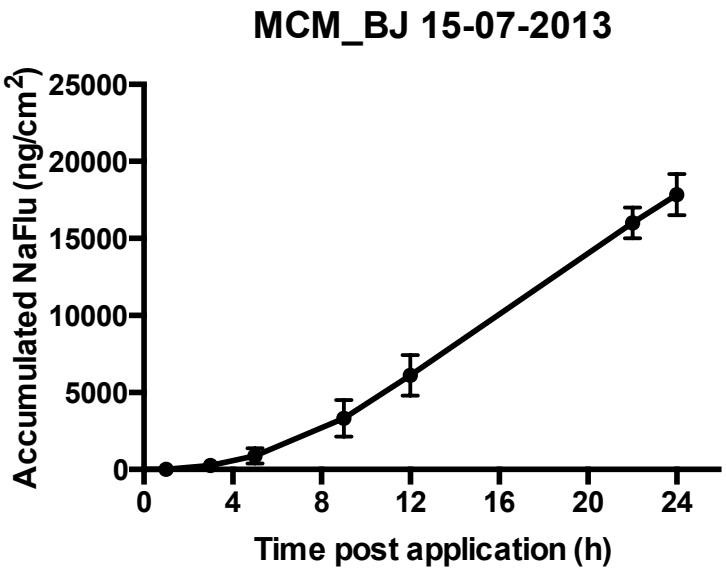

Appendix 7.12 Cumulative transdermal delivery of NaFlu through mouse skin *in vitro* over 24 hours. This formulation contained 1.2 mg/mL NaFlu and was described in Table 3.2. Each point represents means ± standard deviation of 3 to 4 biological replicates.

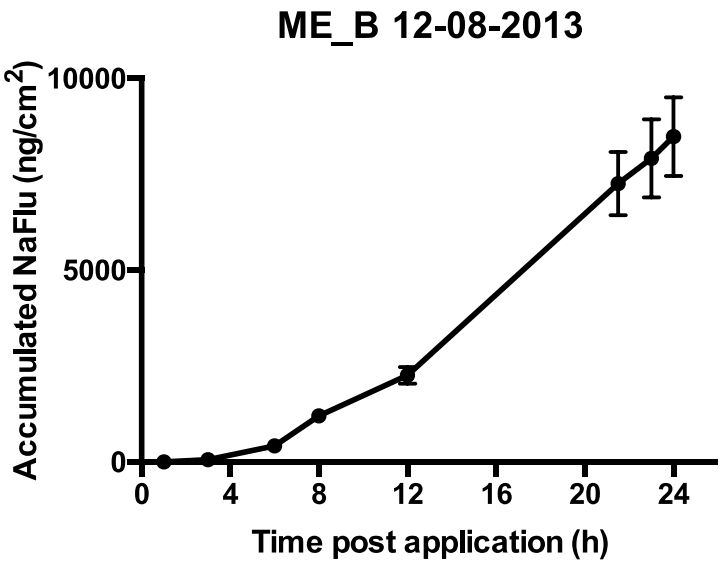

Appendix 7.13 Cumulative transdermal delivery of NaFlu through mouse skin *in vitro* over 24 hours. This formulation contained 1.2 mg/mL NaFlu and was described in Table 3.3. Each point represents means ± standard deviation of 3 to 4 biological replicates.

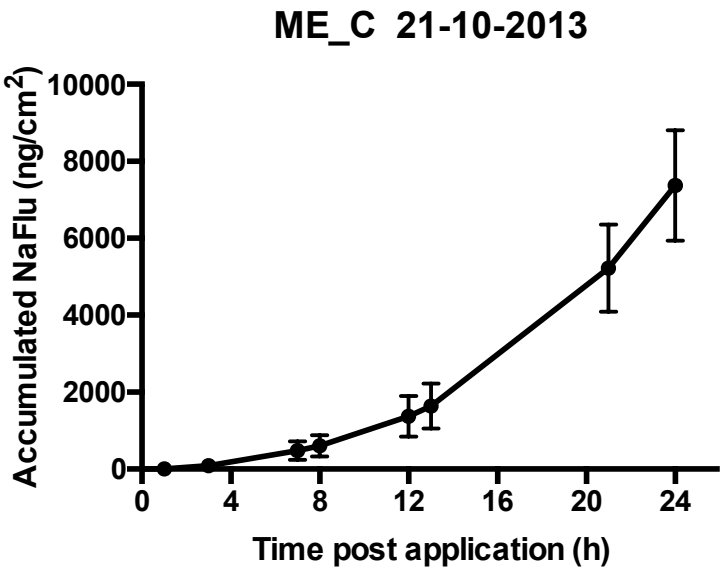

Appendix 7.14 Cumulative transdermal delivery of NaFlu through mouse skin *in vitro* over 24 hours. This formulation contained 1.2 mg/mL NaFlu and was described in Table 3.3. Each point represents means ± standard deviation of 3 to 4 biological replicates.

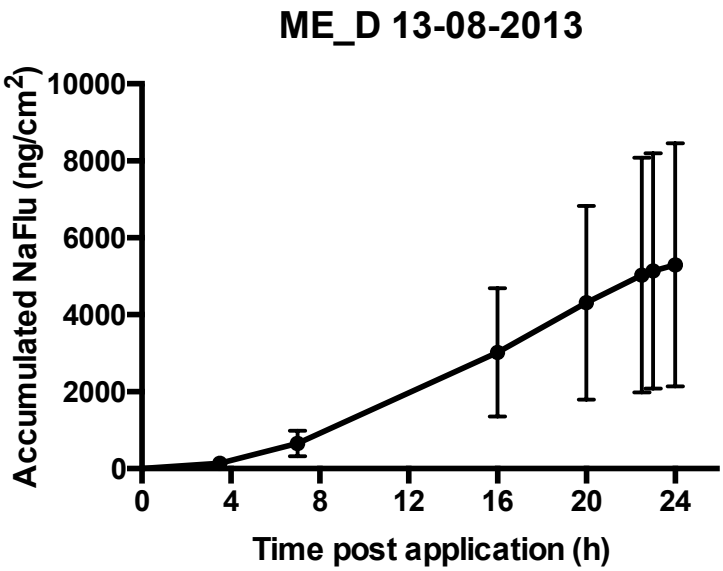

Appendix 7.15 Cumulative transdermal delivery of NaFlu through mouse skin *in vitro* over 24 hours. This formulation contained 1.2 mg/mL NaFlu and was described in Table 3.3. Each point represents means ± standard deviation of 3 to 4 biological replicates.

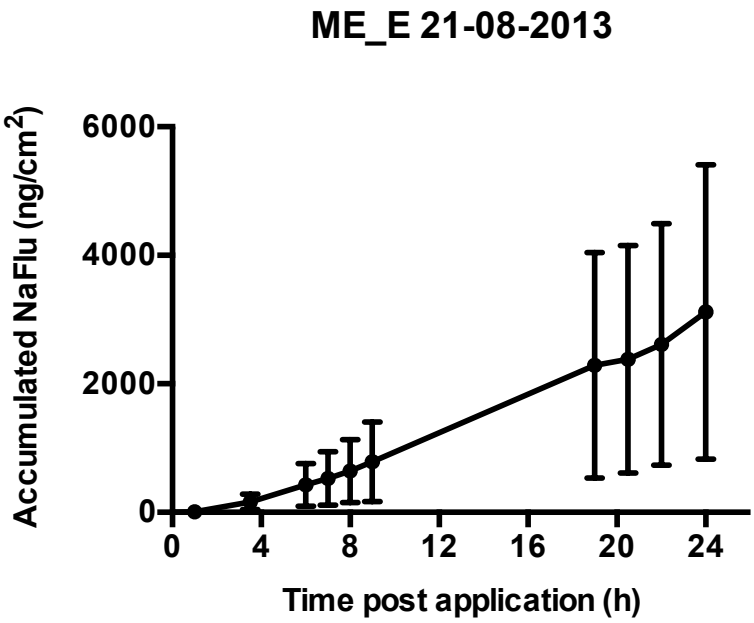

Appendix 7.16 Cumulative transdermal delivery of NaFlu through mouse skin *in vitro* over 24 hours. This formulation contained 1.2 mg/mL NaFlu and was described in Table 3.3. Each point represents means ± standard deviation of 3 to 4 biological replicates.

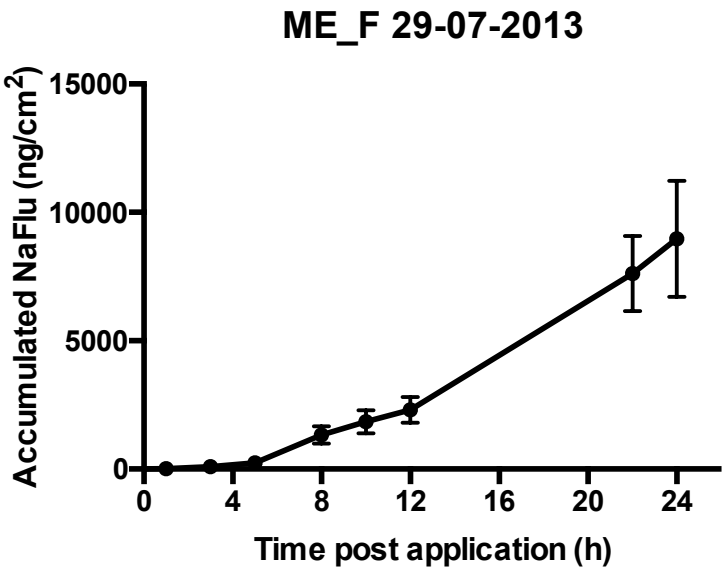

Appendix 7.17 Cumulative transdermal delivery of NaFlu through mouse skin *in vitro* over 24 hours. This formulation contained 1.2 mg/mL NaFlu and was described in Table 3.3. Each point represents means ± standard deviation of 3 to 4 biological replicates.

7.4 Transdermal delivery assay of NaFlu (MCM/EtOH based formulations)

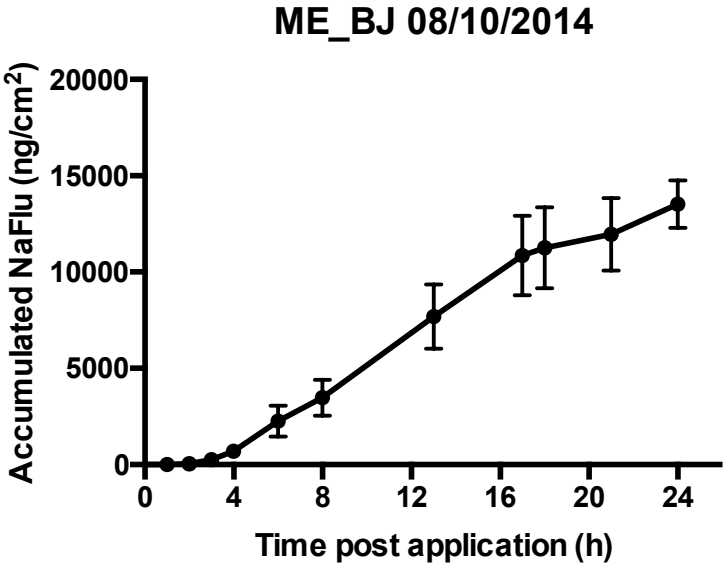

Appendix 7.18 Cumulative transdermal delivery of NaFlu through mouse skin *in vitro* over 24 hours. This formulation contained 1.2 mg/mL NaFlu and was described in Table 3.4. Each point represents means ± standard deviation of 3 to 4 biological replicates.

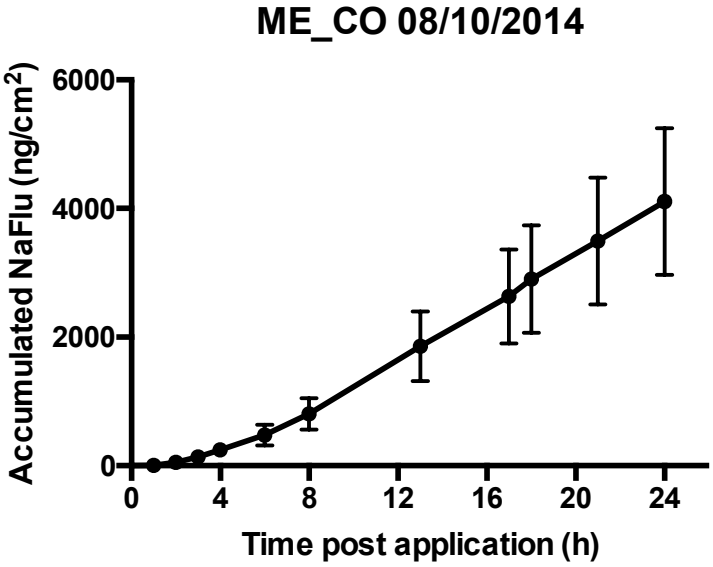

Appendix 7.19 Cumulative transdermal delivery of NaFlu through mouse skin *in vitro* over 24 hours. This formulation contained 1.2 mg/mL NaFlu and was described in Table 3.4. Each point represents means ± standard deviation of 3 to 4 biological replicates.

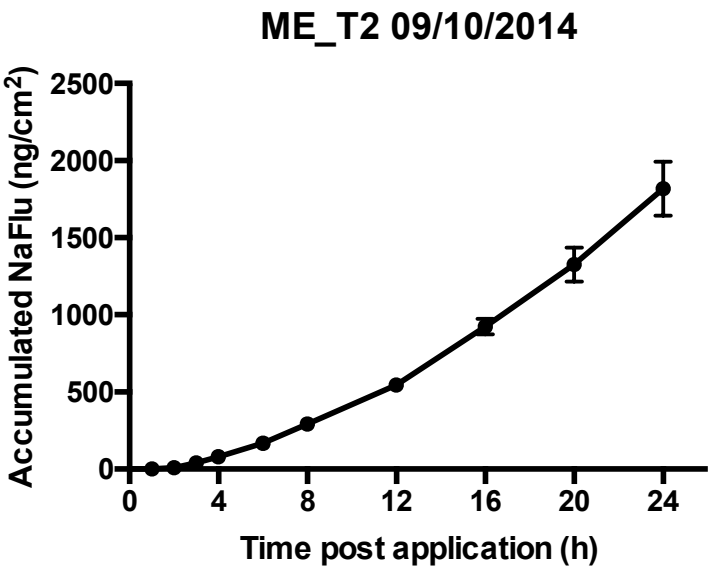

Appendix 7.20 Cumulative transdermal delivery of NaFlu through mouse skin *in vitro* over 24 hours. This formulation contained 1.2 mg/mL NaFlu and was described in Table 3.4. Each point represents means ± standard deviation of 3 to 4 biological replicates.

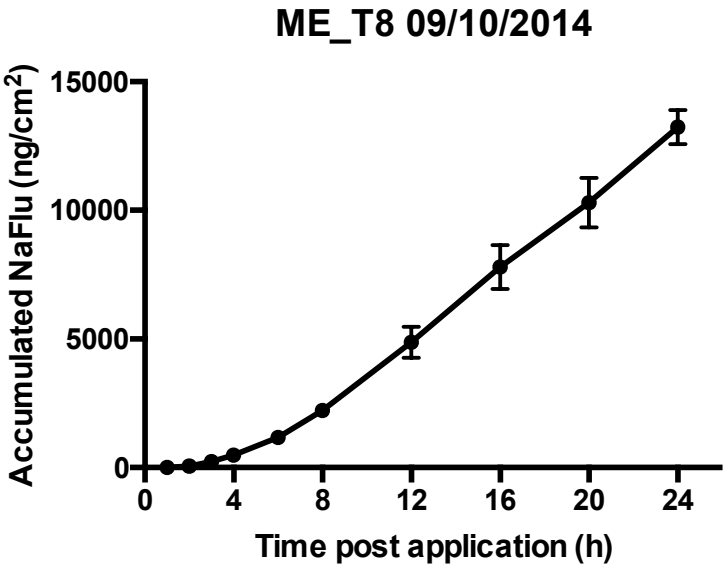

Appendix 7.21 Cumulative transdermal delivery of NaFlu through mouse skin *in vitro* over 24 hours. This formulation contained 1.2 mg/mL NaFlu and was described in Table 3.4. Each point represents means ± standard deviation of 3 to 4 biological replicates.

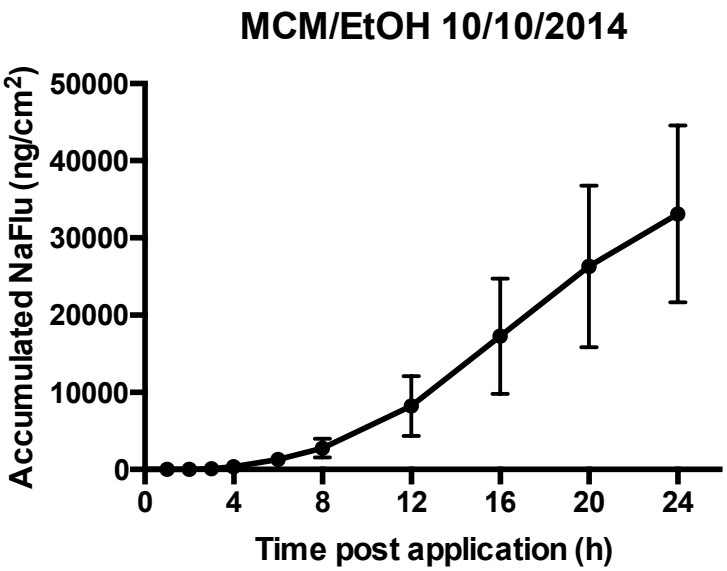

Appendix 7.22 Cumulative transdermal delivery of NaFlu through mouse skin *in vitro* over 24 hours. This formulation contained 1.2 mg/mL NaFlu and was described in Table 3.4. Each point represents means ± standard deviation of 3 to 4 biological replicates.

7.5 Transdermal delivery assay of gentamicin (MCM/EtOH based formulations)

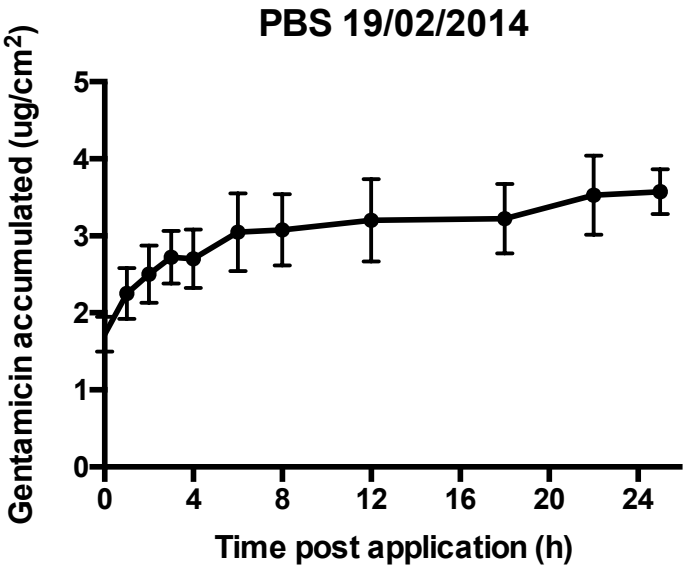

Appendix 7.23 Cumulative transdermal delivery of gentamicin through mouse skin *in vitro* over 24 hours. This formulation contained 20 mg/mL gentamicin that was spiked with 0.5 µCi tritium labelled gentamicin and was described in Table 3.4. Each point represents means ± standard deviation of 3 to 4 biological replicates.

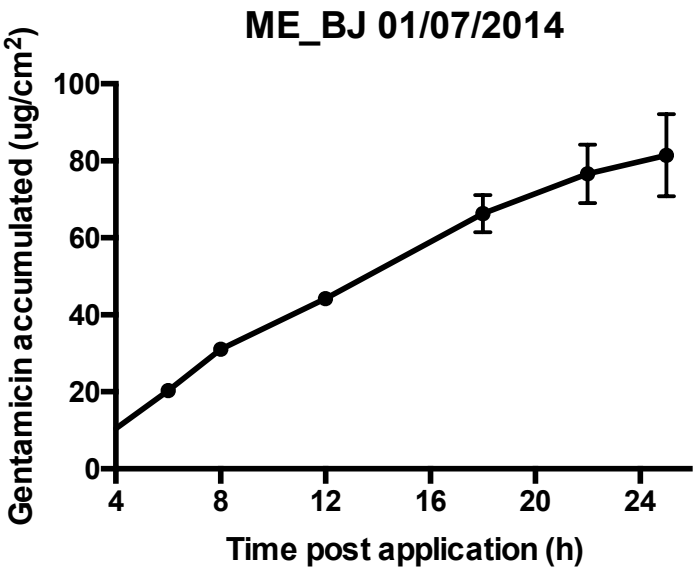

Appendix 7.24 Cumulative transdermal delivery of gentamicin through mouse skin *in vitro* over 24 hours. This formulation contained 20 mg/mL gentamicin that was spiked with 0.5 µCi tritium labelled gentamicin and was described in Table 3.4. Each point represents means ± standard deviation of 3 to 4 biological replicates.

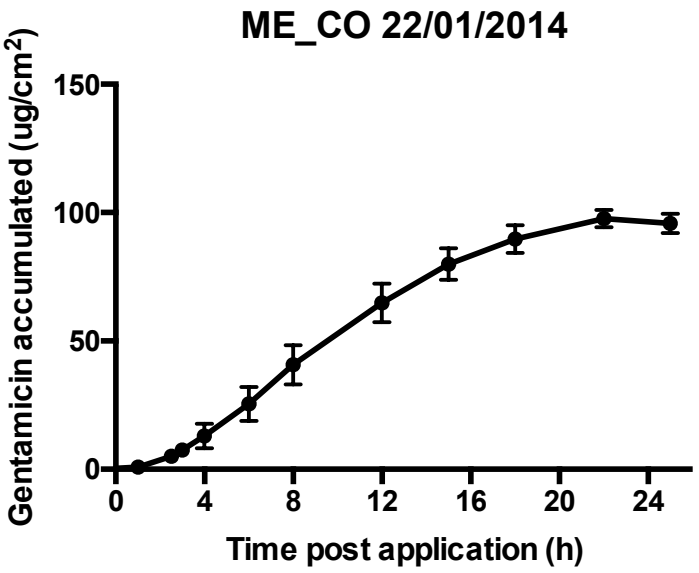

Appendix 7.25 Cumulative transdermal delivery of gentamicin through mouse skin *in vitro* over 24 hours. This formulation contained 20 mg/mL gentamicin that was spiked with 0.5 µCi tritium labelled gentamicin and was described in Table 3.4. Each point represents means ± standard deviation of 3 to 4 biological replicates.

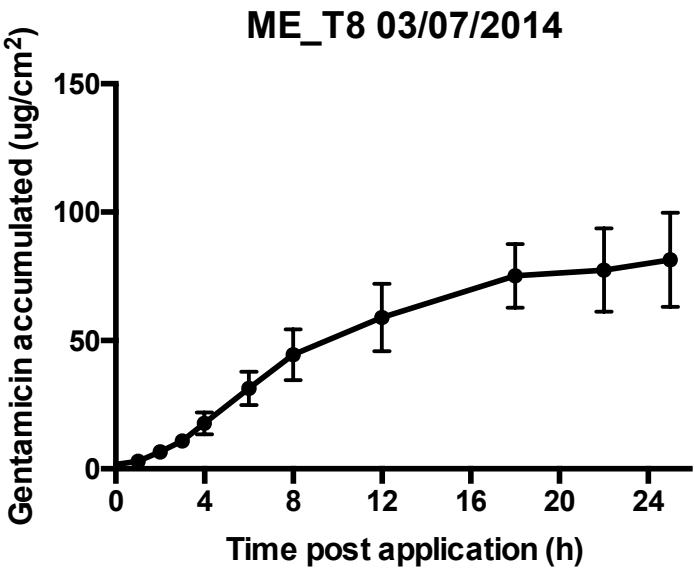

Appendix 7.26 Cumulative transdermal delivery of gentamicin through mouse skin *in vitro* over 24 hours. This formulation contained 20 mg/mL gentamicin that was spiked with 0.5 µCi tritium labelled gentamicin and was described in Table 3.4. Each point represents means ± standard deviation of 3 to 4 biological replicates.

7.6 Bio-distribution assay of gentamicin (MCM/EtOH based formulations)

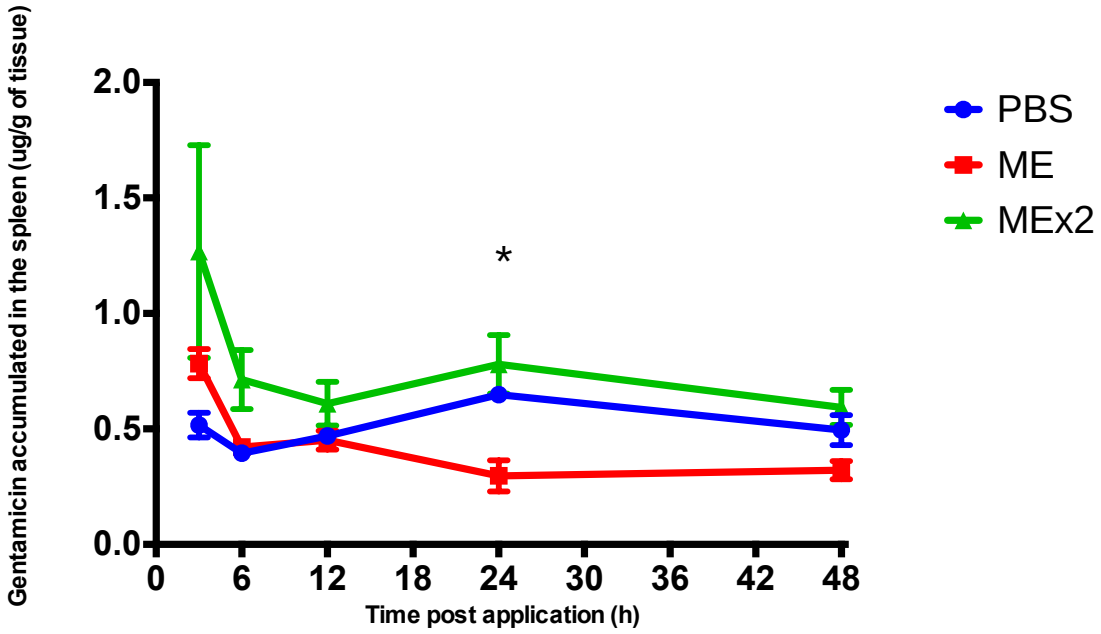

Appendix 7.27 Cumulative gentamicin amount in the spleen of mice *in vivo* over 48 hours. All formulations contained 10 mg/mL gentamicin that was spiked with 0.5 µCi tritium labelled gentamicin and are described in Table 3.4. Each point represents means ± standard error of the mean (SEM) of 3 to 4 biological replicates. At 24 h, the amount of gentamicin in spleen was significantly lower after ME treatment when compared to the PBS treatment (indicated with *, $p < 0.05$).

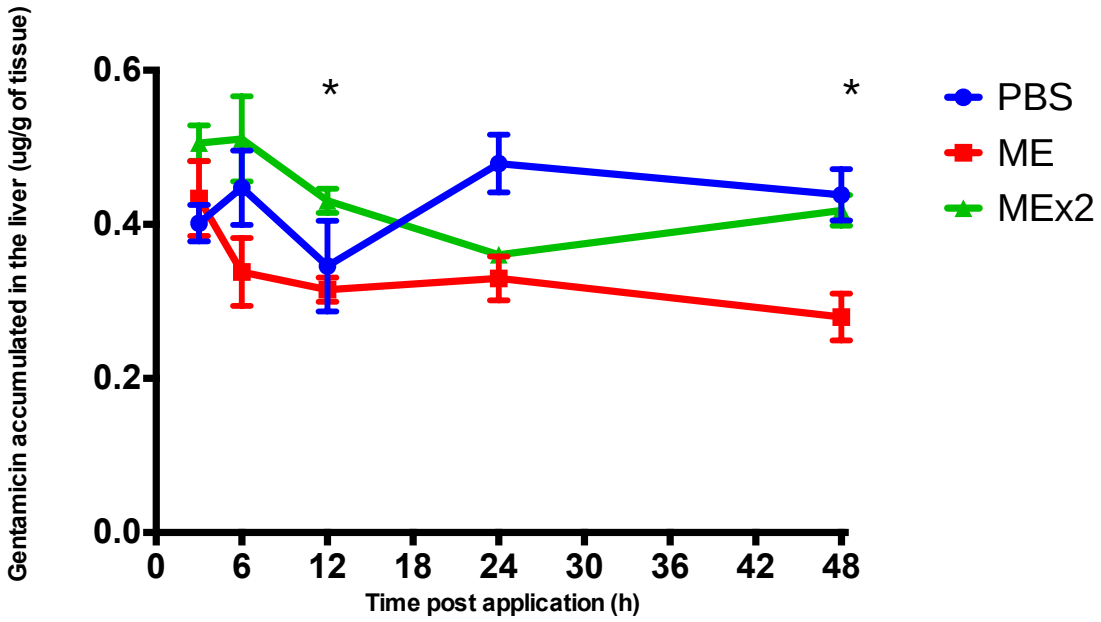

Appendix 7.28 Cumulative gentamicin amount in the liver of mice *in vivo* over 48 hours. All formulations contained 10 mg/mL gentamicin that was spiked with 0.5

µCi of tritium labelled gentamicin and are described in Table 3.4. Each point represents means ± standard error of the mean (SEM) of 3 to 4 biological replicates. At 12 h and 48 h, the amount of gentamicin in liver was significantly lower after ME treatment when compared to the MEx2 treatment (indicated with *, $p < 0.05$).

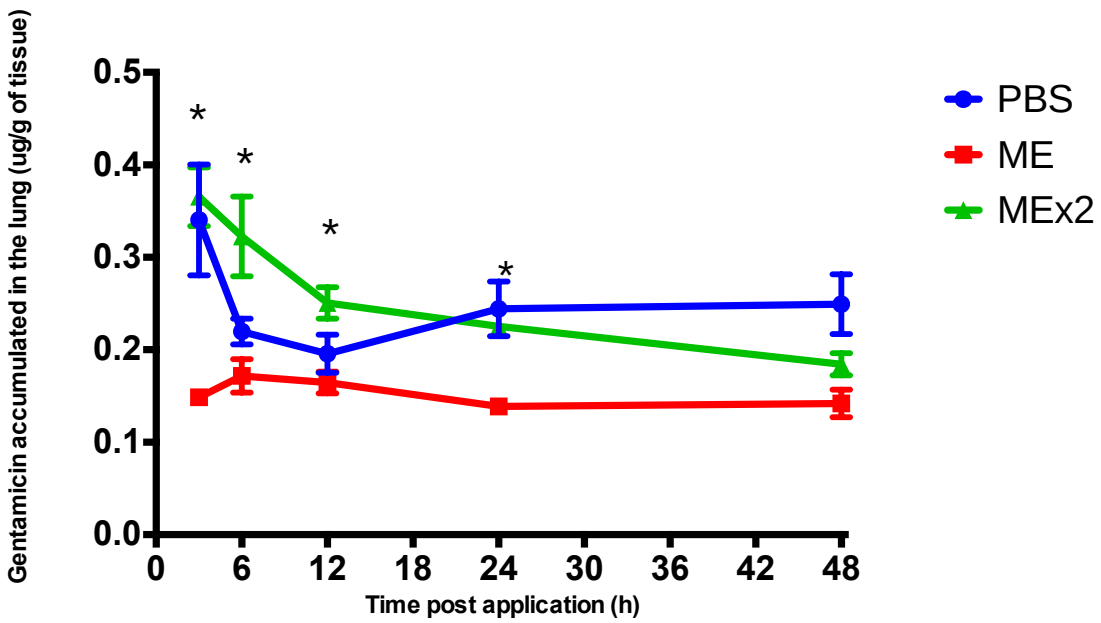

Appendix 7.29 Cumulative gentamicin amount in the lung of mice *in vivo* over 48 hours. All formulations contained 10 mg/mL gentamicin that was spiked with 0.5 µCi of tritium labelled gentamicin and are described in Table 3.4. Each point represents means ± standard error of the mean (SEM) of 3 to 4 biological replicates. At 3 h, 6 h, 12 h and 24 h, the amount of gentamicin in lung was significantly lower after ME treatment when compared to the MEx2 treatment (indicated with *, $p < 0.05$).

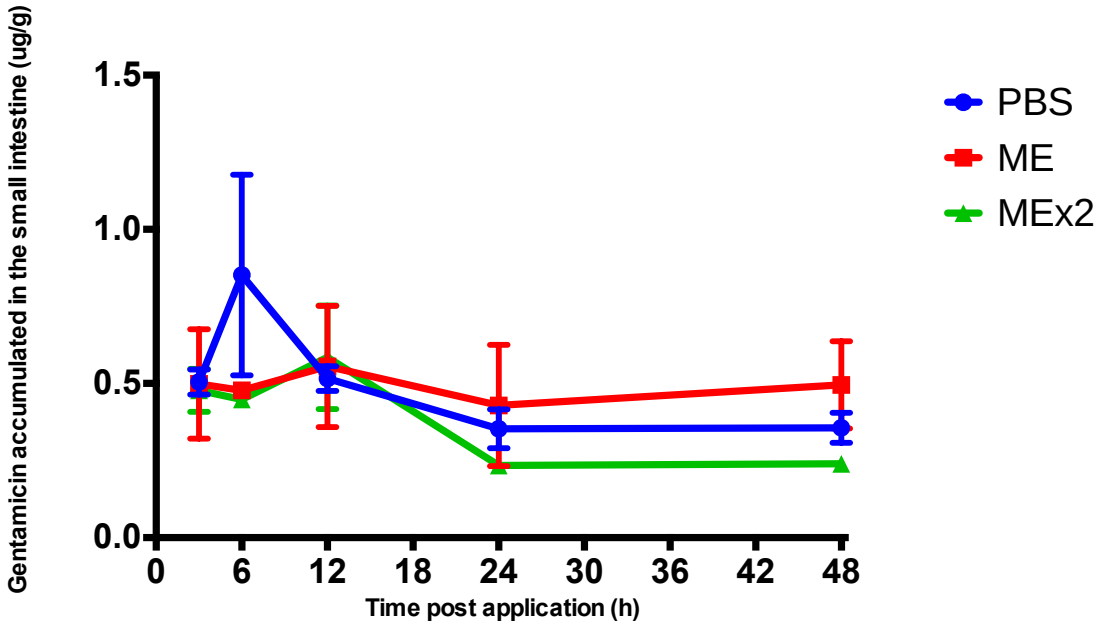

Appendix 7.30 Cumulative gentamicin amount in the small intestine of mice *in vivo* over 48 hours. All formulations contained 10 mg/mL gentamicin that was spiked with 0.5 µCi tritium labelled gentamicin and are described in Table 3.4. There is no significant different between each treatment group. Each point represents means ± standard error of the mean (SEM) of 3 to 4 biological replicates.

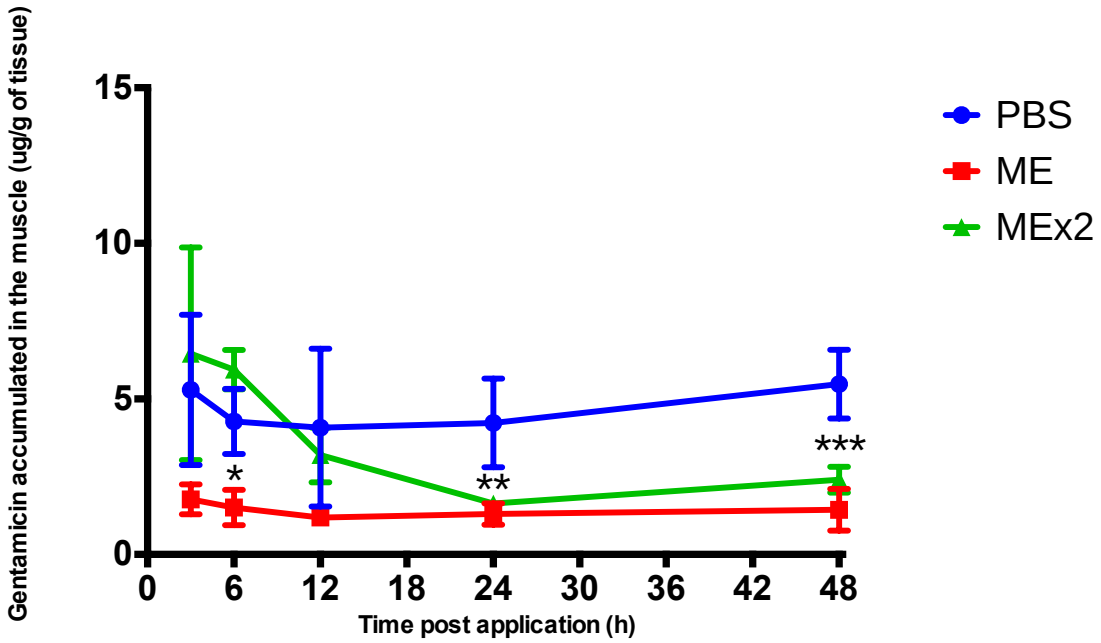

Appendix 7.31 The transdermal permeation gentamicin amount accumulated in the underneath muscle at the site of topical application of mice *in vivo* over 48 hours. All formulations contained 10 mg/mL gentamicin that was spiked with specific amount

of tritium labelled gentamicin and are described in Table 3.4. Each point represents means ± standard error of the mean (SEM) of 3 to 4 biological replicates. At 6 h, the amount of gentamicin in the muscle was significantly lower after ME treatment when compared to the PBS and MEx2 treatment (indicated with *, $p < 0.05$). At 24 h, the amount of gentamicin in the muscle was significantly lower after ME treatment than that after PBS treatment group (indicated with **, $p < 0.05$). The gentamicin amounts in the muscle after both ME treatment and MEx2 treatment were significantly lower than the PBS treatment in the 48 h (indicated with ***, $p < 0.05$).

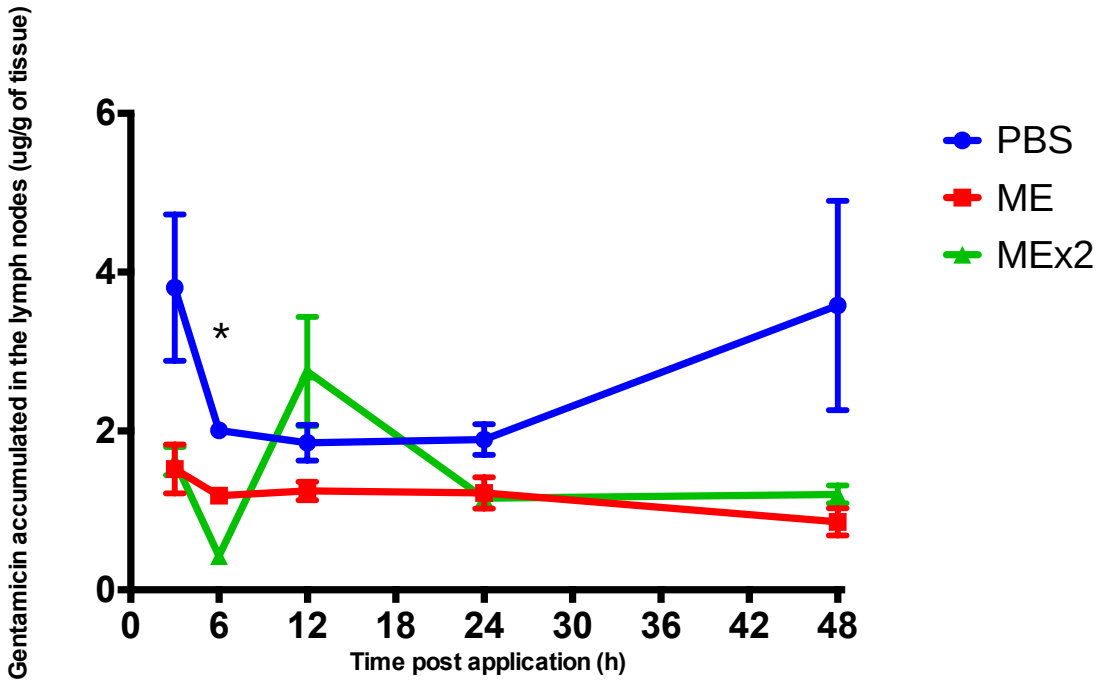

Appendix 7.32 Cumulative gentamicin amount in the lymph nodes of mice *in vivo* over 48 hours. All formulations contained 10 mg/mL gentamicin that was spiked with 0.5 µCi of tritium labelled gentamicin and are described in Table 3.4. Each point represents means ± standard error of the mean (SEM) of 3 to 4 biological replicates. At 6 h, the amount of gentamicin in the lymph nodes was significantly lower after ME treatment when compared to the PBS treatment (indicated with *, $p < 0.05$).